Optimization of Operating Parameters for Minimum Mechanical Specific Energy in Drilling

Todd Robert Hamrick

Dissertation submitted to the
College of Engineering and Mineral Resources
Department of Mechanical and Aerospace Engineering
at West Virginia University
in partial fulfillment of the requirements
for the degree of

Doctor of Philosophy
Mechanical Engineering

Approved by

Bruce Kang, PhD, Committee Chairperson
James Smith, Ph.D.
Larry Banta, Ph.D.

Department of Mechanical and Aerospace Engineering

Keith Heasley, Ph.D.

Department of Mining Engineering

Wu Zhang, Ph.D

Department of Energy, United States of America

Morgantown, West Virginia
2011

Keywords: Drilling Optimization, MSE, Mechanical Specific Energy, Rock Drilling

Abstract

Optimization of Operating Parameters for Minimum Mechanical Specific Energy in Drilling

by Todd Robert Hamrick

Efficiency in drilling is measured by Mechanical Specific Energy (MSE). MSE is the measure of the amount of energy input required to remove a unit volume of rock, expressed in units of energy input divided by volume removed. It can be expressed mathematically in terms of controllable parameters; Weight on Bit, Torque, Rate of Penetration, and RPM. It is well documented that minimizing MSE by optimizing controllable factors results in maximum Rate of Penetration. Current methods for computing MSE make it possible to minimize MSE in the field only through a trial-and-error process. This work makes it possible to compute the optimum drilling parameters that result in minimum MSE. The parameters that have been traditionally used to compute MSE are interdependent. Mathematical relationships between the parameters were established, and the conventional MSE equation was rewritten in terms of a single parameter, Weight on Bit, establishing a form that can be minimized mathematically. Once the optimum Weight on Bit was determined, the interdependent relationship that Weight on Bit has with Torque and Penetration per Revolution was used to determine optimum values for those parameters for a given drilling situation.

The improved method was validated through laboratory experimentation and analysis of published data. Two rock types were subjected to four treatments each, and drilled in a controlled laboratory environment. The method was applied in each case, and the optimum parameters for minimum MSE were computed. The method demonstrated an accurate means to determine optimum drilling parameters of Weight on Bit, Torque, and Penetration per Revolution. A unique application of micro-cracking is also presented, which demonstrates that rock failure ahead of the bit is related to axial force more than to rotation speed.

Dedication

For my family.

Acknowledgements

A project of this size and duration is only possible with a great deal of support. My wife, Debbie, has been my greatest benefactor, and I could not have done it without her unwavering devotion. I would also like to thank my kids, Scott and Caroline, for their patience and inspiration. My parents, Louis and Barbara Hamrick are the most generous people I have ever encountered, and I could never have even begun the project without their backing. My father, through his company Northco, was particularly generous with lending machine time and funding for experimentation at the end of the project when all other sources were exhausted.

I would like to thank URS Corporation and National Energy Technology Laboratory for providing infrastructure and financial support. Technical and moral assistance was lent by many people, including each member of my committee. Each of them deserves a measure of appreciation for their individual and collective service. Of particular assistance outside of my committee were Peter Zhang, who was always available for help sample preparation, and Jared Tannenbaum, who helped with load cells and micro-cracking.

Table of Contents

List of Figures

List of Tables

1. Introduction

Research on extreme drilling is ongoing at the National Energy Technology Laboratory of the Department of Energy. Their Extreme Drilling Laboratory was particularly interested in research of fundamentals of drilling and improving drilling efficiency. One method of measuring efficiency is through Mechanical Specific Energy (MSE), which measures energy expenditure required for material removal. It is well understood that maximum efficiency can be found at the point where MSE is at its lowest, and it has been used for years in industry as an efficiency measurement tool.

Most research regarding MSE focused on its use as a gauge, indicating the relative effects of changes to efficiency, but little work has been published that seeks to minimize MSE mathematically. Researchers at the Extreme Drilling Lab recognized that the traditional MSE equation consists of a set of interrelated parameters. They initiated work that established mathematical relationships between the parameters in order re-write the MSE equation in terms of controllable parameters. This work expands upon that pioneering effort, re-writing the MSE equation in terms of a single parameter.

2. Literature Review

Background

Early drilled wells using a percussion bit have been produced for centuries, but the need to go deeper in order to access resources further below the surface with less effort brought about new technologies. The first drilled well in America was completed in 1808 by David and Joseph Ruffner near Charleston, WV. Human muscle power was used to drive a percussion bit into the bedrock, with a spring pole attached to pull the bit upward ready for another strike. The same technology was used to drill the nation's first oil well in Titusville, PA in 1859. Petroleum oil satisfied increased demand for Kerosene, which replaced whale oil in lamps.[1] In 1909, Howard Hughes Sr. famously patented the first roller cone drill bit, which revolutionized the well drilling industry. The new technology increased rates of penetration, thus decreasing cost per foot, and such bits are still in wide use today.[2]

As conventional formations are exhausted or placed out of reach by political or environmental influences, unconventional resources such as deep formation drilling grow in importance, and are expected continue to grow in importance into the foreseeable future. In the transportation sector alone, worldwide oil consumption is expected to grow by 45% from 2007 to 2035. Natural gas consumption is expected to increase by 44% in the same time frame, and prices for both are expected to remain strong. Strong prices are important, as this provides the capital required for exploration.[3]

In the late 1970's new bit technology based on man-made diamonds emerged. The Poly-crystalline Diamond Compact (PDC) cutter was developed, which consists of a tungsten carbide backing matrix with a thin diamond face on one end. PDC Cutters can be custom made in nearly any configuration, but typical cylinder diameters range from 2 mm to 24.5 mm and lengths range from 3 mm to 24.5 mm. Rectangular cutters are also common, with the diamond on one of the large faces. Bit technology to arrange the cutters in the most advantageous manner includes aspects important to the driller such as wear, bore-hole sizing, and fluid flow. While roller cone bits are used today for relatively shallow wells, they have been supplanted by PDC bits in deep wells.[4]

Deep natural gas formations are an increasingly important resource, growing from 7% of all natural gas production in 1999 to an estimated 14% in 2010 worldwide. Deep well drilling can be defined as any well drilled deeper than 15,000 feet. At these depths the ambient environment is at high temperature (>250C) and extremely high pressure (>10,000psi), which is often referred to as HTHP. Rocks are often abrasive, extremely hard, and drilling fluids used are corrosive. In such wells half of the total drilling costs can be expended in the last 10% of the

hole. For that reason optimizing Rate of Penetration (ROP) is critical to cost effective well drilling, especially at extreme depths.4

Mechanical Specific Energy

The concept of Mechanical Specific Energy (MSE) was introduced by Teale in 1965. Teale defined MSE as the mechanical work done to remove a unit volume of material. In this regard it is a type of efficiency that evaluates "work in" versus "volume of material out," and the units can be expressed in ft-lb/ft^3 or in psi.[5]

Teale understood that minimizing MSE meant maximum possible excavation, and would result in maximum rate of penetration. With regards to rotary drilling he said, "Breaking the debris into 'smaller fragments than necessary' may have a disproportionate effect on the energy needed to excavate the given volume." This means that rocks broken into pieces smaller than necessary for excavation would result in more energy expenditure than required, and rocks broken into pieces too large for evacuation would consume energy in their necessary re-breaking. He tested this theory and found that MSE plotted against Rate of Penetration did result in either a minimum or a point of diminishing return.5

MSE Applied to PDC Drilling

Although the concept of MSE was proposed by Teale in the mid-1960's and PDC Bits were developed in the late 1970's, the literature has no important effort to apply MSE minimization concepts to PDC rock drilling bits until later. Early tests to understand rock breakage mechanisms and performance characteristics of PDC bits were carried out in the 1980's with no mention of MSE.[6, 7]

Zeuch and Finger found in 1985 that cutters used more energy in their first pass than in subsequent passes when the parent rock had been pre-damaged. The report said, "Cuts in pre-damaged rock remove more chips per unit work than in virgin rock." Zeuch and Finger noted that their tests were carried out in atmospheric temperature and pressure, and that increased borehole and confining pressure and/or temperature may make a difference in the failure mechanisms, but that work does not appear in the literature. They also observed that cracks are nucleated some distance in advance of the tip of the cutter, but they did not compute or mention MSE.[8]

In 1987 Wojitanowicz and Kuro attempted to quantify maximum bit performance both computationally and experimentally. While they did not employ MSE, they did recognize that an optimum Weight on Bit and RPM level would result in maximum bit performance, i.e.

maximum Rate of Penetration. They also proposed measuring performance characteristics in real time and using those figures to compute optimum controllable drilling parameters.[9]

In 1997 Huang and Wang conducted coring bit tests using experimental design. They proposed an equation for computing the specific energy required to cut the kerf. They observed that at very low Weight on Bit the energy level was dominated by friction, and that increased Weight on Bit corresponded to increased torque and lower specific energy. However they failed to report that there is an optimum Weight on Bit that resulted in optimum Specific Energy.[10]

At about the same time in 1997, Ersoy and Waller conducted an early test that used MSE as a metric. They were most interested in comparing drilling detritus particle size on three coring bit types; a PDC pin coring bit, a diamond impregnated bit and a hybrid. They found that the PDC pin bit produced larger particle sizes than the diamond impregnated bit, which is logical as larger physical size of the pins compared with the impregnated diamonds allows the bit to take a bigger bite, which results in a greater penetration per revolution. The PDC pins will break off larger pieces of the rock, while the diamond impregnated bit can only grind. They observed that the optimal penetration per revolution has to do with the clearance between the highest point of the cutter and the bit matrix, and a higher Weight on Bit than is physically possible with a given configuration will result in stall, not increased Rate of Penetration. They also observed that an optimally low Mechanical Specific Energy could be obtained at an optimal Weight on Bit, with a steady production of drilling detritus and a balanced bit wear. [11]

Ersoy followed up this work in 2003 with a similar study on circular rock saws. As with the coring bits, he found that MSE can be used to quantify efficiency of rock cutting for all types of rock working including sawing, cutting, excavation and drilling. He noted that increasing feed rate was associated with decreasing MSE up to a point, but further increase in feed rate caused little or no decrease in MSE, in some cases MSE increased, and machinery could be induced to stall or fail if depth of cut was too high. Very high depth of cut also resulted in excessive tool wear.[12]

By the mid 2000's commercial interests had developed sophisticated hole logging techniques, and drilling efficiencies had improved through experience of trial and error. At the same time improvements to drilling were made possible by innovations in all aspects of the industry including bit design, drilling fluids, rig design, and many other parameters. MSE began to emerge as a method for improving efficiency of drilling at all levels including rigs and bits, and industrial researchers began studying this metric. Although industrial research began using MSE evaluation heavily, academic researchers did not give it the same level of importance, with some exceptions. 4

Caicedo and Calhoun created a method of predicting Rate of Penetration of a given bit using MSE, and they successfully tested the method on rigs in 2005 using real time data.[13] In 2008 Armenta heuristically derived a bit-specific hydraulic term to modify Teale's MSE equation, which he called Drilling Specific Energy. He postulates that a major part of bit efficiency comes from its hydraulic performance, and this term takes hydraulic performance into account for specific bits at specific Weight on Bit.[14]

In 2005 seminal work on using MSE for optimum Rate of Penetration on drilling rigs in real time was initiated by Dupriest, Koederlitz and Weis while working for Exxon Mobile. They modified a drill rig data logging system to compute MSE based on data available at the surface of the rig site. They were able to accurately diagnose drilling problems and take appropriate steps to correct them. Because of the improvements in efficiency made possible by monitoring MSE, it quickly became a standard in rig data surveillance. While a useful tool, MSE surveillance did not tell the drilling operators and engineers what caused inefficiency or what to do to eliminate potential problems. This was remanded to the experience of the operators. [15, 16]

Within a year Dupriest reported that Exxon Mobile had expanded MSE surveillance across its entire global organization, using it on all drill rigs worldwide, drilling some 4.5 million feet annually. They identified 40 different Rate of Penetration limiters, only four of which were related to the bit. They began using MSE as an indicator, and changed company work flow procedures to pursue increased Rate of Penetration through local optimization and, when local optimization techniques were exhausted, through engineering design.[17]

By 2007 Dupriest, with Remmert and Witt, claimed to have saved $54M and set 50 new drilling records, while simultaneously implementing one of the best safety records in the industry. They made improvements to the surveillance package as they moved up on the learning curve, implementing such improvements as vibrational analysis, Bottom Hole Assembly (BHA) design improvements, and lithology records based on wells drilled previously in a given region. This was of particular interest in Qatar.[18]

Similar successes were reported around the world. Off the coast of California the process was implemented to deliver a 5-well project 138 days ahead of schedule and 44% under budget.[19] In Australia problematic borehole behaviors were overcome through MSE management. Seven wells were drilled in record setting time in regions that have historically been difficult to drill due to unstable boreholes. Part of the success is attributed to improved BHA design to overcome vibration problems.[20] A similar project was undertaken in Germany that did not utilize the MSE monitoring, but BHA's were modified for improved vibration control, along with monitoring and control of RPM and Weight on Bit. The result was record performance for diamond impregnated bits in very hard rocks.[21] Dupriest reported in 2009 that the process identified bit steerability and whirl as a major cause of reduced Rate of Penetration, and efforts

to mitigate the problems were monitored and successfully mitigated through MSE surveillance. Steerability is the ability to control the direction of drilling, and whirl is a type of vibration.[22]

Laboratory Scale Drilling

Several researchers employed the use of small scale drilling in laboratory settings. Teale investigated MSE computations for several types of stone drilled with 1 11/16 two-wing carbide bits.5

In 1997 Reddish and Yasar used a hand held drill fitted with a masonry bit as a portable quasi-nondestructive rock strength testing apparatus. While their energy measurement method was dubious, they obtained valid comparative data that agreed with Teale's thesis. They were successful in creating the basis for a portable testing device based on MSE using simple equipment including a standard masonry bit.[23]

In 2006 Stavropoulou used the same type of bit in a fully instrumented machining center for validating numerical Finite Element Analysis. Among their findings were a linear relationship between Penetration per Revolution and both Weight on Bit and Torque. They also determined that the small bits tend to crush the rock rather than chipping it at very high (600) RPM.[24]

Also in 2006 Abd Al-Jalil determined residual stress developed after unloading of brittle material, causing nucleation and growth of cracks. Also Weight on Bit was the most critical factor in crack nucleation below the bit.[25]

In 2008 Mosley, et al. also used a fully instrumented machining center for the study of wear and fracture mechanisms of Poly-Crystalline Diamond Compact (PDC) cutters. They used various sizes of PDC insert coring bits ranging from 52-152 mm with 3-5 PDC cutters per bit, and drilled at RPMs ranging from 440-1100 min^{-1}.[26]

In 2009 a similarly instrumented machining center and was employed by Hamade, et al. for studying wear of cutters and cutting forces while drilling Basalt on Mars. That work used a single 25 mm PDC coring bit, and ran at 60-180 RPM but at very low feeds of no greater than 0.002 in/rev, which would result in grinding only. They derived equations for expected torque and Weight on Bit based on tool wear, rock strength and other drilling parameters. The drilling parameters in the equations were fitted based on actual conditions. The scope of Hamade's work was tool wear, and drilling efficiency was not mentioned, but Hamade did publish his raw data which is analyzed in this work.[27]

As work to improve rates of penetration was underway in the mid-2000s, industrial researchers wanted to determine what the major factors in drilling were. They wanted to know which of

many factors were the most important to increasing rate of penetration, so they joined forces with the government to benchmark the process. A deep drilling simulation research program was carried out in a joint venture by the petroleum industry and National Energy Technology Laboratory at the Department of Energy between 2002 and 2007. Its formal name was "DeepTrek Phase I and II, An Industry/DOE Program to Develop and Benchmark Advanced Diamond Product Drill Bits and HP/HT Drilling Fluids to Significantly Improve Rates of Penetration," but it is generally referred to as Deeptrek. The purpose of that work was to benchmark improved rates of penetration by studying full scale drilling in simulated high pressure and high temperature environments. The work was essentially a screening study, testing 37 different combinations of drill bits, rock types, and drilling fluids. It published the most extensive data set that can currently be found in the literature.[28]

Mathematical Analysis using MSE

There are examples of efforts to improve drilling performance through mathematical analysis, but few of these used MSE as a metric or had a thorough experimental component.

Huang used an experimental design to study drilling efficiency in 1997. He introduced the concept of specific kerfing energy, which is similar to MSE, but did not mention Teale's work. He noted a linear relationship between Weight on Bit and Torque, and a non-linear relationship between Weight on Bit and Penetration per Revolution. An equation for specific kerfing energy as a function of Weigh on Bit alone appears in the work, and Weight on Bit is concluded to be the most influential factor in specific energy. The L-shaped nature of specific energy is also noted. It is unclear if this work is an independent finding of Teale's earlier research, but the results and conclusions are much the same.[10]

Gerbaud developed a mathematical model of the interaction between the rock and the bit, and used it with some practical success in the mid 2000's. That work did not use MSE, but it did some experimentation and related various parameters. A linear relationship between Weight on Bit and Torque is noted. Also of interest is a non-linear relationship between Weight on Bit and Penetration per Revolution. 6

Armenta made an effort to improve the Teale MSE equation in 2008 by adding a term. The added hydraulic parameter was intended to account for removal of detritus from under the bit. No experimentation was conducted, but comparisons with field data were made.[14]

The Caicedo and Calhoun work modified the MSE equation with a bit-specific sliding friction term. This term was based in part on the confined compressive strength of the rock, and was used to modify the Torque component when accurate Torque data was unavailable. The

Torque term in the Teale equation was replaced with the modified Torque term, and the Teale MSE equation was rearranged so that it solved for Rate of Penetration. This was used to predict rate of penetration in field drilling with some success under limited conditions.

RPM Analysis

When RPM is mentioned in the literature it is recognized that in field drilling RPM is related to vibration.

In 1992 Langeveld conducted some early studies on bit whirl and stick-slip behavior of PDC bits. He determined that torque control considerably improved the condition, and improved efficiency in drilling. He concluded that an optimum RPM was related to vibration, and not necessarily rock cutting. [29, 30]

Whirl resistant bits were developed, and the relationship between vibration, RPM, and Torque variation became better understood. It became clear that vibration plays an important role in optimum RPM, and that variable control of torque plays an important role in vibration control.[31, 32]

In his study of bit performance in hard rocks, Mensa-Wilmot emphasized that high penetration per hour usually noted at high RPM in softer formations was due to the increased Penetration per Revolution, and not the cutting mechanism. If RPM is too low, then stick-slip may occur, causing vibrational problems. If RPM is too high, then excess wear will result. RPM can be optimized between these potential outcomes, but it is not a function of other drilling parameters.[33]

3. Major Contribution of This Work

The major contribution of this work is in finding an improved method for computing optimum parameters that will result in minimum MSE, and therefore maximum efficiency in drilling. Current understanding of influences on MSE is limited to experience based knowledge and MSE computations that involve three or four input parameters. This work simplifies the MSE computation by reducing it to a single input parameter, thereby simplifying the minimization process.

A mathematical theory was developed in the work and validated through its application to experimental results. It is further validated through application to published data. The method simplifies a complex and experience based process to a certain and calculable equation based on readily measureable parameters. It will benefit researchers and industry by creating a method for computing the optimum parameters at the minimum MSE by using readily available data. No other work can be found in the literature that seeks to minimize MSE mathematically through rewriting the MSE equations and to validate the theory experimentally.

Teale wrote in 1965, "*For a practical tool operating at a fixed rotation speed in a particular rock, it is to be expected that the specific energy at low thrust will be high. It will fall fairly rapidly, as the thrust increases, until it reaches a value beyond which it will either continue to decrease so slowly as to remain virtually constant, or will actually start to rise again. The lowest value attained is a measure of the maximum efficiency of the particular tool in the particular operating conditions. It enables comparison to be made with any other type of tool operating in the same rock. Its characteristics; whether it occurs as a sharp turning point at one particular thrust, or remains constant over a range of thrusts, are of considerable interest*."[5]

Work to date has used MSE as an industrial tool, as seen in the works by Dupriest and others. While significant improvements in Rates of Penetration in industrial applications have been documented, the optimum that Teale understood existed cannot be determined with existing methods. So while efforts to use MSE as a tool for efficiency improvement have been successful, none have characterized MSE mathematically in a way that allows for its minimizing through the computation of optimum parameters.

Finally this work publishes a set of experimental data larger than can be found elsewhere in the literature. Most researchers publish little or no experimental data or use field data for theoretical validation. The data published in this work is of interest to researchers, drillers, equipment designers, and others involved in the drilling industry. Its principles could potentially be applied to any scale or type of drilling in any material, and thus may have broad applications beyond its original intentions.

4. Mechanical Specific Energy (MSE) Equation Transformation

Fundamental Equation

MSE is defined as Energy-In divided by Volume-Out.

$$MSE = \frac{Total\ Energy\ Input}{Volume\ Removed} \tag{1}$$

Volume of a drill hole is simply cross sectional Area multiplied by depth of penetration (Δh), and Work Energy can be described as Force multiplied by distance. In drilling there are two forces acting on the bit; Weight on Bit (axial force) and Torque (rotational force). These are additive to MSE, so there are two terms in the MSE Equation.

$$MSE = \frac{Vertical\ Energy\ Input}{Volume\ Removed} + \frac{Rotational\ Energy\ Input}{Volume\ Removed} \tag{2}$$

$$MSE = \frac{WOB * \Delta h}{Area * \Delta h} + \frac{Torque * 2\pi * \#of\ Rotations}{Area * \Delta h} \tag{3}$$

The distance travelled by the bit (Δh) during a given interval is the penetration per time (ROP) divided by rotations per time. This is also known as depth of cut or as Penetration per Revolution. On a per-minute basis,

$$\Delta h = \frac{Penetration\ Per\ Minute}{RPM} = \frac{ROP}{RPM} = P \tag{4}$$

Therefore the MSE equation derived from Teale appears in Equation 5.5

$$\mathrm{MSE} = \frac{\mathrm{WOB}}{\mathrm{Area}} + \frac{2\,\pi * \mathrm{RPM} * \mathrm{Torque}}{\mathrm{Area} * \mathrm{ROP}} \tag{5}$$

Where:

MSE = Mechanical Specific Energy (psi)
WOB = Weight On Bit (lb)
RPM = Rotations Per Minute
Torque = Rotational torque (in-lb)
Area = Cross sectional area of bit (in^2)
ROP = Rate of Penetration (in/hr)
P = Penetration Per Revolution (in/rev)

By definition MSE is a measure of material removal efficiency, and Teale recognized it as a potentially important tool in analyzing rock drilling.[5] It is well understood that MSE is expected to be high at low rates of penetration, and decrease as penetration rate increases. At some point MSE will either remain flat with increasing penetration rate, or MSE will begin to climb again. An example of this can be seen in Figure 1 from Deeptrek.

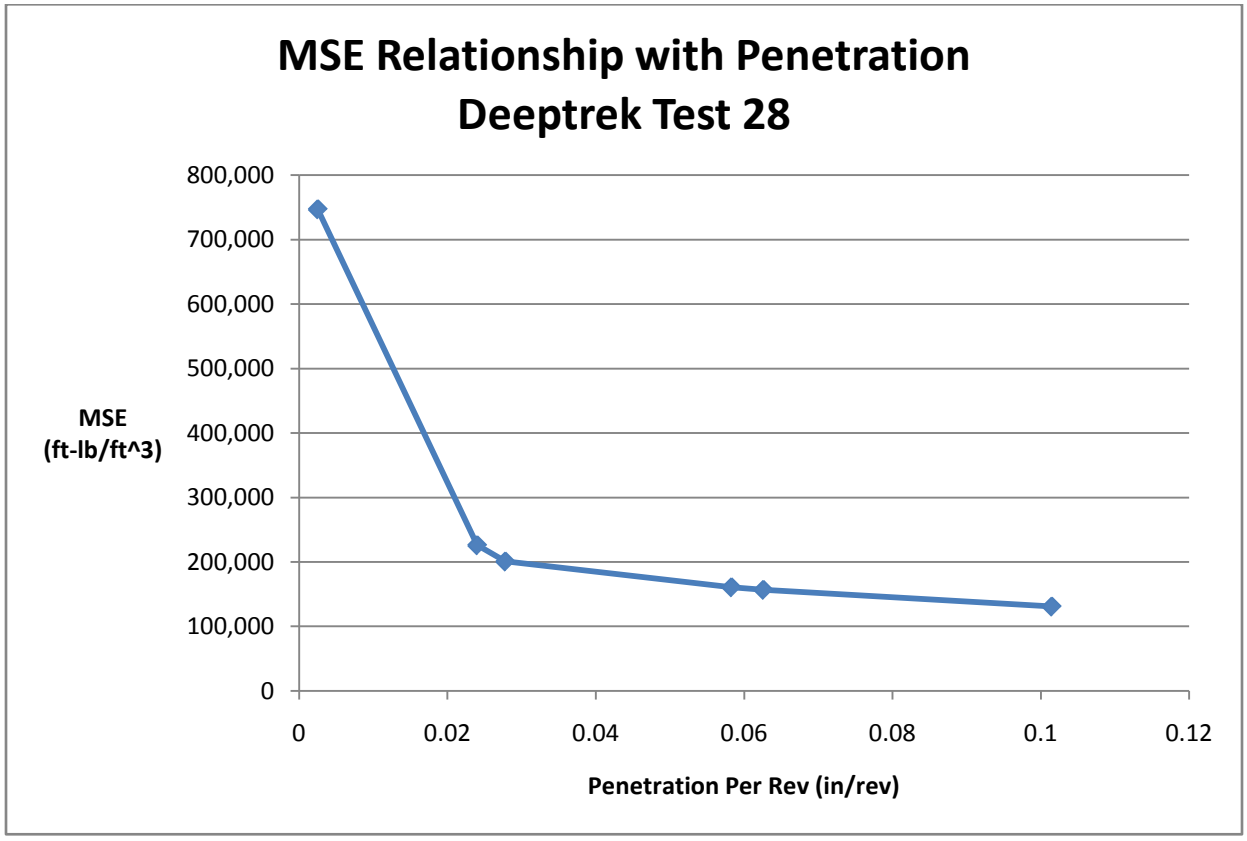

Figure 1 MSE Decreases with Increasing Penetration Rate to A Steady State [28]

This L or U-shaped response of MSE is due to the mechanics of cutting, and is directly related to depth of cut. Small depth of cut is associated with grinding and high friction forces, resulting in high MSE and low Rate of Penetration. Much energy is expended in grinding detritus that has already been separated from the parent. As depth of cut increases, cutting behavior changes from scraping and grinding to fracture and breakage of rock. Higher depth of cut causes chipping and breakage of material in larger pieces, with less reduction to smaller pieces through regrinding, resulting in lower MSE because of the more efficient volume removal.[5] This can be seen in Figure 2, where small depth of cut results in powdered detritus and large depth of cut results in fractures breaking away large chips.[34]

Figure 2 Comparison of Cutting Particle Size Between Small and Large Depth of Cut [34]

There is, however, a limitation to the decrease in MSE that can be achieved. As depth of cut increases further and the size of the chips that must be removed becomes large, and the energy required to break them away from the parent becomes very high. This high level of energy input results in an increase in MSE in very high penetration rates. Therefore as Teale understood, an optimum set of parameters with regard to MSE including Weight on Bit, Torque, RPM and Rate of Penetration, must exist for any given set of drilling conditions.

MSE Minimization Analysis

From the literature, MSE typically makes an L or U-shaped graph when plotted against Weight on Bit. This is due to the fact that Weight on Bit and Penetration per Revolution are related, and that relationship is non-linear. When seeking a minimum MSE, the point where this graph reaches a minimum indicates the optimum Weight on Bit for that particular set of drilling conditions

Theoretically one could simply choose the data point where the lowest MSE occurs and use the parameters that produced that point. However that may be misleading, and would put excessive reliance on a single data point, assuming that one data point fell near the actual minimum. This is especially true when working with the wide variability common in geologic materials. Also, data that covers such a wide range is seldom readily available. A better approach provides the minimum based on all of the available data, even if there are no points in close proximity to the actual minimum.

Assumptions

The Teale equation is difficult to minimize mathematically because it is a function of three parameters. This work recognizes that those parameters are inter-related, and makes assumptions about that relationship. The Teale equation is re-written as a function of one of those parameters so that a minimum might be found mathematically.

Assumption 1: The three parameters of Weight on Bit, Torque, and Rate of Penetration are related to one another, implying that MSE is a function of three interrelated, not independent, parameters. It is intuitive that increasing axial force on the bit results in increased penetration rate and increased torsional force. This important observation means that if the relationship can be established, MSE can be written in terms one parameter instead of three.

Assumption 2: The relationship between Weight on Bit and Torque can be described as linear within a normal processing range. This is well established in the literature, and appears in Teale's work. [5,6,9] The Deeptrek tests also indicate a linear relationship between Torque and Weight on Bit. One example can be seen in Figure 3. [28]

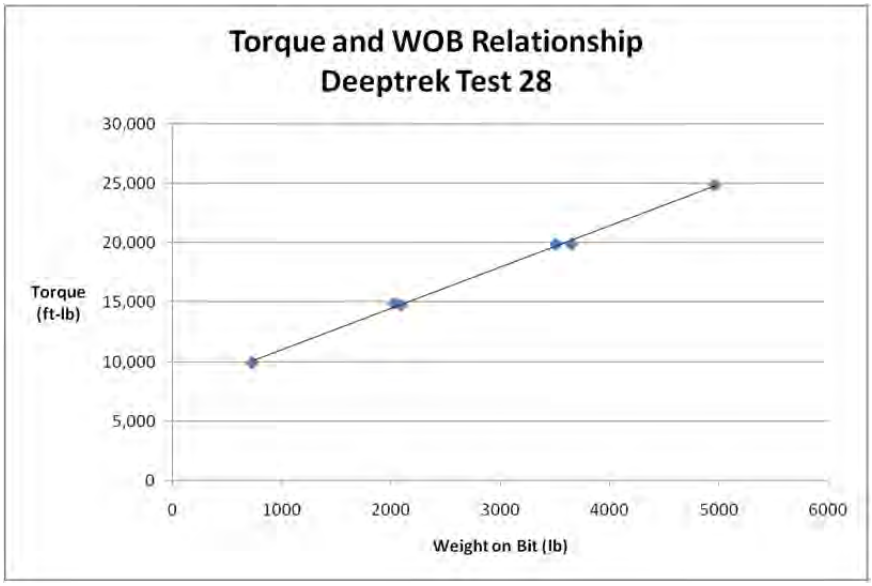

Figure 3 Deeptrek Example of Linear Relationship Between WOB and Torque. [28]

Under this assumption Torque can be written as a linear function of Weight on Bit

$$Torque = f(WOB) = A_0 + A_1 * WOB \quad (6)$$

The A coefficients have no direct physical meaning, but are influenced by the strength of the relationship. The slope of the line is affected by the response of Torque to the Weight on Bit force, and is subject to change that depends on drilling conditions. It is important to note that the linearity assumption is valid only in a range of reasonable processing. It would be expected

that at the condition where Weight on Bit is equal to zero, the Torque would also equal zero. This can be influenced by rock type, bit type and wear, hydrostatic pressure, fluids in use, and many other factors. The value of the coefficients is unique to a given set of drilling conditions.

Assumption 3: Penetration per Revolution can be represented as a second order polynomial function of Weight on Bit within a normal processing range. A non-linear relationship is established in the literature and in the Deeptrek Data, but the assumption of a quadratic function seems to be unique to this work. [5,6] The second order polynomial was selected based on curve fitting of data sets as they became available, as this was the best fit according to the determination coefficient (R^2) of all of the ten possible fits that were tested. An example from Deeptrek can be seen in Figure 4, with a second order polynomial curve fitted to the data. [28]

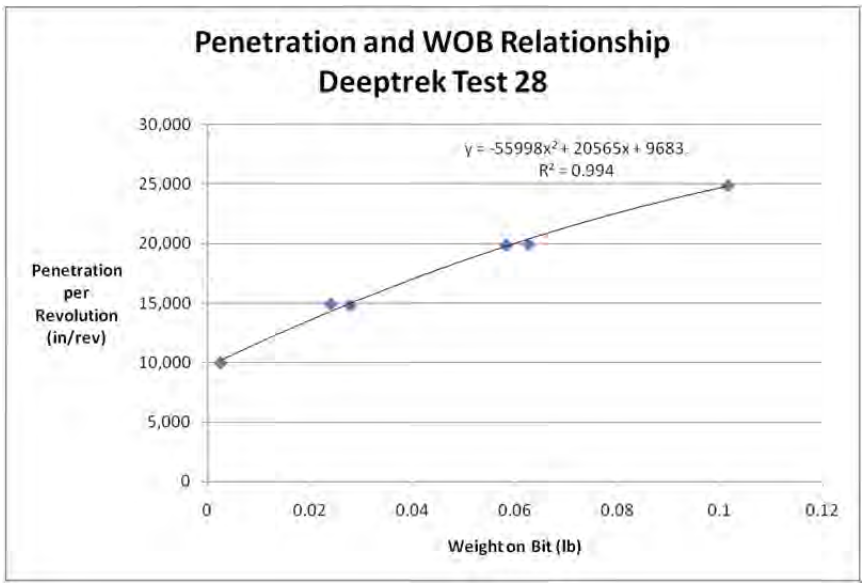

Figure 4 Deeptrek example of quadratic relationship between WOB and Penetration per Revolution. [28]

Under this assumption the Penetration per Revolution can be written as a quadratic function of Weight on Bit.

$$P = g(WOB) = B_2 * WOB^2 + B_1 * WOB + B_0 \quad (7)$$

As with the Torque equation the B parameters have no physical meaning, are valid only within a normal processing range, and the values are subject to a specific set of drilling conditions. It would be expected that if Weight on Bit is equal to zero, the Rate of Penetration would also be zero.

Assumption 4: Within a normal industrial operating range, RPM is limited primarily by factors not related to MSE. This implies that Penetration per Revolution governs MSE, and not

revolutions per time. This is borne out in Teale's MSE equation, as RPM only appears in it along with Penetration per Time. The time factor can be removed by using Penetration per Revolution. By definition the Rate of Penetration (ROP) can be divided by RPM to arrive at p (Penetration per Revolution).

$$P = \frac{ROP}{RPM} \tag{8}$$

Using this value, the MSE equation on a per revolution basis becomes

$$\mathrm{MSE} = \frac{\mathrm{WOB}}{\mathrm{Area}} + \frac{2\,\pi * \mathrm{Torque}}{\mathrm{Area} * \mathrm{P}} \tag{9}$$

From Equation 5 it can be seen that MSE is a function of Weight on Bit, Torque, RPM and Penetration per Minute. This can be reduced to three parameters, as seen in Equation 9, to Weight on Bit, Torque and Penetration per Revolution.

Transformation of MSE Equation

Using these assumptions the Teale MSE equation can be transformed into a function of only one parameter, that being Weight on Bit. Rewriting Equation 9, the MSE equation becomes

$$\mathrm{MSE} = \frac{\mathrm{WOB}}{\mathrm{Area}} + \frac{2\,\pi * \mathrm{f(WOB)}}{\mathrm{Area} * \mathrm{g(WOB)}} \tag{10}$$

$$\mathrm{MSE_H} = \frac{\mathrm{WOB}}{\mathrm{Area}} + \frac{2\,\pi * (\mathrm{A_0} + \mathrm{A_1} * \mathrm{WOB})}{\mathrm{Area} * (\mathrm{B_2} * \mathrm{WOB^2} + \mathrm{B_1} * \mathrm{WOB} + \mathrm{B_0})} \tag{11}$$

The most important aspect of this equation is that at a minimum value can be computed where the A and B coefficients are known. The minimum and maximum point(s) of a polynomial equation can be found where the first derivative is equal to zero. The first derivative of the Equation 11 is

$$\mathrm{MSE_H}' = \frac{1}{\mathrm{Area}} + \frac{2\,\pi * \mathrm{A_1}}{\mathrm{Area} * (\mathrm{B_2} * \mathrm{WOB^2} + \mathrm{B_1} * \mathrm{WOB} + \mathrm{B_0})} - \frac{2\,\pi * (\mathrm{A_0} + \mathrm{A_1} * \mathrm{WOB})(2\mathrm{B_2} * \mathrm{WOB} + \mathrm{B_1})}{\mathrm{Area} * (\mathrm{B_2} * \mathrm{WOB^2} + \mathrm{B_1} * \mathrm{WOB} + \mathrm{B_0})^2} \tag{12}$$

When MSE_H' is set equal to zero and simplified algebraically, the minimums and maximums can be found at the roots of Equation 13.

$$\begin{aligned} 0 = {} & B_2 * WOB^4 + 2B_1B_2 * WOB^3 + (B_1{}^2 + 2B_2B_0 \\ & - 2\pi A_1B_2) * WOB^2 \\ & + (2B_1B_0 - 4\pi A_0B_2) * WOB \\ & + (B_0{}^2 + 2A_1B_0 - 2\pi A_0B_1) \end{aligned} \tag{13}$$

A fourth order polynomial has four roots. In practical applications of the types of graphs seen in drilling, this equation typically has one positive real root, one negative real root, and a pair of complex conjugates. Only the positive real root has physical meaning, which corresponds to the optimum Weight on Bit (WOB_{opt}) at the minimum MSE.

The optimum Weight on Bit (WOB_{opt}) found at the positive real root of Equation 13 can be used in the Torque and Penetration per Revolution Equations 6 and 7 to compute the optimum values of those parameters.

$$Torque_{opt} = f(WOB_{opt}) = A_0 + A_1 * WOB_{opt} \tag{14}$$

$$P_{opt} = g(WOB) = B_2 * WOB_{opt}{}^2 + B_1 * WOB_{opt} + B_0 \tag{15}$$

5. Stiletto Experimental Apparatus and Instrumentation

In order to prove the MSE_H theory, experimental analysis was completed. This study evaluated two different rock types subjected to four sets of drilling conditions, creating eight unique data sets. An apparatus, nicknamed "Stiletto," was designed and constructed that could hold rock samples and drill them at specified penetration rates and RPM settings while measuring Weight on Bit and Torque. These parameters were measured at 30 or more data points per data set. The apparatus and instrumentation used for the experiments is summarized here, while a detailed description including calibration appears in Appendix A.

Machinery

Testing the theory required drilling under a wide range of controlled conditions, so a drill press with a wide range of penetration per revolution and RPM settings was selected. A press like the one in Figure 5 was generously made available by Northco Corporation of Morgantown, WV. This is a large radial drill press with a wide range of RPM and Penetration per Revolution settings. The RPM and Penetration per Revolution settings were calibrated to ensure accuracy.

Figure 5 Radial Drill Press Like the One Used in This Experiment

Fixturing

A rock holding fixture was designed and built to hold the samples and the load cells, as can be seen in Figure 6. The drill fixture used a three-jaw chuck as a sample holder. A load cell for measuring Weight on Bit (axial force) was located below the sample holder. A thrust bearing was also located below the sample holder so that the torque arm could rotate freely with minimal friction. A load cell used for measuring torque was located at the tip of the torque arm.

Figure 6 Rock Holding Fixture with Integrated WOB and Torque Load Cells

Data Acquisition

The data acquisition system was comprised of two main parts; the sensor suite and the software.

Load cells were used to measure Weight on Bit and Torque, and a fiber-optic sensor was used to measure RPM. The sensor readers, power supply, voltage divider, and data acquisition board were mounted to a custom-built mounting board, which appears in Figure 7.

Figure 7 Sensor Suite Mounting Board

National Instrument's LabVIEW programming software was used to control the data acquisition device and for data collection. The software was capable of capturing data from all three sensors and storing it for later retrieval. Screen shots of the front and back panels can be seen in Figure 8.

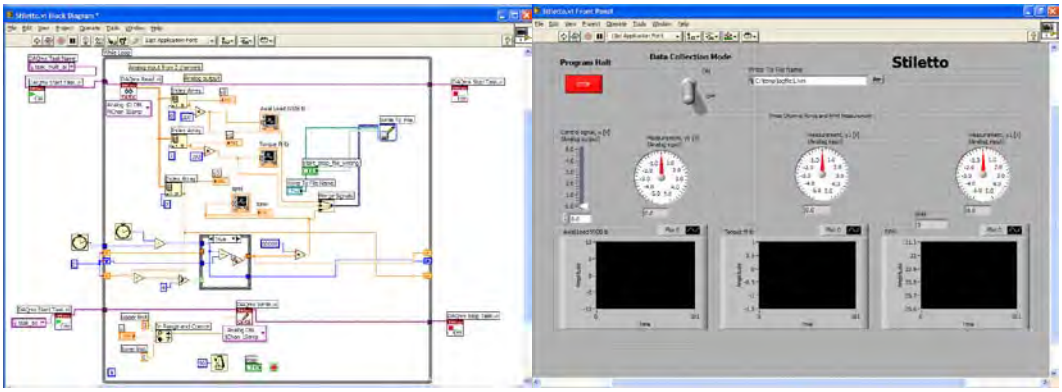

Figure 8 LabVIEW Program Used for Data Collection. Back Panel Left, Front Panel Right.

6. Drilling Experiments

Sample Preparation

All samples were prepared first by coring 2 inch diameter samples from parent slabs. This was accomplished using a diamond embedded coring bit, with water used for cooling and detritus flushing. Samples longer than 4 inches in length were cut into 4 inch segments using a diamond wet saw, while some shorter segments were used because of breakage of the cores. These operations may be seen in Figure 9. In each case samples were numbered using a standard numbering system which described everything about the sample within its numbering and lettering scheme. The numbering system was: 'XX (rock type)'## (slab number)'X# (diameter)'H# (hole number)'X (portion of sample). So for example CM23D2H4A would be a Carthage Marble sample, slab number 23, Diameter 2-inch, Hole 4, segment A. The two types of rocks used for this experiment were Carthage Marble (CM) and Terretek Sandstone (TS). Segments were lettered starting at the top of the slab.

Figure 9 Rock Coring from Parent Slabs and Cutting Segments With Wet Saw

In order to ensure that samples would fit squarely and vertically in the sample holder of the drill fixture, both ends of all of the samples were faced in a lathe using a carbide tipped lathe tool. While clamped in the lathe, centering holes were also created in the samples using a ½ inch masonry drill bit as a centering bit. This ensured that the drill bit would seek the center of the sample when drilling began in the fixture. The turning portions of sample preparation may be seen in Figure 10.

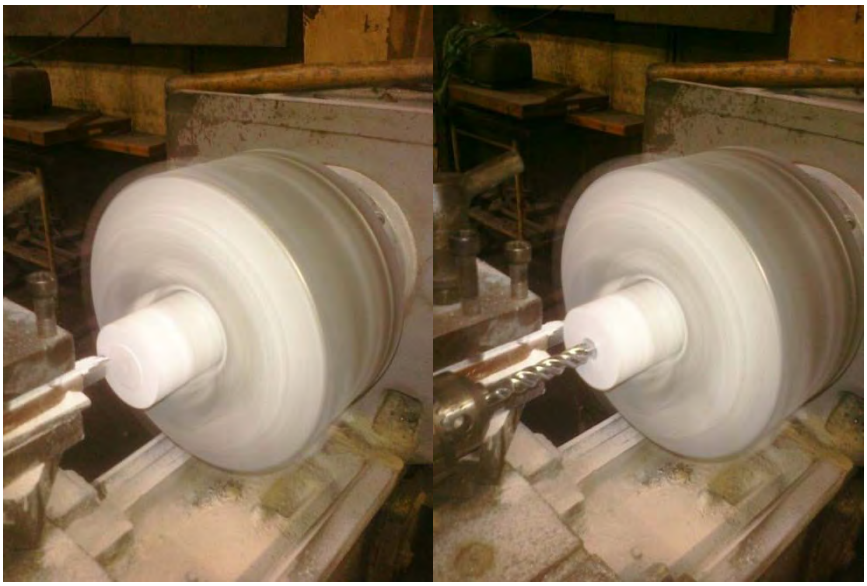

Figure 10 Left: Facing the End of the Sample. Right: Centering

For ambient samples and for those subjected to confining pressure only, no additional sample preparation was necessary. For heated rocks, samples were next placed in an oven set at 450 F and soaked at that temperature for a minimum of 2 hours.

Experiments and Methodology

Drilling was all conducted on the same drill press with the same fixture. An example from one of the experiments can be seen in Figure 11.

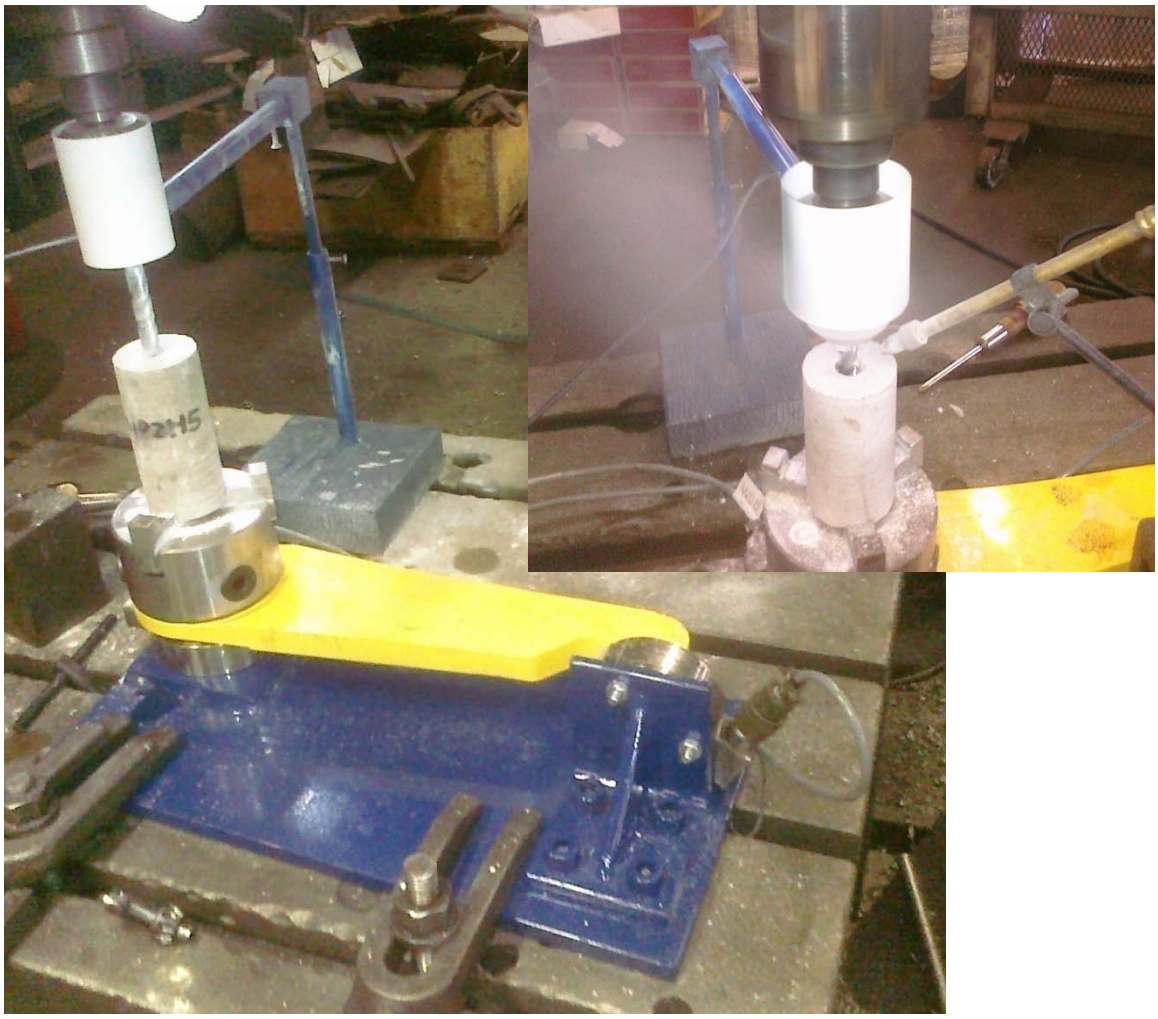

Figure 11 Drilling Apparatus Conducting Drilling Experiment. Inset: Close Up of Drilling

An air nozzle was placed above the sample, directing compressed air at the top of the hole to blow detritus out of the hole and clear the flutes of the bit. Trials were conducted at the outset of testing proving that this was adequate for detritus clearing of the flutes. Trials showed that drilling forces were the same either with or without air clearing so long as detritus cleared. If the flutes of the bit clogged with detritus, drilling forces were not at steady state, and a gradual increase in drilling forces resulted. Air clearing did not affect forces but did ensure consistent clearing for steady state of drilling forces. For this reason an air nozzle was used to clear detritus on all tests. In all cases except the increased confining pressure tests, samples were clamped in the sample holder and checked that it was plumb. If necessary the hole was made deeper so that the bit was fully engaged in the rock before data was collected.

Once the apparatus was set up and tested to ensure that signals were being properly received by the software, testing was initiated. The data collection window in the software allowed data

to be collected without restarting the program between tests. A file name was selected that was meaningful to the data being collected. The software was designed so that when data collection switch was engaged, a file with that name was created automatically and data was saved until the data collection switch was disengaged.

The appropriate RPM and Penetration per Revolution were set on the drill press. The drill press quill was adjusted to just above the rock sample, and then the machine clutch was engaged. Data collection was initiated after the bit was fully engaged and had reached steady state. An attempt was made to record at least 30 revolutions of the bit for each test. After the time required to reach this number of revolutions had elapsed, the data collection switch in the software was disengaged, the machine clutch was disengaged, and the quill was immediately raised. The data collection system and machine were then readied for another data point.

During testing it was discovered that Carthage Marble had little tendency to dull the bits, but the Terretek Sandstone dulled them after drilling about four inches of rock. Bits were sharpened at four inch intervals when drilling Terretek Sandstone to ensure that a sharp bit was always used. Bits were re-sharpened no more than twice.

The bits used in this work, illustrated in Figure 12, can drill up to two inches in depth. Samples were reused until the two inch depth was reached, and then inverted so that the maximum amount of sample could be used. Samples were nearly always consumed completely. This ensured the most efficient use of sample material.

Figure 12 Drill Bits Used For All Experiments.
Inset Left: Standard Tip. Inset Right: Two Wing Bit

Heated Rock Variant

For the heated rock variant, samples were prepared as for the other experiments. They were then placed in a preheated oven at 450˚ F for a minimum of two hours. Samples were removed from the oven and immediately placed in the sample holder and drilled. All sample collection was completed within ten minutes of removal from the heat soak. It is assumed that they did not cool off enough to make a difference to the data.

Confining Pressure Variant

Elevated confining pressure was accomplished through the use of a Roctest Telemac Hoek Cell. All samples used were two inches in diameter and four inches long. The Hoek cell was designed for samples up to six inches long, so a spacer was required to fill the additional length. A requirement was that neither the Hoek cell nor the Stiletto apparatus be modified, which necessitated an adapter. For this purpose a custom made spacer was created that was 2 inches in diameter and 2 3/4 inches long. The additional length allowed the spacer to protrude from the bottom of the Hoek Cell, which was mounted in the sample holder and clamped securely. This put the top of the sample to be drilled at the top of the Hoek cell. When pressurized, the Hoek cell squeezed both the rock sample and the spacer, securely holding it to the fixture. The setup can be seen in Figure 13.

Figure 13 Hoek Cell Mounted in the Stiletto Apparatus. A Spacer Was Clamped in the Sample Holder, and the Hoek Cell Squeezed Both the Spacer and the Rock

Care was taken that the hydraulic pressurizing hose was on the same line of action with the torque arm. This ensured that the hose did not pull on the torque arm and influence the torque reading. For all experiments pressure was checked just prior to data collection to ensure that the cell was at the correct pressure for the drill test. For all experiments, care was taken to ensure that the hole was deep enough in the sample that the rock was subjected to the confining pressure and not too close to the surface to be out of the influence of the pressure. Use of a Hoek cell to induce confining pressure for drilling cannot be found in literature, and is believed to be unique to this work.

7. Experimental Results

Samples of two types of rock were each subjected to four identical treatments, making a total of eight complete data sets. The rock types were Carthage Marble and Terretek Sandstone. These were selected in order to replicate the rock types from the Deeptrek study, the material properties of which can be found in Table 1.

Table 1 Basic Rock Properties of Rock Samples[28]

Rock/Attribute Property	Carthage Marble	Terretek Sandstone
Bulk density	2.65 g/cm3	2.47 g/cm3
Unconfined compressive strength	16,000 psi	19,000 psi
Porosity	1.40%	7.00%
Permeability	0.002 millidarcy	0.1 millidarcy

The four treatments were:

A) Ambient temperature and pressure

B) Elevated temperature to 450 F, ambient pressure

C) Elevated Confining Pressure to 1500 psi, ambient temperature

D) Ambient temperature and pressure drilled with a 2-wing bit.

The apparatus had inputs of RPM and Penetration per Revolution and outputs of Weight on Bit and Torque. Set point ranges for RPM were based on settings used in the Deeptrek study, which had a median of 90. Penetration per Revolution was set low at the outset of each test and increased incrementally until laboratory computations of MSE found that it had increased or reached a plateau. An effort was made to complete 30 revolutions of the bit where possible.

Data Reduction and Processing

Data Reduction was conducted by first importing the raw data into a spreadsheet. Points not intended as part of the data collection were trimmed, and the data was inspected to ensure that steady state conditions were reached. This was done by plotting Weight on Bit and Torque over time and adding linear trend lines to each plot. The slope of the trend lines was inspected to ensure that it was near zero, indicating steady state. Reported values were averages taken over the entire time interval. All of the spreadsheet data is made available in electronic form in Appendix C.

Results Analysis

For each variant a set of some 30 data points were generated. Regressions of the data were used to compute the A and B coefficients from Equations 6 and 7 repeated here.

$$Torque = f(WOB) = A_0 + A_1 * WOB \tag{16}$$

$$P = g(WOB) = B_2 * WOB^2 + B_1 * WOB + B_0 \tag{17}$$

These coefficients were also used in the MSE and MSE' equations.

$$\mathrm{MSE_H} = \frac{\mathrm{WOB}}{\mathrm{Area}} + \frac{2\,\pi * (\mathrm{A_0} + \mathrm{A_1} * \mathrm{WOB})}{\mathrm{Area} * (\mathrm{B_2} * \mathrm{WOB}^2 + \mathrm{B_1} * \mathrm{WOB} + \mathrm{B_0})} \tag{18}$$

$$\begin{aligned} 0 = {} & \mathrm{B_2} * \mathrm{WOB}^4 + 2\mathrm{B_1B_2} * \mathrm{WOB}^3 + (\mathrm{B_1}^2 + 2\mathrm{B_2B_0} \\ & - 2\pi\mathrm{A_1B_2}) * \mathrm{WOB}^2 \\ & + (2\mathrm{B_1B_0} - 4\pi\mathrm{A_0B_2}) * \mathrm{WOB} \\ & + (\mathrm{B_0}^2 + 2\mathrm{A_1B_0} - 2\pi\mathrm{A_0B_1}) \end{aligned} \tag{19}$$

In each case the fourth order polynomial of MSE' was found to have only one positive real root. This corresponded to the optimum Weight on Bit for that data set, and was used to compute the optimum MSE, Torque, and Penetration per Revolution from the equations above.

In order to further substantiate the validity of the proposed MSE analysis in this work, published data from the work of others was also analyzed. One of the primary reasons for generating the experimental data for this work was that little such published data is available. Determination of optimal conditions was not part of the scope of the Deeptrek study, but several experiments did have the necessary and sufficient data, and three of them were analyzed. One data set from a completely different source was also analyzed.

Details of computations for each of the twelve variants are found in Appendix B.

Table 2 contains a summary of all of the optimum parameters from both the experimental tests conducted for this work and those from published sources.

Table 2 Summary of Optimum Conditions for All Experiments

						Optimum Values			
Test	Rock Type	UCS (ksi)	Bit Type	Bit Size (in)	Drill Fluid Base	Penetr. (in/rev)	WOB (lb)	Torque (in-lb)	MSE (ksi)
CM Amb	Marble	16	Masonry	1/2	None	0.040	434	45.5	38.2
CM Hot	Marble	16	Masonry	1/2	None	0.051	455	42.7	29.0
CM Hoek	Marble	16	Masonry	1/2	None	0.028	218	27.3	32.7
CM 2 Wing	Marble	16	Masonry	1/2	None	0.017	248	64.7	123
TS Amb	Sandstone	19	Masonry	1/2	None	0.016	361	55.7	110
TS Hot	Sandstone	19	Masonry	1/2	None	0.016	329	53.1	106
TS Hoek	Sandstone	19	Masonry	1/2	None	0.018	312	53.4	97.8
TS 2 Wing	Sandstone	19	Masonry	1/2	None	0.015	265	56.6	129
Deep 5	Marble	16	PDC	6	Water	0.044	18,600	9,150	94.6
Deep 3	Sandstone	19	Roller Cone	6	Water	0.011	27,900	8,070	163
Deep 17	Shale	9.8	Impregnated	6	Oil	0.014	28,900	19,800	324
Hamade	Basalt	34.8	Coring	1.5 x 1	None	0.002	66	31	131

In order to investigate the scalability of the improved method, the axial pressure (WOB/Area) was also investigated. Table 3 shows the axial pressure in psi for all tests at the computed optimum conditions.

Table 3 Axial Pressure at Optimum Conditions for All Tests

Carthage Marble					Terretek Sandstone					Shale	Basalt
Ambient	Heated	Pressure	2 Wing	Deep 5	Ambient	Heated	Pressure	2 Wing	Deep 3	Deep 17	Hamade
2210	232	1110	1270	324	1840	1670	1590	1350	985	1020	67

Ambient Standard Bit Results

The optimum Rate of Penetration is much higher for Marble than Sandstone under ambient conditions. This is reasonable given the differences in their respective UCS values. The softer material is considered easier to drill, so the optimum penetration is expected to be higher at lower Weight on Bit and Torque and lower MSE.

Elevated Temperature Results

Increased temperature is expected to make each type of rock easier to drill relative to ambient, and that is observed in the data. The optimum Rate of Penetration for Marble is higher than for ambient with only a modest increase in Weight on Bit. For Sandstone the Rate of Penetration is the same, but at a lower Weight on Bit and Torque. The MSE is lower for heated rock as compared with ambient temperature in both materials.

A further comparison of heated rocks is of interest. Table 4 shows a comparison of drilling forces between ambient and heated Carthage Marble pulled from the data. The Weight on Bit and Torque were each reduced by about 30% by heating.

Table 4 Comparison of Drilling Forces Between Ambient and Heated Samples in Marble

		Ambient Marble		Heated Marble	
RPM	in/Rev	WOB (lb)	Torque (in-lb)	WOB (lb)	Torque (in-lb)
21	0.018	214	30.5	104	22.2
21	0.047	762	61.5	486	50.0
43	0.008	104	20.0	67.5	14.4
43	0.018	216	33.2	128	24.5
43	0.033	480	61.2	378	38.5
133	0.018	192	30.0	118	12.6
133	0.033	382	38.4	364	26.0
Average		336	39.2	235	26.9

Table 5 shows similar data for Terretek Sandstone. In that case Weight on Bit was reduced by 26% and Torque by 20%.

Table 5 Comparison of Drilling Forces Between Ambient and Heated Samples in Sandstone

		Ambient Sandstone		Heated Sandstone	
RPM	in/Rev	WOB (lb)	Torque (in-lb)	WOB (lb)	Torque (in-lb)
21	0.005	221	34.2	94	34.3
21	0.008	246	37.9	152	33.5
21	0.01	270	40.3	193	38.0
21	0.012	391	54.4	256	50.9
21	0.018	386	56.5	264	49.1
21	0.021	452	66.3	273	54.0
86	0.005	179	36.5	112	16.5
86	0.008	206	39.8	142	18.5
86	0.010	213	39.5	188	23.1
86	0.012	309	55.1	270	35.6
86	0.018	338	57.4	282	37.7
100	0.005	137	22.8	109	25.3
100	0.008	159	25.3	151	27.3
100	0.010	192	29.0	182	30.3
100	0.012	283	45.3	235	38.2
100	0.018	304	51.1	262	41.2
Average		268	43.2	198	34.6

Elevated Confining Pressure Results

In the results of samples subjected to elevated confining pressure, the optimum Rate of Penetration for Marble is considerably lower than for ambient, but the drilling forces and MSE are also lower. In Sandstone the optimum Rate of Penetration is slightly higher, but the drilling forces and MSE are lower than for ambient. These results indicate that elevating the confining pressure makes drilling easier. This is the result of induced stress in the radial direction, making it require less work to promote failure.

Two Wing Bit Results

In the results of drilling Marble with the two-wing bit the Rate of Penetration is much lower when compared with the standard bit. The Weight on Bit is also lower, but the Torque is higher. For Sandstone the Rate of Penetration is only slightly lower, but again the Weight on Bit it is lower and the Torque is higher when compared with the standard bit.

The higher Torque is likely due to the bit design. In the standard masonry bit all of the material is removed by cutting, except that in the center, which is ground under the point of the bit. In contrast the two-wing bit leaves a column of un-drilled rock 0.080 inch in diameter in the center which must be removed in order for the bit to advance. It is likely that it is twisted off and not ground away, as the Weight on Bit is lower and the Torque is higher when compared with the standard bit. Because Torque is higher, MSE is higher in both cases, particularly Marble.

Results Summary

Eight versions of drilling were conducted for this work, with more extensive and thorough data collection than can be found elsewhere in the literature. Four complete sets of corroborative data from published sources were also analyzed, each of which was generated under completely different conditions. These include PDC, impregnated, and roller cone bits in diameters from 6 inch drilling bits to 1 ½ inch coring bits, drilling with and without fluids, and four different types of rock.

In all cases optimum values of Weight on Bit, Torque and Penetration per Revolution were computed. The optimum values of Torque and Penetration per Revolution were computed based on assumptions about the nature of the inter-relationship that those parameters share with Weight on Bit. The improved equation creates a method for computing these optimum parameters that is not possible with conventional methods.

8. Results of RPM Analysis

It is generally expected that at a given rate of Penetration per Revolution, Weight on Bit will increase as RPM increases. The families of graphs of Weight on Bit by RPM in Figure 14 and Figure 15 show that the trends are generally flat or slightly upward, as expected. This illustrates that for a constant Penetration per Revolution there is a weak connection between Weight on Bit and RPM.

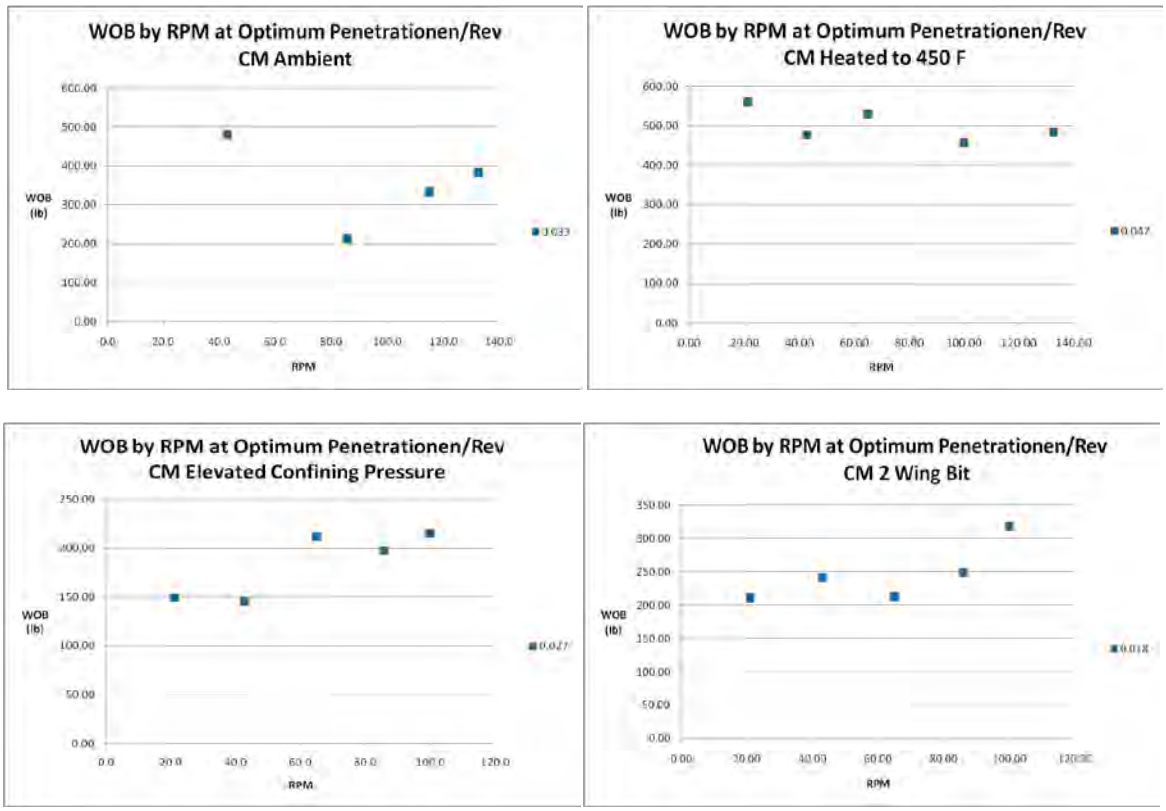

Figure 14 Family of RPM to Weight on Bit Relationships at Optimum Penetration per Revolution for Carthage Marble Experiments

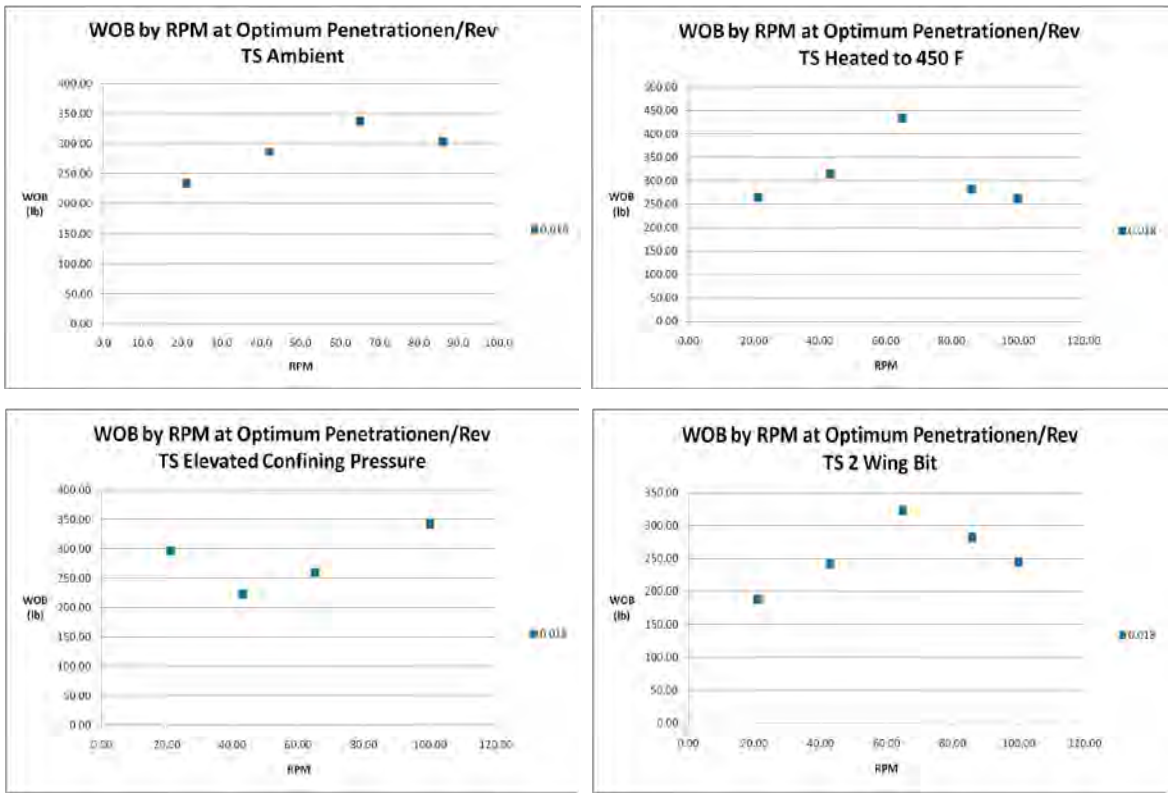

Figure 15 Family of RPM to Weight on Bit Relationships at Optimum Penetration per Revolution for Terretek Sandstone Experiments

As seen in the Results sections of this work, plots of MSE against Weight on Bit, Torque, and Penetration per Revolution indicate a U- or L- shaped graphs, suggesting that an optimum exists for each that produces a minimum value of MSE. If an optimum RPM could be determined by finding a minimum MSE, then a U- or L- shaped graph of MSE plotted as a function of RPM would be expected. Such graphs are presented in Figure 16 for Carthage Marble and Figure 17 for Terretek Sandstone. Such a U-shaped graph could possibly be described in only three of the plots using the Teale equation, and none of the plots using the improved equation, indicating that such a correlation is weak or non-existent.

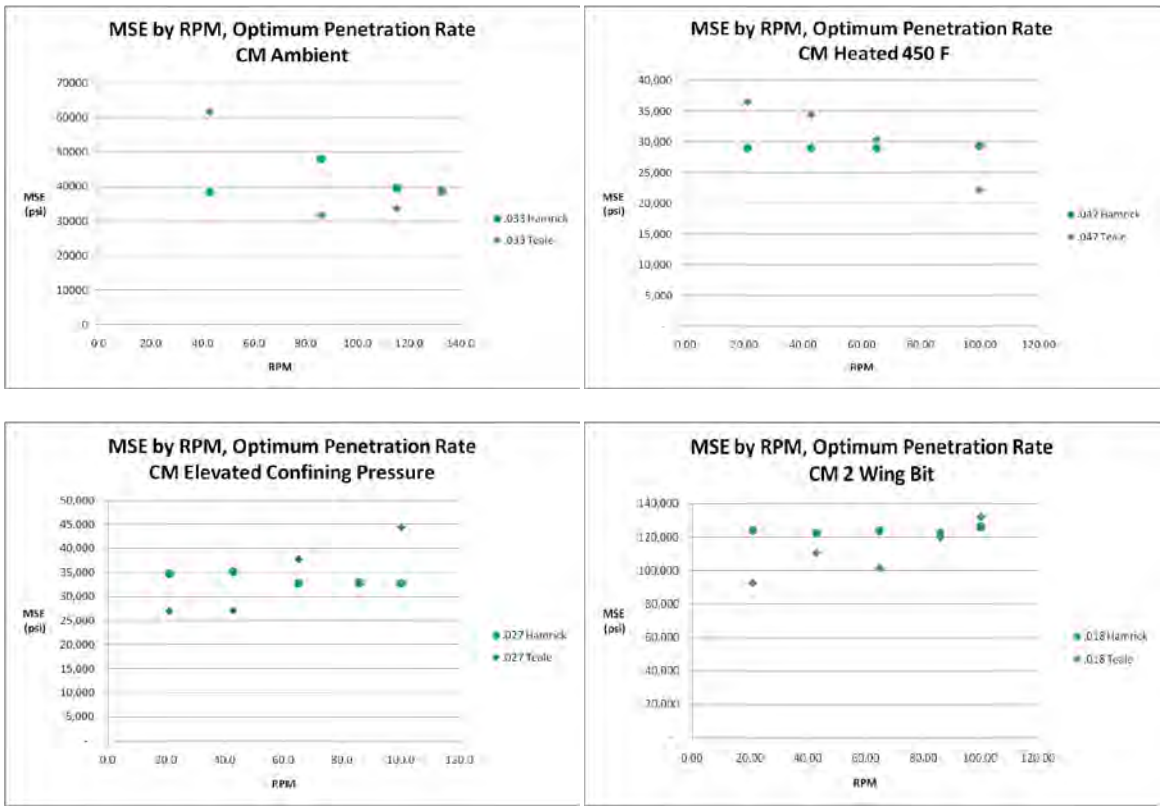

Figure 16 Family of MSE to RPM Relationships at Optimum Penetration per Revolution for Carthage Marble Experiments Computed Using Both MSE Equations

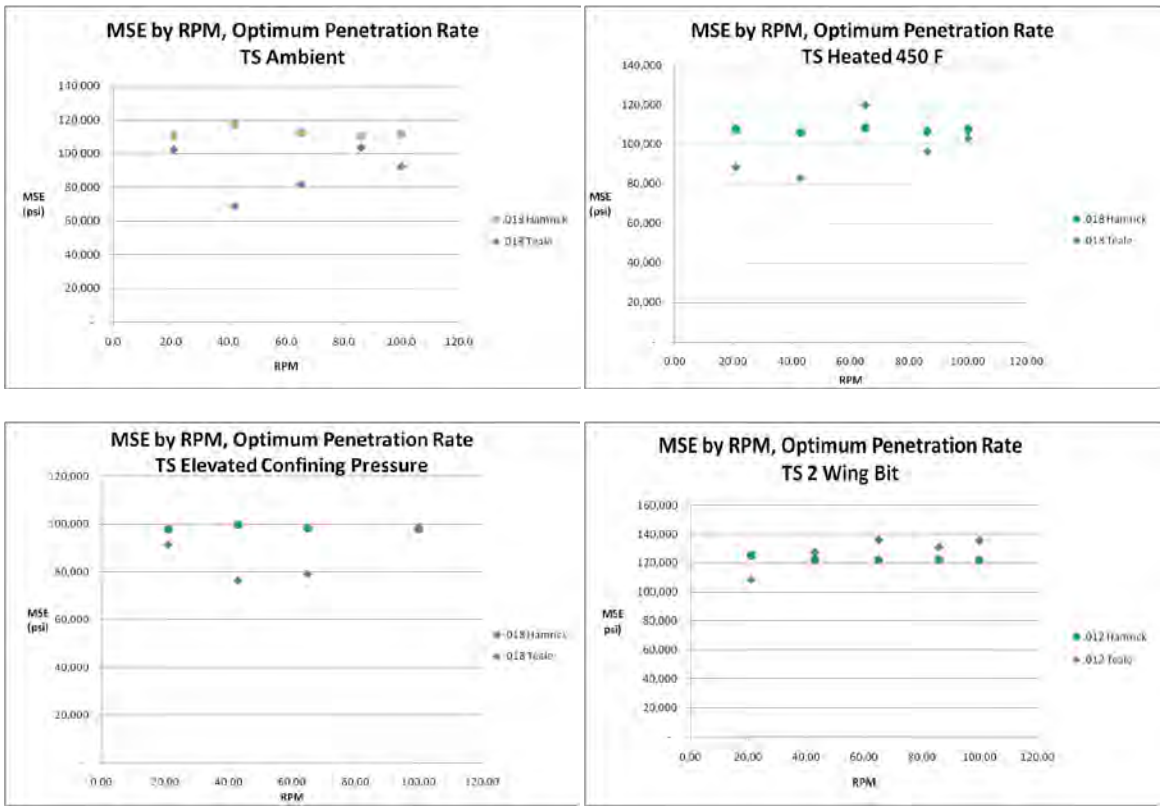

Figure 17Family of MSE to RPM Relationships at Optimum Penetration per Revolution for Terretek Sandstone Experiments Computed Using Both MSE Equations

From the literature it is known that cutters tend to consume more energy in their first pass than they do in subsequent passes. This is due to damage ahead of the bit, which weakens the rock. Weight on Bit influences damage ahead of the bit more than rotation speed, and thus Weight on Bit is a greater influence on MSE.[8, 25, 26]

Micrographs of the region in front of the bit demonstrate this principle. Specimens of both rock types were drilled at high and low RPM and high and low Penetration per Revolution. These were then filled with a two-part epoxy using a contrasting dye in order to better see the rock. A common ink was used as the dye, but was applied to the epoxy for the first time for this project after some experimentation. The specimens were then sectioned so that the hole was cut vertically perpendicular to the cross section, thus exposing the sides and bottom of the drilled rock. Micrographs were taken at an area below the bit along the cutting surface, as indicated in Figure 18. Such micrographs do not appear in the drilling literature, and appear to be unique to this work.

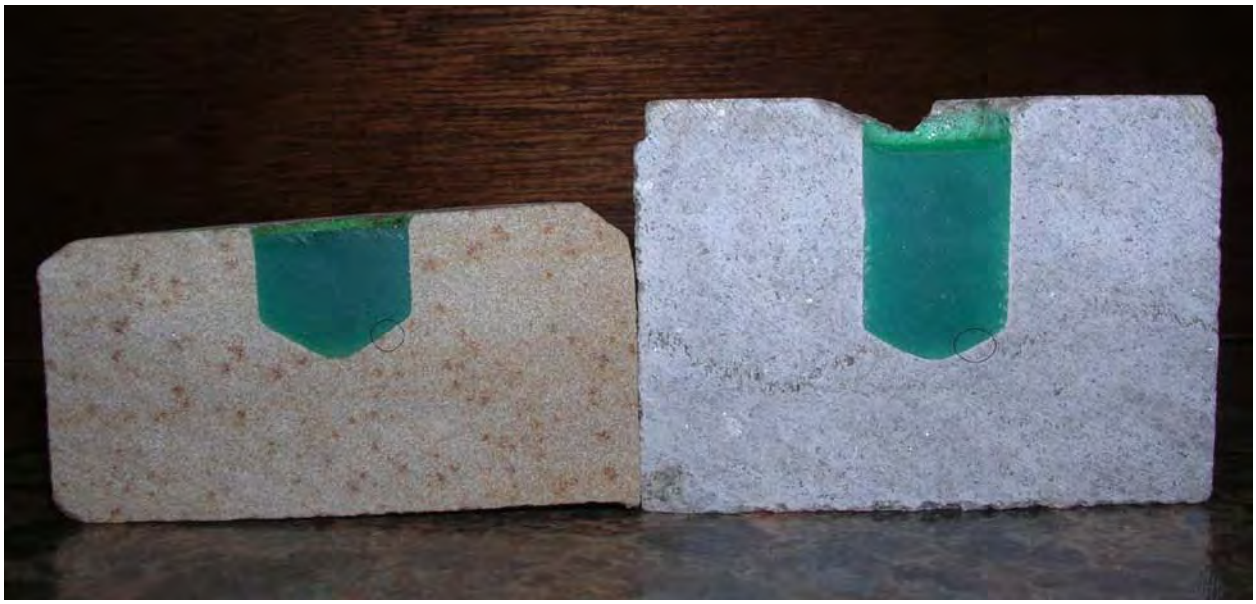

Figure 18 Typical Sectioned Specimens Used for Micrographs, With Area Examined Indicated. Terretek Sandstone Left, Carthage Marble Right. The Stylolite in the Marble is not a Crack.

In Figure 19 the top photo shows sandstone drilled at 43 RPM and 0.018 in/rev, while the bottom shows sandstone drilled at the same penetration per revolution and a much higher RPM of 100. Despite the difference in RPM, the cracking is nearly the same. In both cases cracks run parallel to the surface of the cut edge, and crushing is apparent along the edge. Some rough surface can be seen where cracks have propagated into the uncut portion and removed material, or where grains have been crushed or plucked from the matrix. The opposite may be seen in Figure 20, which was drilled at the same high RPM of 100, but a low penetration of 0.003 in/rev. In that photo no cracks and little crushing of grains are visible.

Force measurements of these tests can be found in Table 6. There is a slight difference between forces measured when comparing high and low RPM. However the difference is significatly greater for the high and low Penetration per Revolution rate. High Weight on Bit accounts for damage ahead of the bit more than does high RPM.

Table 6 Weight on Bit and Torque Values for Terretek Sandstone Samples in Micrographs

RPM	in/Rev	WOB (lb)	Torque (in-lb)
42	0.018	234	38.0
100	0.003	79	14.6
100	0.018	303	51.1

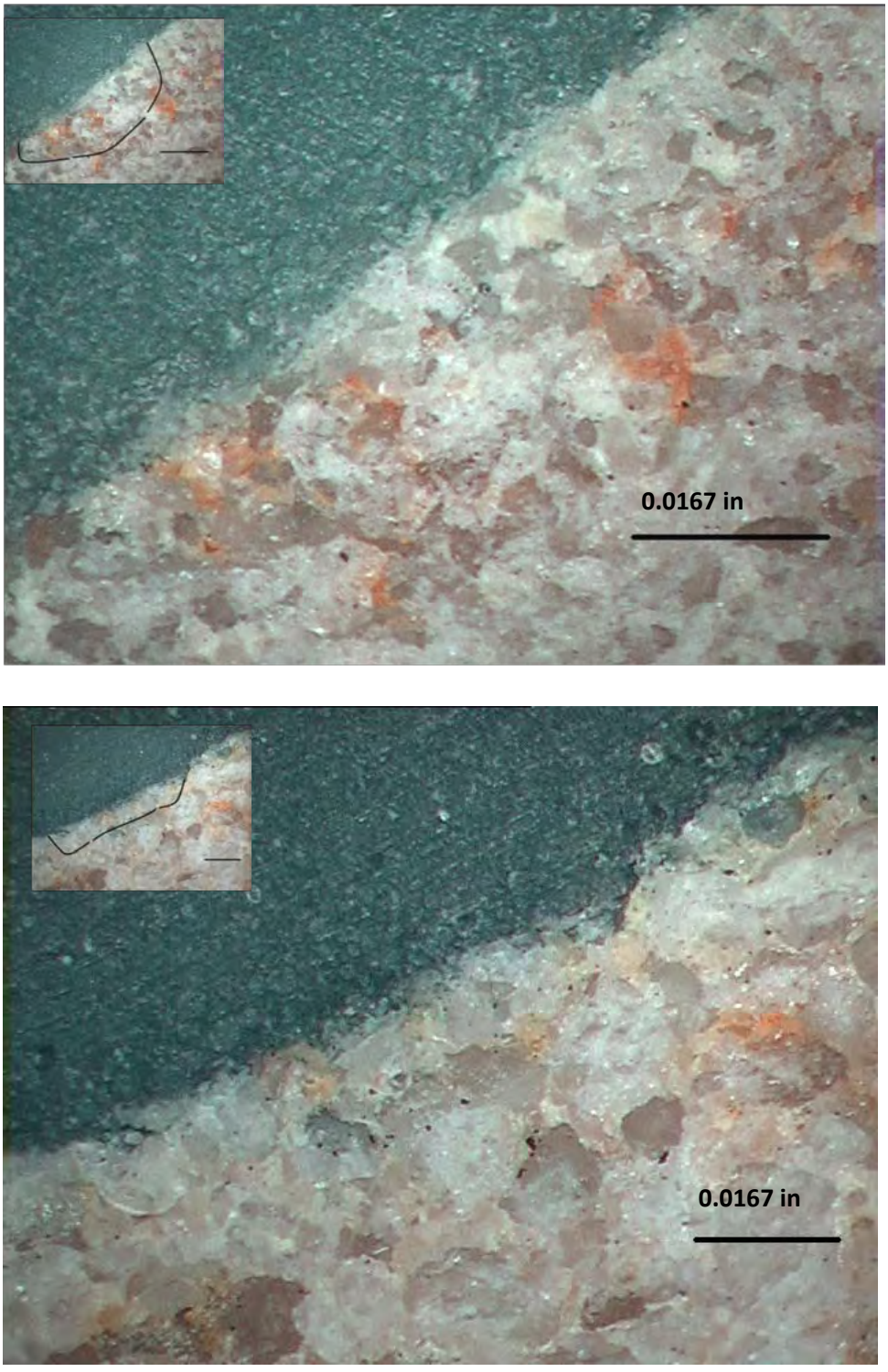

Figure 19 Micrographs of Ambient Sandstone Below Drill Bit. Top; 42 RPM and 0.018 in/rev, Bottom; 95 RPM and 0.003 in/rev. Insets denote approximate locations of cracks. Note the Similar Cracking and Rough Surface of the Two Having the Same Pentration Rate at High and Low RPM.

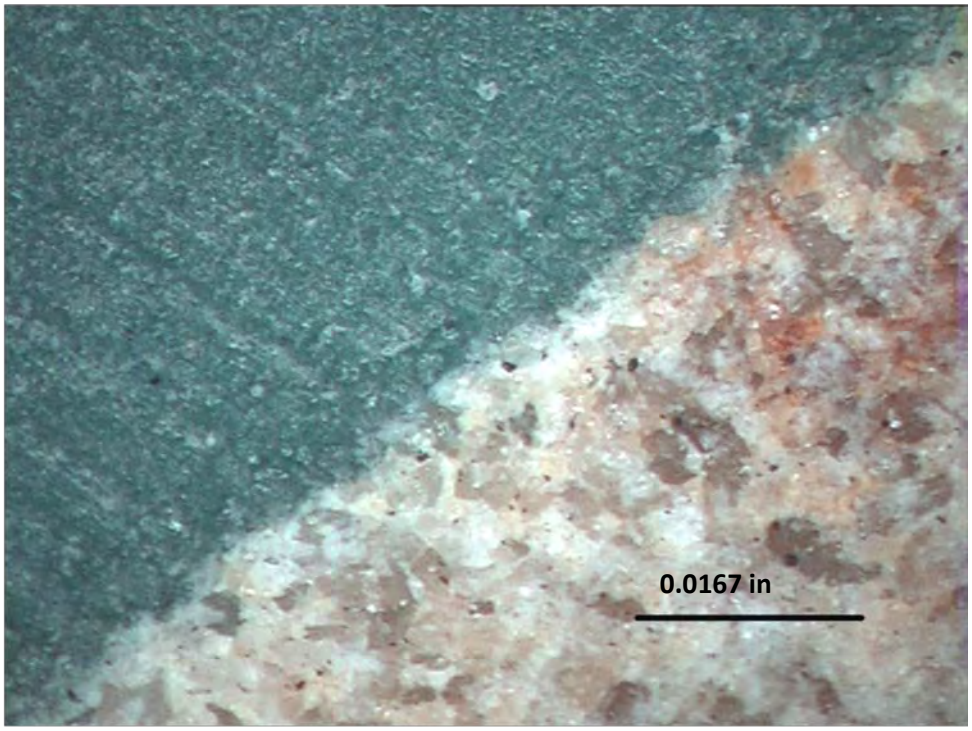

Figure 20 Micrograph of Ambient Terretek Sandstone Below Drill Bit at 100 RPM and 0.003 in/rev. Note the Smooth Surface and No Cracking at Low Penetration Per Revolution, Even at High RPM.

A similar argument can be made for Carthage Marble under similar conditions. Figure 21 shows two Marble specimens drilled at 0.033 in/rev penetration, with the top photo at 43 RPM and the bottom photo at 133 RPM. Despite the significant difference in RPM, very similar cracks can be seen in each specimen running parallel to the cut surface, with some surface roughness also visible. In Figure 22 the opposite can be seen. This was drilled at the high RPM of 133, and at a low penetration rate of 0.003 in/rev. In that photo no cracks can be found and the surface is smooth. The Weight on Bit and Torque values can be seen in Table 7, where much higher forces are generated by the higher penetration, resulting in more cracks ahead of the bit. While the lower forces of the low penetration rate result in no cracking.

Table 7 Weight on Bit and Torque Values for Carthage Marble Samples in Micrographs

RPM	in/Rev	WOB (lb)	Torque (in-lb)
43	0.033	480	61.2
133	0.003	57	14.6
133	0.033	382	38.4

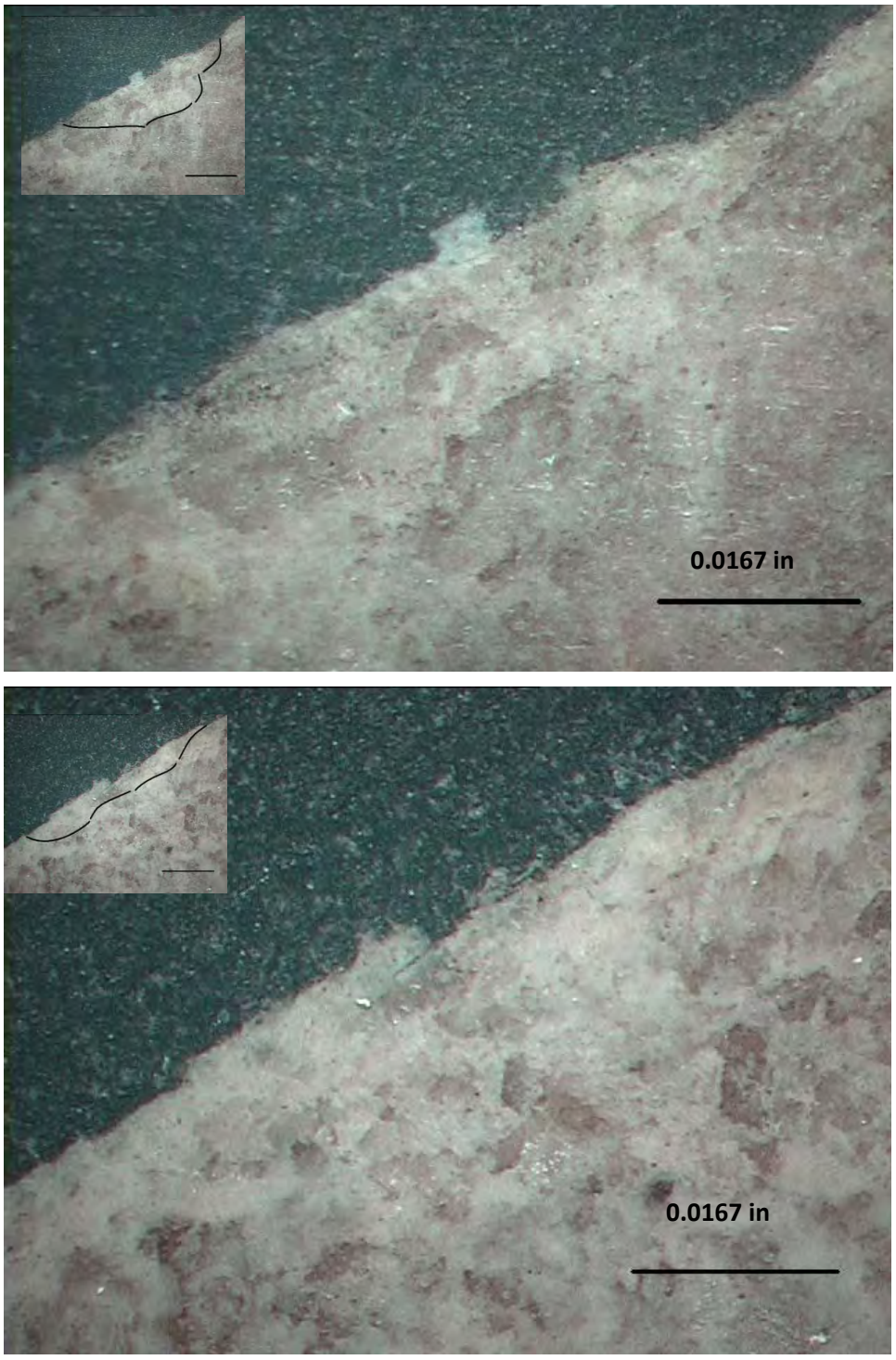

Figure 21 Micrographs of Ambient Marble Below Drill Bit. Top; 42 RPM and 0.033 in/rev, Bottom; 133 RPM and 0.033 in/rev. Insets denote approximate locations of cracks. Note the Similar Cracking and Rough Surface of the Two Having the Same Pentration Rate at High and Low RPM.

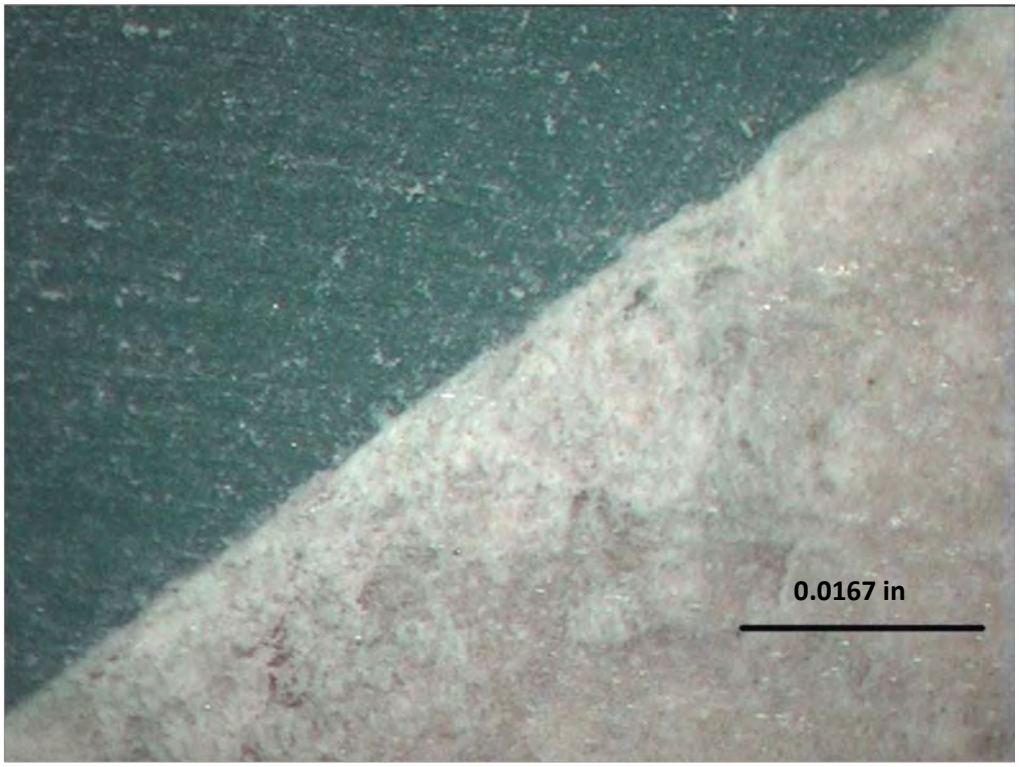

Figure 22 Micrograph of Ambient Marble Below Drill Bit at 133 RPM and 0.003 in/rev. Note the Smooth Surface and No Cracking at Low Penetration Per Revolution, Even at High RPM.

The fracture observations in these experiments indicate that RPM does not contribute significantly to MSE due to rock failure. By contrast, drillers find that RPM is a factor in MSE in field applications. The practice of the drill-off test is conducted by first varying the Weight on Bit until a minimum MSE is found, and then by varying the RPM until a new minimum is found.[15] Based on the cracking analysis in this work the RPM effect on MSE is not connected to the cutting of the rock by the bit. It has been shown that RPM has little effect on damage ahead of the bit, and little correlation to MSE in the data.

Industry found that only about 10% of limitations to rate of penetration are related to the bit.[17] The literature suggests that the correlation between RPM and Torque in field drilling is due to drill string vibration. It does not anticipate a correlation between RPM and Weight on Bit due to rock failure.[29, 30, 31, 32, 33] The experimental apparatus used in this work minimized drill string vibration in comparison with full scale field drilling rigs, so that effect is negligible in these data sets. With vibration minimized, the effect of RPM is more clearly seen as having little effect on rock failure. Another possible cause of increased MSE unrelated to cutting at high RPM is evacuation of detritus. Detritus removal is a function of bit and drill string design, and high RPM can overload the evacuation mechanism, resulting in regrinding of detritus and increased MSE.[14,24]

9. Conclusions

An improved method for computing Mechanical Specific Energy (MSE) was developed and validated. The improved method recognizes that the three parameters that are used to compute MSE are inter-related. Mathematical relationships between the parameters were assumed, and the conventional MSE equation was re-written in terms of one parameter, Weight on Bit. The roots of the first derivative of the re-written equation yielded the optimum Weight on Bit, which was used in the assumed mathematical relationships to determine the optimum Torque and Penetration per Revolution.

The method was validated through a more extensive experimentation than can be found elsewhere in the literature. It was also validated through its application to published data. The twelve validations spanned disparate drilling conditions including various rock types, bit types, bit sizes, temperatures, pressures, and use of fluids.

The method successfully computed optimum parameters for each data set. Any optimum point should be located at the minimum MSE. The optimum value computed for each parameter in each case fell at or near where the minimum MSE for that point was located. It is therefore a reasonably accurate method for computing optimum drilling parameters.

Through micro crack analysis it was shown that Weight on Bit is a greater contributor to damage ahead of the bit than RPM. This suggests that Weight on Bit governs MSE due to rock failure more than RPM.

This method is limited to computation only over the range of data collected, and cannot extrapolate beyond its span. It can find a minimum MSE only where a minimum exists. It is also limited to drilling due to the geometry assumed in the development.

10. Suggested Further Research

Additional research should bring the concept of MSE minimization to field drilling through the improved equation. Modern sophisticated drill rigs are already equipped with the measurement devices, but do not use MSE minimization in the manor described in this work. A simple algorithm can be written to determine the A and B parameters using linear regression, and the optimum Weight on Bit, Torque and Penetration per Revolution found using Equation 13.

The relationship between RPM and Torque, and thus between RPM and MSE, is not a function of rock breakage, but is instead related to drill string vibration, detritus removal, or other factors. Additional work should be conducted to measure and quantify these effects on Torque, RPM, Penetration Rates, and MSE in field drilling.

All testing done for this work was conducted at ambient hydrostatic pressure. Research suggests that increased hydrostatic pressure significantly changes apparent rock properties, so much of this work can be made more representative to field conditions by conducting similar tests at higher hydrostatic pressure and temperature, known as HPHT conditions.

All testing was done with drilling in rocks, but the method could apply to other types of machining in other materials. The method could be applied to feed and speed computations for machining and cutting of a variety materials. It can also be applied to excavation such as road headers, continuous miners, long-wall miners, and tunnel boring machines. This could result in improved efficiency in manufacturing a wide range of products and processes.

The effect of Weight on Bit with crack nucleation and expansion in rock has been little studied, and additional work in this area could be fruitful in creating a better understanding of that relationship, leading to improved bit designs and drilling methods.

A multivariate regression analysis of the data sets would determine which parameters were of greater influence and by how much. Such information would be valuable for drillers and researchers interested in improving efficiency.

Nomenclature

BHA – Bottom Hole Assembly
Bit – Collection of cutting elements
Cutter - Single cutting element
Detritus – Cuttings and material removed during drilling
HTHP – High Temperature, High Pressure
MSE - Mechanical Specific Energy
MSE_H – Mechanical Specific Energy as proposed in this work
P – Penetration pre Revolution
PDC - Poly-Crystalline Diamond (A type of cutter)
PDC Bit – A bit made up of multiple PDC cutters
ROP - Rate of Penetration
RPM - Revolutions per Minute
UCS – Unconfined Compressive Strength
WOB - Weight on Bit

Appendix A – Detail of Stiletto

Machinery

Testing the theory required drilling under a wide range of controlled conditions, so a drill press with a wide range of penetration per revolution and RPM settings was selected. A press like the one in Figure 23 was made available. This is an American Hole Wizard radial drill press, with 28 RPM settings and 16 Penetration per Revolution settings.

Figure 23 Radial Drill Press Like the One Used in This Experiment

In order to prove the accuracy of the RPM settings of the drill press, a hand held optical tachometer, Extech model number 461825, was used to test all of the settings in the low range of the machine. The hand held tachometer is an optical device that senses the pulse of a reflective tape applied a rotating object, and computes the pulses over time to display RPM.

First a piece of clean paper was taped snugly to the drill chuck and tested with the handheld tachometer. The tachometer detected no pulses with only the clean paper, so it was calculating no false RPM readings. A piece of reflective tape was applied to the paper, and the machine RPM settings were tested for accuracy at all of its low range settings. Table 8 shows that the tachometer read consistently 3-5 percent higher than the machine settings, with an average of 3.9 percent difference. The handheld tachometer settings were considered to be more accurate, so these values were used in all reported data.

Table 8 Tachometer Calibration of the Drill Press Used for Experiments

RPM Measurement		
Machine	Hand Tach	% Difference
20	21	4.8
31	31.5	1.6
36	37	2.7
41	42.7	4.0
47	49.9	5.8
54	55.1	2.0
62	65	4.6
72	74.3	3.1
83	85.8	3.3
95	100	5.0
109	115.1	5.3
126	132.6	5.0
145	150.7	3.8
167	172.5	3.2
	Average	+3.9

The penetration per revolution settings were calibrated with the use of a micrometer and a stopwatch at two RPM settings, as seen in Figure 24. First a micrometer, Mitutoyo Corp. Model ID-C125EB, was clamped in the drill fixture sample holder, and a probe with a flat end was clamped in the drill chuck. In this arrangement the probe pushed downward on the micrometer as it advanced. Since the micrometer rod was centered on the flat probe end, it was immune to any effects of rotation. A handheld tachometer was used to measure the RPM just before the penetration test. At the start of the penetration test the probe end was brought onto the micrometer probe so that it was actively pushing it down, then the penetration clutch of the drill press was disengaged and the micrometer was set to zero. The drill press clutch was

engaged simultaneously with the start of a stop watch, and after a time interval the drill press clutch was disengaged simultaneously with the stopping of the stopwatch. These actions were necessarily done by hand. The recorded measurements can be seen in Table 9.

Figure 24 Calibrating the Penetration per Revolution of the Drill Press Used in Testing

There is only one motor that runs the entire drill press, so the penetration per revolution of the quill is mechanically geared to the drive motor. Because of this arrangement, the penetration per revolution must be consistent with the number of revolutions over time. The percent difference noted in the table is likely caused by inconsistencies in the hand operation of the stopwatch and clutch engagement lever. Since no major discrepancies are noted and the source of error in this test is identified, the penetration per revolution settings of the drill press are considered to be accurate, and were used in all data reported.

Table 9 Penetration per Revolution Calibration of Drill Press

Rate of Penetration Measurement						
Machine Set Point		Measurement		Computed		
RPM	Penetration	Hand Tach	Time (s)	Penetration	Micrometer	% Diff
145	0.003	150.6	49.49	0.373	0.371	0.4
145	0.008	150.2	27.81	0.557	0.545	2.2
145	0.018	150.5	12.01	0.542	0.514	5.5
145	0.047	150.5	5.24	0.618	0.630	1.9
20	0.003	20.9	82.4	0.086	0.091	5.4
20	0.018	20.9	65.6	0.411	0.399	3.1
20	0.047	20.9	41.5	0.679	0.689	1.4

Fixturing

The samples used for all experiments were 2 inch diameter cores taken from larger parent slabs. Lengths varied from 1 to 4 inches, with most samples being 4 inches long. A rock holding fixture was designed and built to hold the samples and the load cells, as can be seen in Figure 25.

Figure 25 Rock Holding Fixture with Integrated WOB and Torque Load Cells

The drill fixture used a three-jaw chuck as a sample holder for securely clamping the sample. This type of chuck had several advantages over other types of clamping systems. It included a self-centering feature, changing samples was quick and easy with the use of a chuck key, it accommodated a wide range of variation in sample diameter, and it held samples securely.

Directly below the sample holder was a torque arm. The torque arm was constructed of ¾ inch steel, and was designed to have a distance of exactly 12 inches from the center of the sample holder to the tip of the arm. In this arrangement the pounds indicated by the load cell could automatically be interpreted as foot-pounds. The tip of the torque arm was rounded to reduce friction against the load cell contact. The heavy material was intended to give the arm negligible compliance. For measuring the torque, a load cell was mounted perpendicular to the torque arm, with a rounded load button in place to reduce friction. In order to reduce compliance, the mount for the torque load cell was made from ¼ inch steel angle and gusseted in the center. A single ball spring plunger was used to hold up the end of the torque arm. This held the arm level while minimizing friction.

The pivot of the torque arm was machined in a lathe using a 4-jaw chuck to have an integrated bearing sleeve for a thrust bearing. This allowed the torque arm have the freedom of movement to turn with minimal friction while faithfully transferring axial load through to below. A custom made adapter plate was necessary to transfer the axial load from the thrust bearing to the load cell below. The adapter plate was designed so that all of the force was transferred to the center of the axial (Weight on Bit) load cell. All of these components were

mounted to a single ½ inch thick steel plate, ensuring that measurements were robust and identical between runs.

It was important during set up to ensure that the drill bit was centered above the axial load cell. This was important because an off-center condition would result in erroneous measurements of both the axial and the torsional load cells, especially the latter. This was accomplished by disassembling the torque arm, thrust bearing, and adapter plate from the fixture. A threaded stud was threaded into the load cell button hole in the center of the load cell, and the drill chuck was closed on the stud. In this configuration the drill head and drill fixture were clamped in place, ensuring that the drill chuck would always be directly above the center of the load cell, even after the torque arm assembly was refit. From time to time during drilling the torque arm assembly was removed, and the thrust bearing was cleaned of rock dust to ensure its ease of movement. It was possible to remove, clean, and refit the torque arm assembly without moving either the base of the drill fixture or the quill of the drill press. It was therefore unnecessary to re-center the quill over the axial load cell after cleaning out the thrust bearing.

Data Acquisition:

The data acquisition system was comprised of two main parts; the sensor suite and the software.

Sensor Suite

A 1000 lb Sensotek load cell, serial number 226428, was used to measure the Weight on Bit force, and was mounted below the torque arm of the drill fixture. It was connected to Sensotek load cell reader model 060-3147-01, serial number 485536. A 500 lb Sensotek load cell, serial number 212655, was used for the torque cell. It was connected to Honeywell load cell reader model SC500, serial number 1207334. Both load cells were calibrated using the shunt calibration method and the calibration data as provided by the manufacturer, which can be seen in Figure 26 and Figure 27. In both cases the input and output resistance of the cells were confirmed before calibration. Each load cell reader was configured so that the full range produced a 0-5 volt output signal, each of which was wired to the data acquisition board. The 1000 lb Weight on Bit took the “0” slot and the 500 lb Torque took the “1” slot.

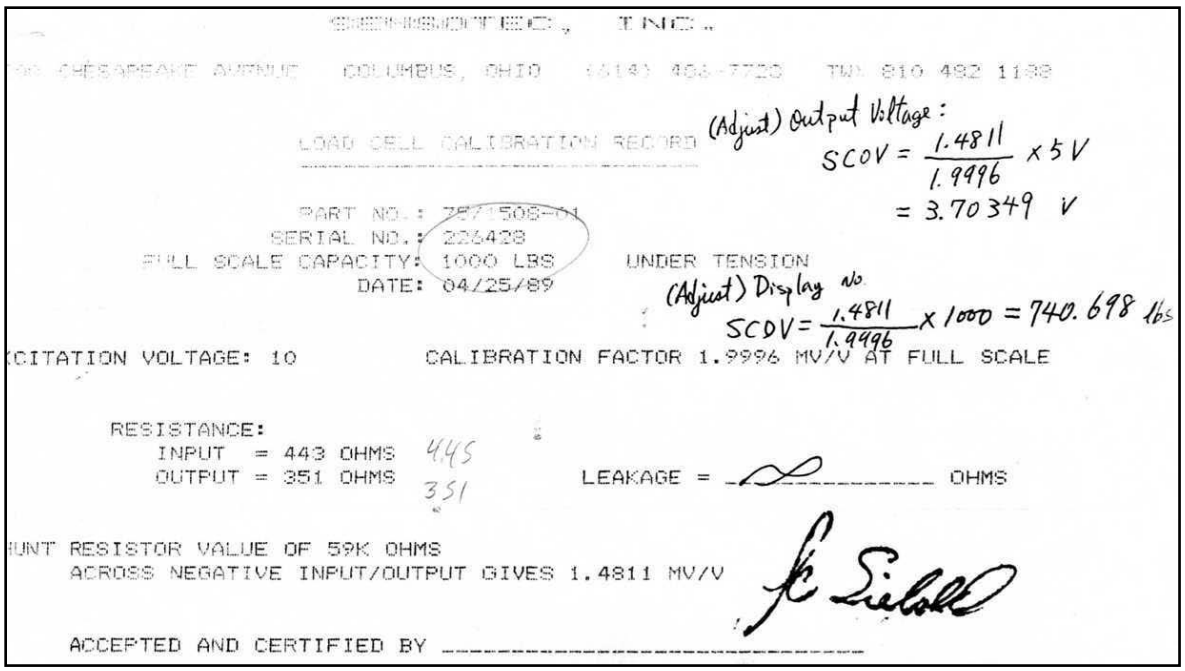

SENSOTEC, INC.

200 CHESAPEAKE AVENUE COLUMBUS, OHIO (614) 486-7723 TWX 810 482 1188

LOAD CELL CALIBRATION RECORD

(Adjust) Output Voltage:
SCOV = 1.4811 / 1.9996 x 5V
= 3.70349 V

PART NO.: 357508-01
SERIAL NO.: 226438
FULL SCALE CAPACITY: 1000 LBS UNDER TENSION
DATE: 04/25/89

(Adjust) Display no
SCOV = 1.4811 / 1.9996 x 1000 = 740.698 lbs

CITATION VOLTAGE: 10 CALIBRATION FACTOR 1.9996 MV/V AT FULL SCALE

RESISTANCE:
INPUT = 443 OHMS 445
OUTPUT = 351 OHMS 351
LEAKAGE = ∞ OHMS

UNT RESISTOR VALUE OF 59K OHMS
ACROSS NEGATIVE INPUT/OUTPUT GIVES 1.4811 MV/V

ACCEPTED AND CERTIFIED BY _____

Figure 26 Manufacturer's Calibration Data for 1000 Pound Load Cell Used for Weight on Bit

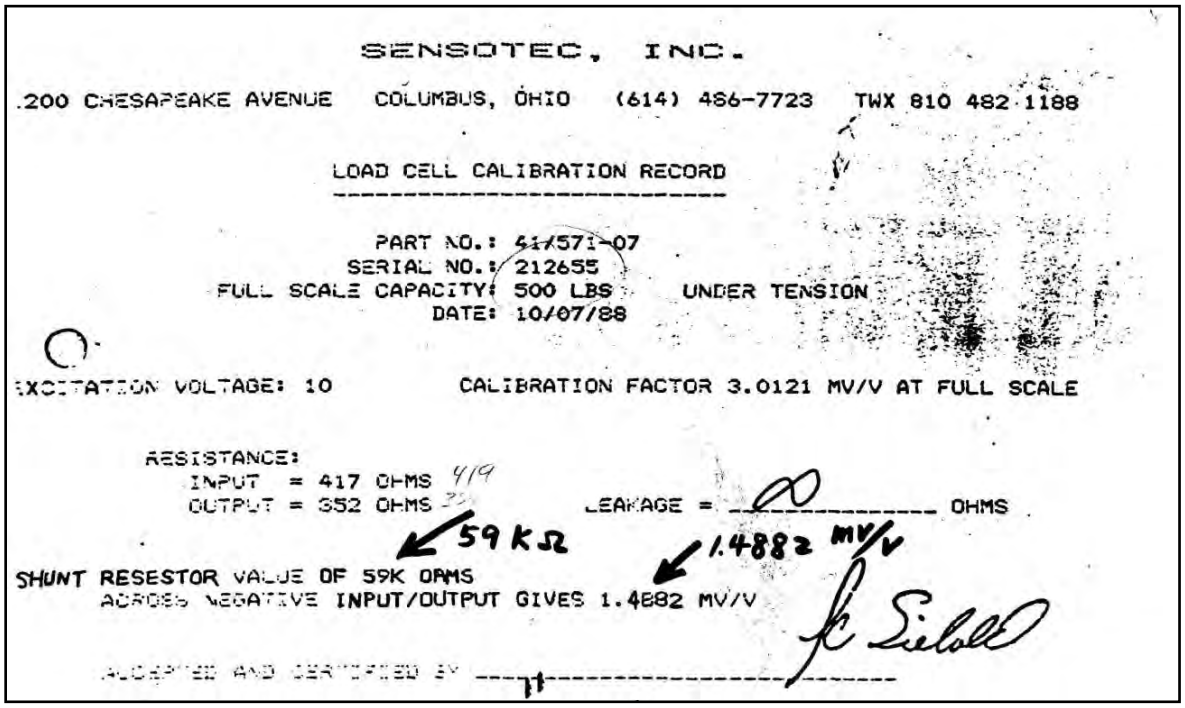

SENSOTEC, INC.

200 CHESAPEAKE AVENUE COLUMBUS, OHIO (614) 486-7723 TWX 810 482 1188

LOAD CELL CALIBRATION RECORD

PART NO.: 41571-07
SERIAL NO.: 212655
FULL SCALE CAPACITY: 500 LBS UNDER TENSION
DATE: 10/07/88

XCITATION VOLTAGE: 10 CALIBRATION FACTOR 3.0121 MV/V AT FULL SCALE

RESISTANCE:
INPUT = 417 OHMS 419
OUTPUT = 352 OHMS
LEAKAGE = ∞ OHMS

59 kΩ
1.4882 MV/V

SHUNT RESESTOR VALUE OF 59K OHMS
ACROSS NEGATIVE INPUT/OUTPUT GIVES 1.4882 MV/V

ACCEPTED AND CERTIFIED BY _____

Figure 27 Manufacturer's Calibration Data for 500 Pound Load Cell Used for Torque

The sensor used for the tachometer was a fiber-optic sensor, Banner Mini-Beam “FP” series. It has a two-lumen sensor probe, and is designed to generate a continuous beam of light in one lumen while sensing for the reflected light using the other lumen. This device is a 12 volt device and the data acquisition board used was only designed to accept up to 5 volts, so a voltage divider was used to bring the signal voltage down below 5 volts.

To use the fiber optic sensor as a tachometer, a clean white paper was securely fastened to the drill chuck, and a dark stripe of tape was applied to the paper. The emitter shined a light onto the paper, and the sensor detected the reflection of the light. When the dark stripe interrupted the surface, the detector sensed no light, and generated a 12 volt pulse for the duration of the presence of the dark stripe. The voltage divider reduced the pulse to 4.8 volts. The 0-4.8 volt signal was connected directly to the data acquisition system, and the computation of RPM was done in the software.

RPM data was collected to ensure that RPM was consistent between runs, and to ensure that RPM was not affected by forces on the drill bit. At no time during drilling was a reduction in RPM noted due to excess demands placed on the machine. Since the RPM was well documented in calibration and no deviation was noted, the RPM data reported was that of the calibration.

The data acquisition board used was a National Instruments NI-6009. This is a USB data acquisition board, and three of its analog channels were used. It was connected to a Dell model PP04L laptop computer, which was used to control the software and collect the data.

Drilling tests were conducted during several sessions over the course of several months. Between tests it was not possible for the equipment to remain in place, so tear down for transport and storage was necessary. The sensor readers, power supply, voltage divider, and data acquisition board were mounted to a purpose-built mounting board, which appears in Figure 28. The mounting board held the wire connections tight during transport and held the load cell readers and fiber optic sensor in place. This was not only convenient, but it ensured consistency between tests and reduced the possibility of damaging to the most sensitive equipment.

Figure 28 Sensor Suite Mounting Board

Software

National Instrument's LabVIEW program was used to control the data acquisition device and for data collection. First the NI-6009 USB data acquisition device was configured to use three analog channels using National Instrument's Measurement and Automation Explorer software. This software is capable of configuring external devices such as the USB Data Acquisition device in order for other software to access it. The LabVIEW program, Stiletto, was created to monitor the three channels and collect the data generated during drilling. In Figure 29 a screen shot of the LabVIEW front panel can be seen. The three channels of the instrument suite can be seen represented by the three dials and strip charts on the panel. The dials indicated the raw voltage from 0-5 volts as input to the data acquisition board. The three strip charts translated these voltage signals into appropriate units. From left to right they were Weight on Bit (lb), Torque (ft-lb), and RPM. The analog output signal to the left of the dials was used for set up of the program and was not used during data collection. Above the dials was the Data Collection Mode area, conveniently located near the Program Halt button. When switched on, the program saved all data from all three channels into a file as indicated in the "Write To File Name" window.

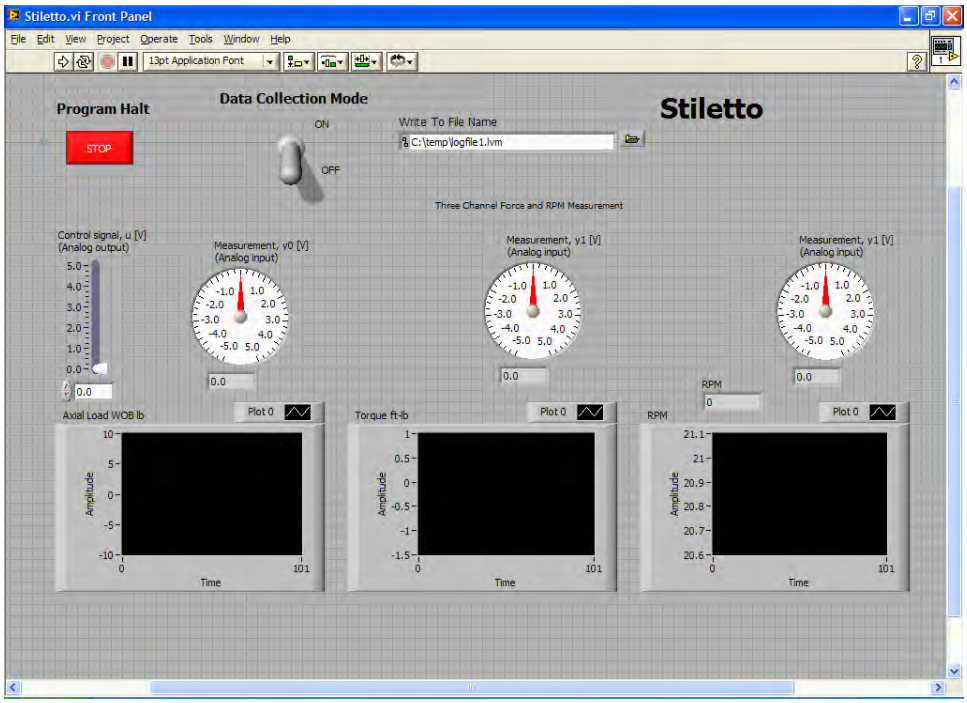

Figure 29 Stiletto LabVIEW Program Front Panel

In Figure 30 the back panel of this program is shown. LabVIEW works by executing anything outside the While Loop once at the start of the program, and then executing everything inside the While Loop continually until the program is stopped. The metronome symbol at the bottom was set to regulate the While Loop execution at once per 50 milliseconds, so the program took 20 data points per second. The top part of the program read the 0-5 volts signals from the three channels connected to the data acquisition board as a three unit array. The “0” slot was the axial Weight on Bit load from the 1000 lb load cell, which was set to display both the raw voltage on a dial indicator and the converted load in pounds on a strip chart. The “1” signal was the voltage from the 500 lb load cell used to measure torque. Its signal was displayed in the same way as the axial load, except that its strip chart measured in units of ft-lb. It was confirmed that these converted signals were the same as those on the external load cell indicators.

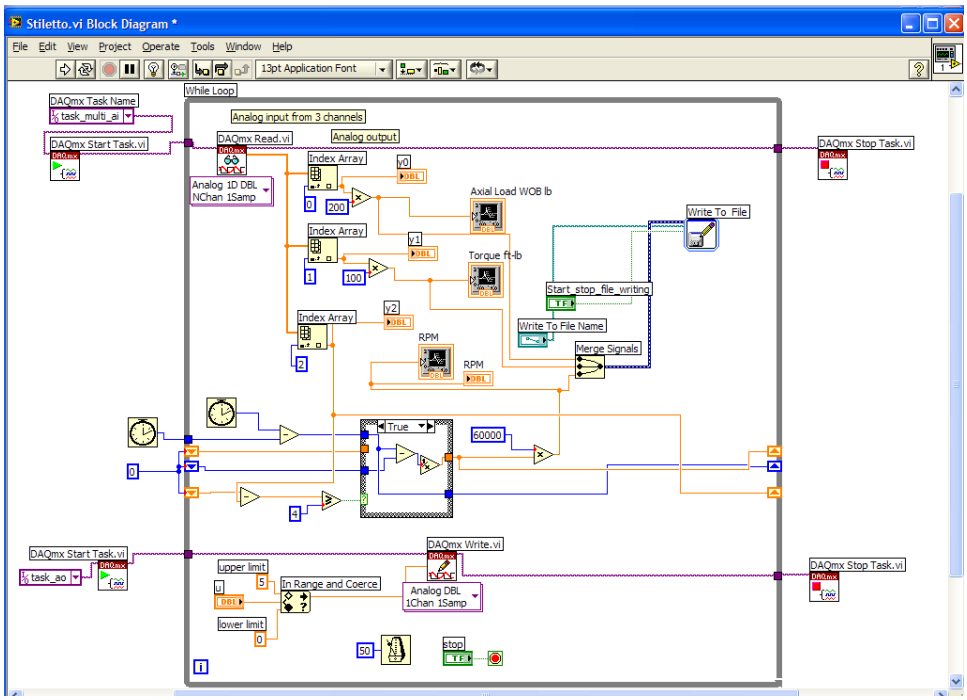

Figure 30 Stiletto LabVIEW Program Back View

The “2” signal was the square wave from the tachometer. Its signal was also displayed in raw voltage on a dial so that its pulse could be seen on the screen, but it required some computation in order to translate the square wave into RPM. It did this by searching for the rising edges of the square waves and computing the time difference between them. For each 50 millisecond increment the program compared the voltage of the square wave with that from the previous iteration to be greater than or equal to 4 volts. If the comparison was false, it passed the voltage and previous time through to the next iteration. If it were true, then it had sensed the rising edge of the square wave. In that case it computed the time difference between the current time and the time of the previous true condition, and converted it to RPM. That value was then displayed on a strip chart and a digital indicator.

All three converted signals were merged to an array and wired to a “Write to File” function. This function was controlled by the lowest area of the program, with a toggle switch controlling when the writing would start and stop on demand. The program saved a comma delimited text file, a format easily opened by spreadsheet software, to the name and directory written in the “Write To File Name” window. The program could run continuously, with the file name changed between tests. Data from consecutive tests could be taken by switching the toggle OFF, changing the file name, resetting the drill press settings, and switching the toggle ON. File names were designated by a meaningful naming system of ‘Rock Type|Treatment|RPM|Penetration’, so for example CMHOT42018 would be data collected on Carthage Marble heated samples at 42 RPM and 0.018 inch per revolution penetration rate.

Appendix B

Carthage Marble

Ambient Temperature and Pressure

Samples of Carthage Marble at ambient temperature and pressure were drilled using a standard ½ inch masonry bit at various RPM and Penetration per Revolution settings. The data for this variant is displayed in Table 10. The Weight on Bit data plotted against Torque can be seen in Figure 31. Under Assumption 2 a linear relationship was assumed, and the coefficients for the Torque equation were computed by regression.

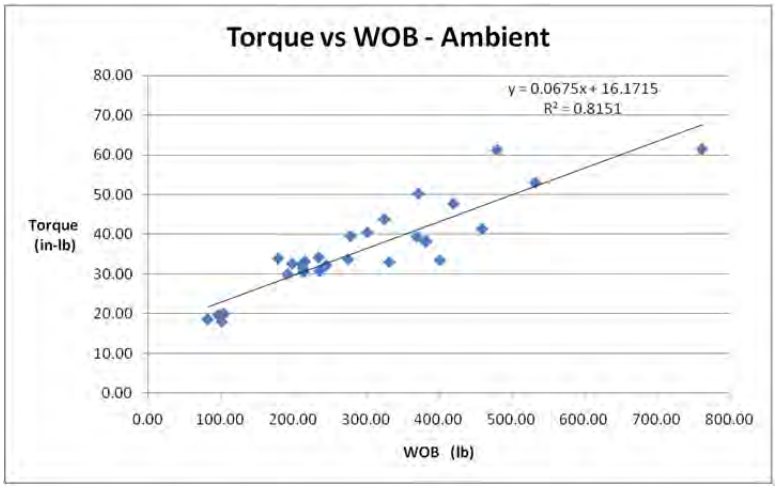

Figure 31 Torque as a Linear Function of Weight on Bit for Ambient Marble

$$Torque = f(WOB) = A_0 + A_1 * WOB \quad (20)$$

$$Torque = f(WOB) = 16.71 + 0.0675 * WOB \quad (21)$$

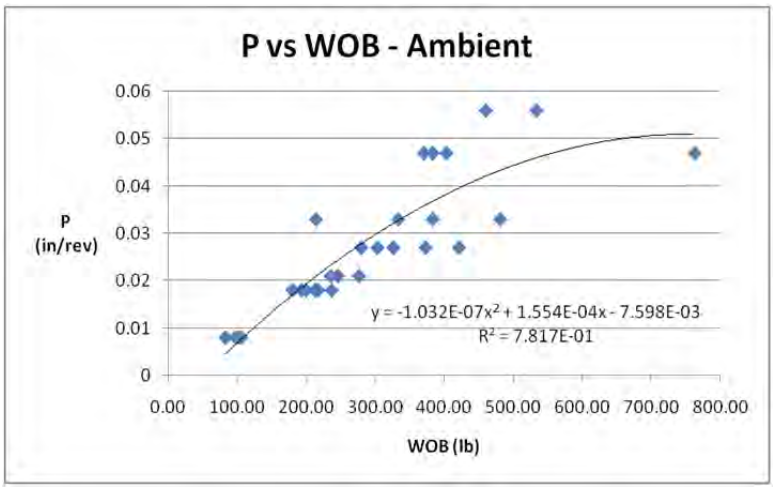

Figure 32 Rate of Penetration as a Function of Weight on Bit for Ambient Marble

Similarly Weight on Bit was plotted against Penetration per Revolution, as can be seen in Figure 32. Under Assumption 3 a second order polynomial relationship was assumed, and the coefficients for the Penetration per Revolution equation were computed by regression.

$$ROP = g(WOB) = B_2 * WOB^2 + B_1 * WOB + B_0 \quad (22)$$

$$ROP = g(WOB) = -1.03\text{E}-07 * WOB^2 + 1.55\text{E}-04 * WOB - 7.60\text{E}-03 \quad (23)$$

The Torque and Penetration per Revolution equations were substituted into the MSE_H equation.

$$\text{MSE}_\text{H} = \frac{\text{WOB}}{\text{Area}} + \frac{2\,\pi * (\text{A}_0 + \text{A}_1 * \text{WOB})}{\text{Area} * (\text{B}_2 * \text{WOB}^2 + \text{B}_1 * \text{WOB} + \text{B}_0)} \quad (24)$$

$$\text{MSE}_\text{H} = \frac{\text{WOB}}{\text{Area}} + \frac{2\,\pi * (16.1715 + 0.0675 * WOB)}{\text{Area} * (-1.03\text{E}-07 * WOB^2 + 1.55\text{E}-04 * WOB - 7.60\text{E}-03)} \quad (25)$$

In Table 10 MSE was computed using both the conventional Equation 9 and the above equation. A comparison is plotted in Figure 33, where the proposed equation has a smoothing effect.

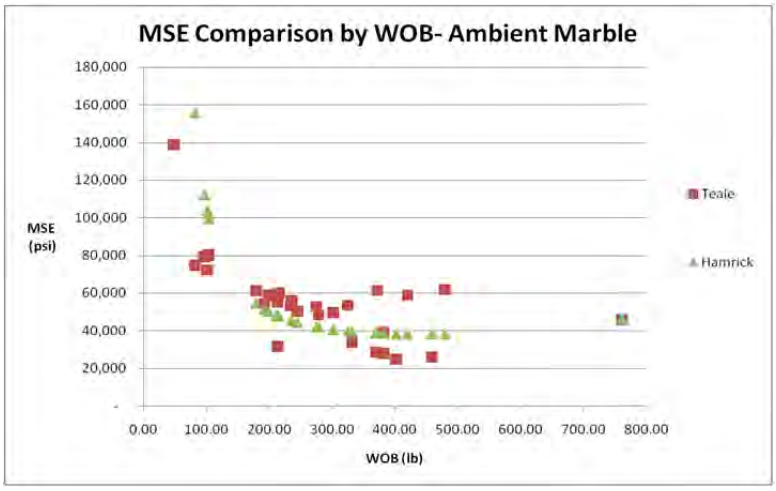

Figure 33 Comparison of Teale and Hamrick MSE Curves

Table 10 Carthage Marble Ambient Temperature and Pressure Results

				Teale	Hamrick
RPM	in/Rev	WOB (lb)	Torque (in-lb)	MSE (ksi)	MSE (ksi)
21	0.018	214	30.5	55.3	47.9
21	0.021	275	33.8	52.9	42.0
21	0.047	762	61.5	45.8	46.4
43	0.008	105	20.0	80.4	99.4
43	0.018	216	33.2	60.1	47.6
43	0.021	245	32.2	50.3	44.3
43	0.033	480	61.2	61.8	38.4
65	0.018	199	32.6	59.0	50.3
65	0.021	235	34.2	53.3	45.4
65	0.027	325	43.8	53.6	39.8
86	0.008	97	19.6	79.1	112
86	0.018	212	32.4	58.7	48.2
86	0.027	302	40.5	49.5	40.6
86	0.033	213	31.5	31.6	48.0
86	0.047	382	38.1	27.9	38.5
115	0.008	82	18.6	74.7	156
115	0.018	179	33.9	61.2	54.4
115	0.027	279	39.5	48.3	41.8
115	0.033	332	33.0	33.7	39.5
133	0.008	103	19.9	80.0	102
133	0.018	192	30.0	54.3	51.5
133	0.027	372	50.3	61.5	38.7
133	0.033	382	38.4	39.1	38.5
133	0.047	370	39.3	28.7	38.7
151	0.008	102	17.9	72.2	104
151	0.018	236	30.8	55.9	45.3
151	0.027	420	47.8	58.7	38.2
151	0.047	402	33.4	24.8	38.3
151	0.056	459	41.4	26.0	38.3

The coefficients determined by regression were used in Equation 13 to compute the polynomial unique to this variant.

$$0 = B_2 * WOB^4 + 2B_1B_2 * WOB^3 + ({B_1}^2 + 2B_2B_0 - 2\pi A_1B_2) * WOB^2 + (2B_1B_0 - 4\pi A_0B_2) * WOB + ({B_0}^2 + 2A_1B_0 - 2\pi A_0B_1)0 \quad (26)$$

$$0 = 1.07E-14 * WOB^4 - 3.2E-11 * WOB^3 + 6.95E-08 * WOB^2 - 1.86E-05 * WOB - 0.019 \quad (27)$$

This polynomial has four roots, which are indicated in Table 11.[35] Only the positive real root has physical meaning, indicating that the optimum Weight on Bit is 435 pounds.

Table 11 Roots of MSE_H Equation for Ambient Marble

Real solutions:
Root 1: -569.2
Root 2: 434.5
Complex roots:
Root 3: 1573.17-2172.71 * i
Root 4: 1573.17+2172.71 * i

Using the modified Torque and Penetration per Revolution equations, optimum values were computed and illustrated in Table 12.

Table 12 Optimum Values of Parameters for Marble

Parameter	Optimum Values
WOB (lb)	435
Torque (ft-lb)	45.5
Penetration (in/rev)	0.040

Plots of MSE against Weight on Bit, Torque and Penetration per Revolution can be seen in Figure 34, Figure 35, and Figure 36.

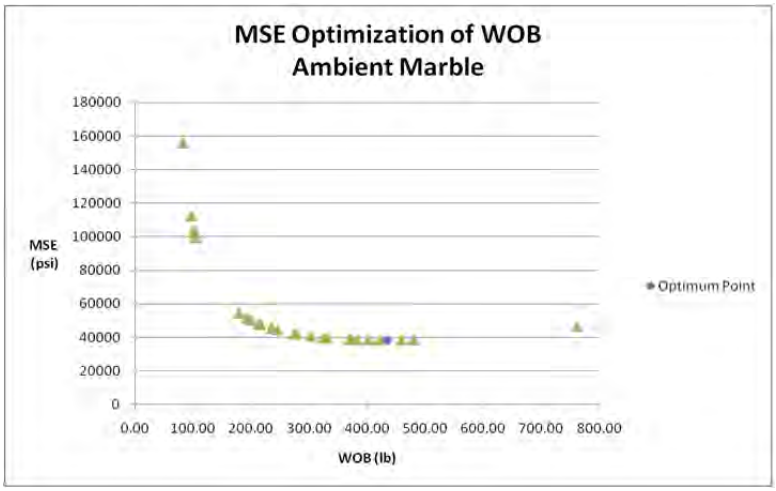

Figure 34 Optimum Weight on Bit Point Indicated for Ambient Marble

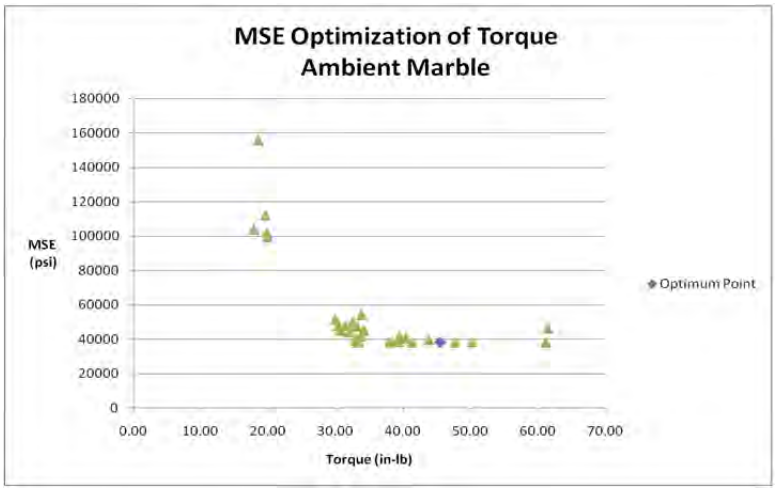

Figure 35 Optimum Torque Point Indicated for Ambient Marble

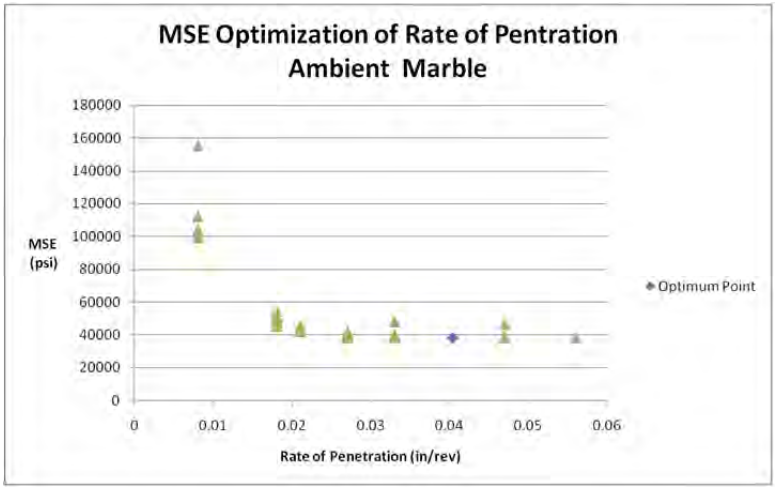

Figure 36 Optimum Rate of Penetration Point Indicated for Ambient Marble

Elevated Temperature and Ambient Pressure

Samples of Carthage Marble were heat soaked in an oven at 450 F for a minimum of two hours, and then drilled using a standard ½ inch masonry bit at various RPM and Rate of Penetration settings. The data for this variant is displayed in Table 13. The Weight on Bit data plotted against Torque can be seen in Figure 37. Under Assumption 2 a linear relationship was assumed, and the coefficients for the Torque equation were computed by regression.

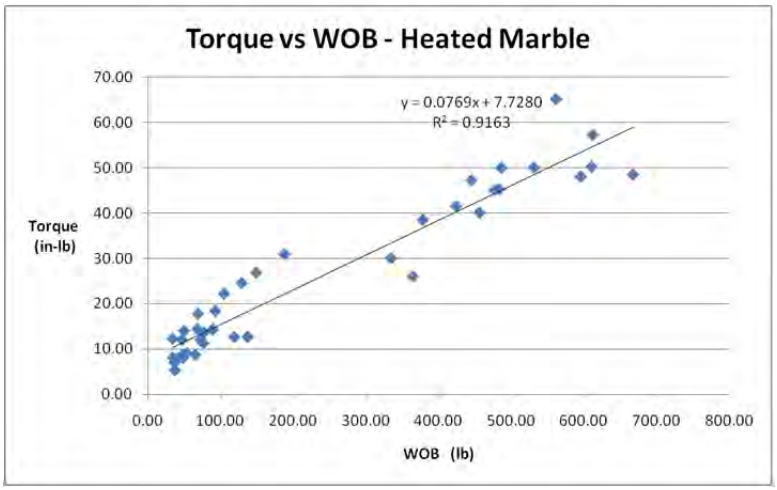

Figure 37 Torque as a Linear Function of Weight on Bit for Heated Marble

$$Torque = f(WOB) = A_0 + A_1 * WOB \tag{28}$$

$$Torque = f(WOB) = 7.728 + 0.0769 * WOB \tag{29}$$

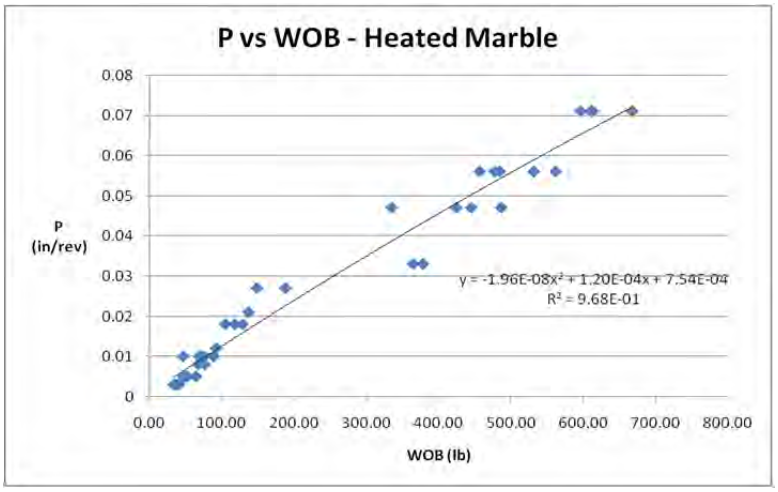

Figure 38 Rate of Penetration as a Function of Weight on Bit for Heated Marble

Similarly Weight on Bit was plotted against Penetration per Revolution, as can be seen in Figure 38. Under Assumption 3 a second order polynomial relationship was assumed, and the coefficients for the Penetration per Revolution equation were computed by regression.

$$ROP = g(WOB) = B_2 * WOB^2 + B_1 * WOB + B_0 \quad (30)$$

$$ROP = g(WOB) = 7.54\text{E}-04 * WOB^2 + 1.20\text{E}-04 * WOB - 1.96\text{E}-08 \quad (31)$$

The Torque and Penetration per Revolution equations were substituted into the MSE_H equation.

$$\text{MSE}_\text{H} = \frac{\text{WOB}}{\text{Area}} + \frac{2\,\pi * (\text{A}_0 + \text{A}_1 * \text{WOB})}{\text{Area} * (\text{B}_2 * \text{WOB}^2 + \text{B}_1 * \text{WOB} + \text{B}_0)} \quad (32)$$

$$\text{MSE}_\text{H} = \frac{\text{WOB}}{\text{Area}} + \frac{2\,\pi * (7.728 + 0.0769 * WOB)}{\text{Area} * (7.54\text{E}-04 * WOB^2 + 1.20\text{E}-04 * WOB - 1.96\text{E}-08)} \quad (33)$$

In Table 13 MSE was computed using both the conventional Equation 9 and the above equation. A comparison is plotted in Figure 39, where the proposed equation has a smoothing effect.

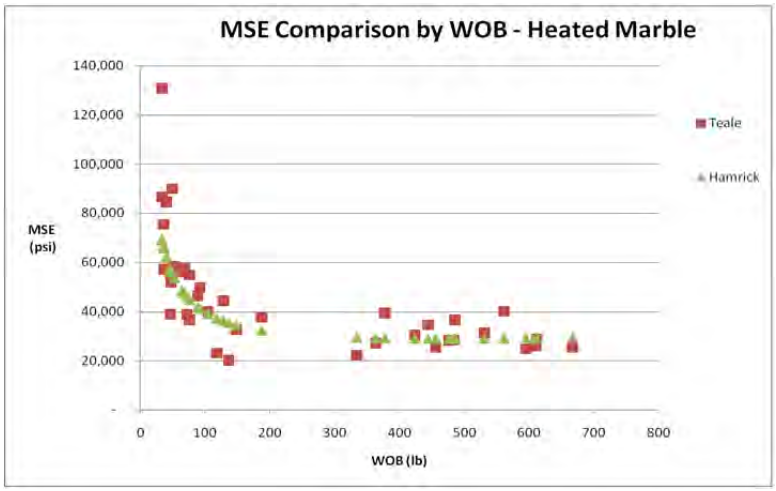

Figure 39 Comparison of Teale and Hamrick MSE Curves

Table 13 Carthage Marble Elevated Temperature Results

				Teale	Hamrick
RPM	in/Rev	WOB (lb)	Torque (in-lb)	MSE (ksi)	MSE (ksi)
21	0.003	34	12.3	131	69.5
21	0.005	49	14.0	89.9	56.0
21	0.008	76	13.6	54.8	44.8
21	0.010	68	17.7	57.1	47.2
21	0.018	104	22.2	40.1	39.1
21	0.027	188	30.9	37.5	32.4
21	0.047	486	50.0	36.5	29.0
21	0.056	562	65.1	40.1	29.2
21	0.071	612	57.2	28.9	29.3
43	0.003	36	7.1	75.4	66.8
43	0.005	53	9.1	58.3	53.8
43	0.008	68	14.4	57.9	47.5
43	0.01	72	12.0	38.7	46.1
43	0.018	128	24.5	44.3	36.2
43	0.027	148	26.9	32.6	34.5
43	0.033	378	38.5	39.3	29.1
43	0.047	445	47.2	34.4	29.0
43	0.056	477	45.0	28.1	29.0
43	0.071	668	48.5	25.2	29.6
65	0.003	34	8.1	86.6	69.2
65	0.005	46	8.6	55.0	57.8
65	0.01	46	12.0	38.7	57.8
65	0.047	424	41.5	30.4	29.0
65	0.056	531	50.0	31.3	29.1
100	0.003	41	7.9	84.5	62.2
100	0.005	48	8.0	51.7	56.9
100	0.010	76	11.3	36.5	44.9
100	0.021	137	12.7	20.0	35.4
100	0.047	335	30.0	22.2	29.4
100	0.056	456	40.0	25.2	29.0
100	0.071	596	48.0	24.7	29.3
133	0.003	37	5.3	57.2	65.9
133	0.005	64	8.7	56.1	48.6
133	0.010	89	14.3	46.3	41.8
133	0.012	92	18.4	49.6	41.1
133	0.018	118	12.6	23.0	37.3
133	0.033	364	26.0	27.1	29.2
133	0.056	484	45.3	28.3	29.0
133	0.071	611	50.2	25.8	29.3

The coefficients determined by regression were used in Equation 13 to compute the polynomial unique to this variant.

$$0 = B_2 * WOB^4 + 2B_1B_2 * WOB^3 + (B_1{}^2 + 2B_2B_0 - 2\pi A_1B_2) * WOB^2 + (2B_1B_0 - 4\pi A_0B_2) * WOB + (B_0{}^2 + 2A_1B_0 - 2\pi A_0B_1)0 \quad (34)$$

$$0 = 1.07E-14 * WOB^4 - 3.2E-11 * WOB^3 + 6.95E-08 * WOB^2 - 1.86E-05 * WOB - 0.019 \quad (35)$$

This polynomial has four roots, which are indicated in Table 14.[35] Only the positive real root has physical meaning, indicating that the optimum Weight on Bit is 455 pounds.

Table 14 Roots of MSE_H Equation for Heated Marble

Real solutions:
Root 1: -497.3
Root 2: 455.2
Complex roots:
Root 3: 6143.5-5006.037 * i
Root 4: 6143.5+5006.037 * i

Using the modified Torque and Penetration per Revolution equations, optimum values were computed and illustrated in Table 15.

Table 15 Optimum Values of Parameters for Heated Marble

Parameter	Optimum Values
WOB (lb)	455
Torque (in-lb)	42.7
Penetration (in/rev)	0.051

Plots of MSE against Weight on Bit, Torque and Penetration per Revolution can be seen in Figure 40, Figure 41, and Figure 42.

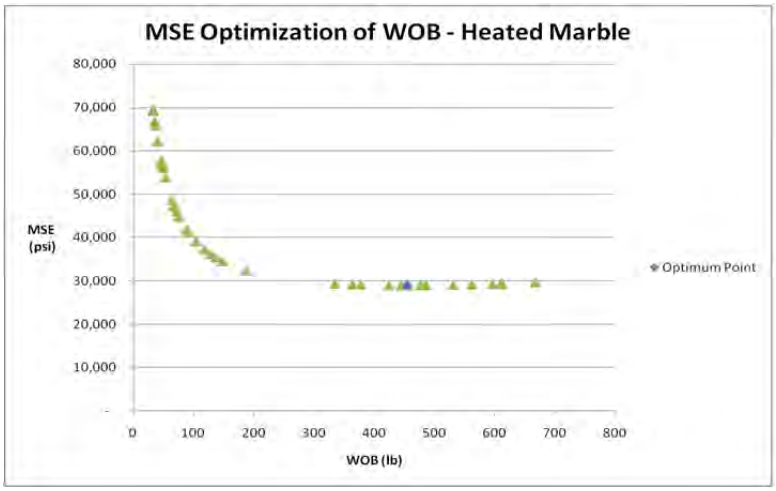

Figure 40 Optimum Weight on Bit Point Indicated for Heated Marble

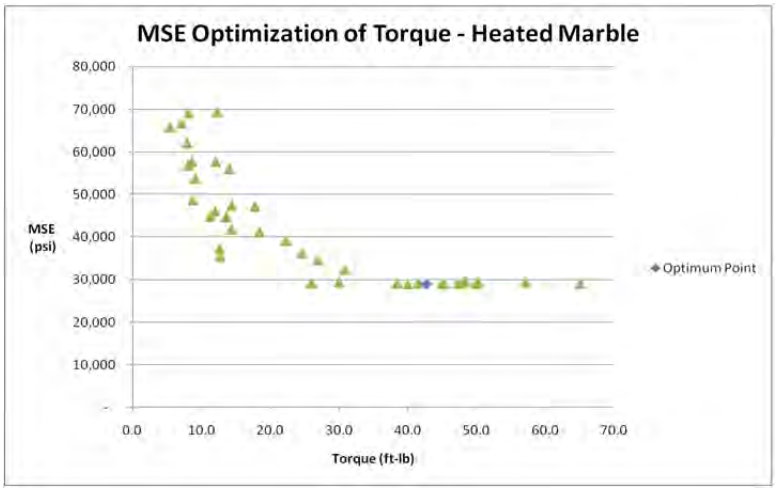

Figure 41 Optimum Torque Point Indicated for Heated Marble

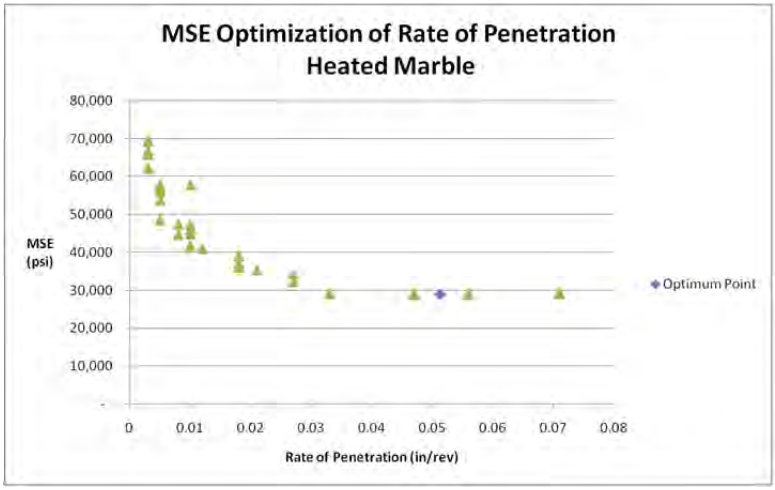

Figure 42 Optimum Rate of Penetration Point Indicated for Heated Marble

Elevated Confining Pressure

Samples of Carthage Marble were placed in a Hoek Cell and pressurized to 1500 psi confining pressure in the drilling apparatus, as described in the Drilling Experiments Section of this work. They were then drilled using a standard ½ inch masonry bit at various RPM and Rate of Penetration settings. The data for this variant is displayed in Table 16. The Weight on Bit data plotted against Torque can be seen in Figure 43. Under Assumption 2 a linear relationship was assumed, and the coefficients for the Torque equation were computed by regression.

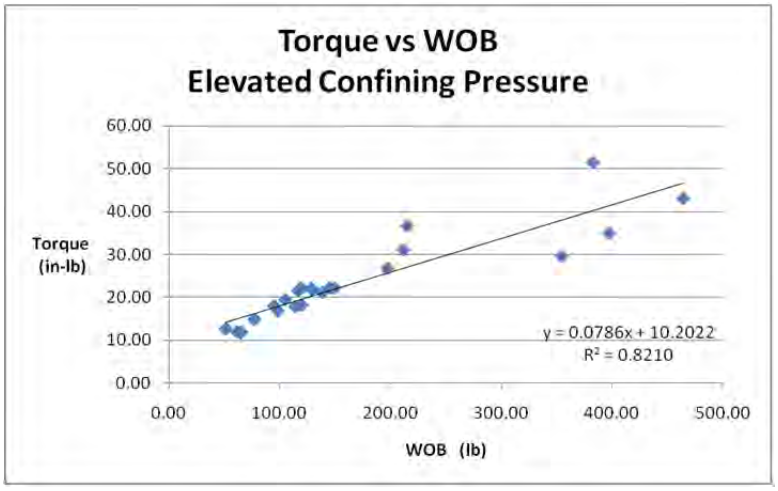

Figure 43 Torque as a Linear Function of Weight on Bit for Marble at Elevated Confining Pressure

$$\text{Torque} = \text{f(WOB)} = \text{A}_0 + \text{A}_1 * \text{WOB} \quad (36)$$

$$\text{Torque} = \text{f(WOB)} = 10.202 + 0.079 * \text{WOB} \quad (37)$$

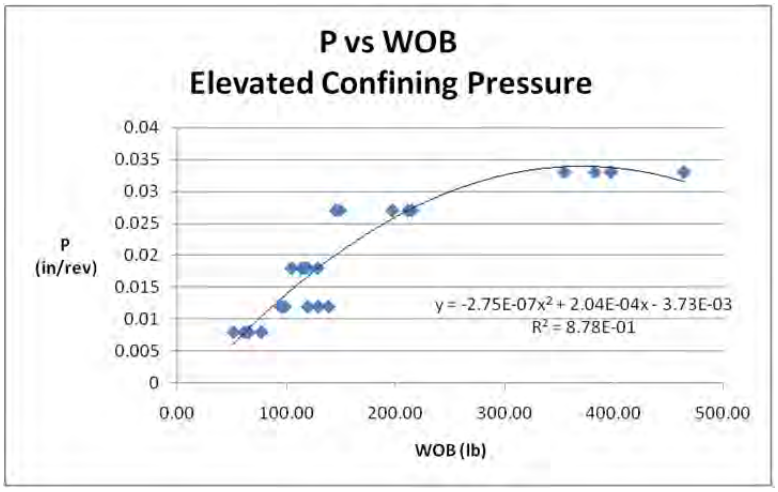

Figure 44 Rate of Penetration as a Function of Weight on Bit for Marble at Elevated Confining Pressure

Similarly Weight on Bit was plotted against Penetration per Revolution, as can be seen in Figure 44. Under Assumption 3 a second order polynomial relationship was assumed, and the coefficients for the Penetration per Revolution equation were computed by regression.

$$\mathrm{ROP} = \mathrm{g(WOB)} = \mathrm{B_2} * \mathrm{WOB^2} + \mathrm{B_1} * \mathrm{WOB} + \mathrm{B_0} \tag{38}$$

$$\begin{aligned}\mathrm{ROP} = \mathrm{g(WOB)} \\ = -2.75\mathrm{E}-07 * \mathrm{WOB^2} + 2.04\mathrm{E}-04 * \mathrm{WOB} \\ - 3.73\mathrm{E}-03\end{aligned} \tag{39}$$

The Torque and Penetration per Revolution equations were substituted into the $\mathrm{MSE_H}$ equation.

$$\mathrm{MSE_H} = \frac{\mathrm{WOB}}{\mathrm{Area}} + \frac{2\,\pi * (\mathrm{A_0} + \mathrm{A_1} * \mathrm{WOB})}{\mathrm{Area} * (\mathrm{B_2} * \mathrm{WOB^2} + \mathrm{B_1} * \mathrm{WOB} + \mathrm{B_0})} \tag{40}$$

$$\begin{aligned}\mathrm{MSE_H} \\ = \frac{\mathrm{WOB}}{\mathrm{Area}} \\ + \frac{2\,\pi * (10.202 + 0.079 * \mathrm{WOB})}{\mathrm{Area} * (-2.75\mathrm{E}-07 * \mathrm{WOB^2} + 2.04\mathrm{E}-04 * \mathrm{WOB} - 3.73\mathrm{E}-03)}\end{aligned} \tag{41}$$

In Table 16 MSE was computed using both the conventional Equation 9 and the above equation. A comparison is plotted in Figure 45, where the proposed equation has a smoothing effect.

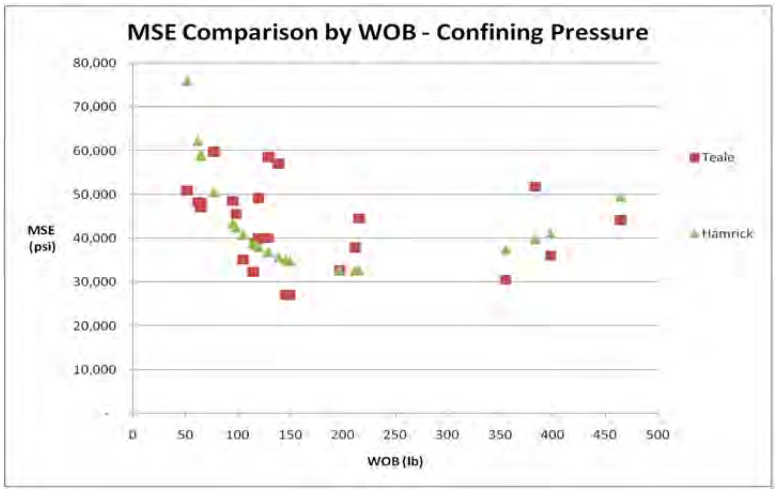

Figure 45 Comparison of Teale and Hamrick MSE Curves

Table 16 Carthage Marble at Elevated Confining Pressure Results

				Teale	Hamrick
RPM	in/Rev	WOB (lb)	Torque (in-lb)	MSE (ksi)	MSE (ksi)
21	0.008	61	12.0	48.1	62.3
21	0.012	98	16.9	45.5	42.5
21	0.018	114	17.8	32.3	39.0
21	0.027	149	22.1	26.9	34.8
21	0.033	355	29.6	30.5	37.6
43	0.008	51	12.6	50.8	76.0
43	0.012	95	18.0	48.5	43.5
43	0.018	128	22.1	40.0	36.9
43	0.027	145	22.2	27.0	35.2
43	0.033	397	35.0	35.9	41.1
65	0.008	65	11.7	47.1	59.2
65	0.012	129	21.7	58.5	36.8
65	0.018	119	22.1	39.9	38.1
65	0.027	212	31.0	37.8	32.7
86	0.008	65	11.9	48.0	58.8
86	0.012	120	18.2	49.1	38.1
86	0.018	117	21.5	38.8	38.6
86	0.027	197	26.7	32.6	32.9
86	0.033	464	43.1	44.1	49.5
100	0.008	77	14.8	59.7	50.6
100	0.012	138	21.1	57.1	35.8
100	0.018	105	19.4	35.1	40.9
100	0.027	215	36.6	44.5	32.7
100	0.033	383	51.3	51.7	39.8

The coefficients determined by regression were used in Equation 13 to compute the polynomial unique to this variant.

$$0 = B_2 * WOB^4 + 2B_1B_2 * WOB^3 + ({B_1}^2 + 2B_2B_0 - 2\pi A_1B_2) * WOB^2 + (2B_1B_0 - 4\pi A_0B_2) * WOB + ({B_0}^2 + 2A_1B_0 - 2\pi A_0B_1)0 \quad (42)$$

$$0 = 7.56E-14 * WOB^4 - 1.12E-10 * WOB^3 + 1.80E-07 * WOB^2 + 3.37E-05 * WOB - 0.0149 \quad (43)$$

This polynomial has four roots, which are indicated in Table 17. Only the positive real root has physical meaning, indicating that the optimum Weight on Bit is 218 pounds.

Table 17 Roots of MSEH Equation for Marble at Elevated Confining Pressure

Real solutions:
Root 1: -341.5
Root 2: 218.1
Complex roots:
Root 3: 803.492-1414.348 * i
Root 4: 803.492+1414.348 * i

Using the modified Torque and Penetration per Revolution equations, optimum values were computed and illustrated in Table 18

Table 18 Optimum Values of Parameters for Heated Marble

Parameter	Optimum Values
WOB (lb)	218
Torque (in-lb)	27.3
Penetration (in/rev)	0.028

Plots of MSE against Weight on Bit, Torque and Penetration per Revolution can be seen in Figure 46, Figure 47, and Figure 48.

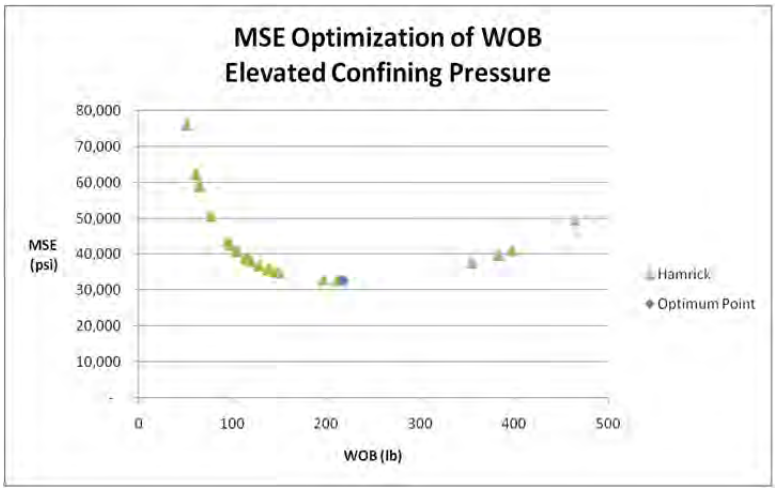

Figure 46 Optimum Weight on Bit Point Indicated for Marble at Elevated Confining Pressure

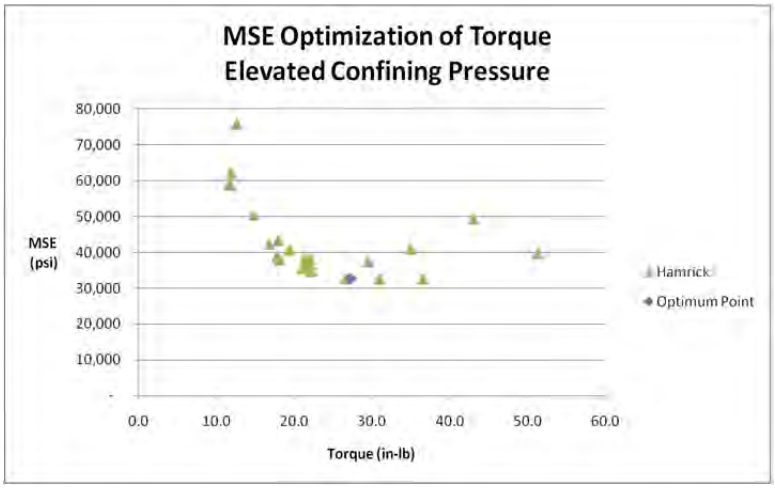

Figure 47 Optimum Torque Point Indicated for Marble at Elevated Confining Pressure

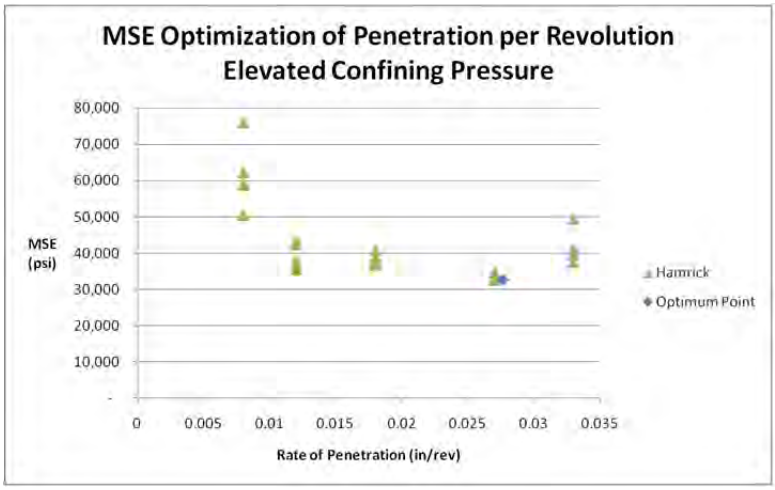

Figure 48 Optimum Rate of Penetration Point Indicated for Marble at Elevated Confining Pressure

2-Wing Bit

Samples of Carthage Marble were drilled in the drilling apparatus at ambient temperature and pressure using a 2-wing ½ inch drill bit as described in the Drilling Experiments Section of this work at various RPM and Penetration per Revolution settings. The data for this variant is displayed Table 19. The Weight on Bit data plotted against Torque can be seen in Figure 49. Under Assumption 2 a linear relationship was assumed, and the coefficients for the Torque equation were computed by regression.

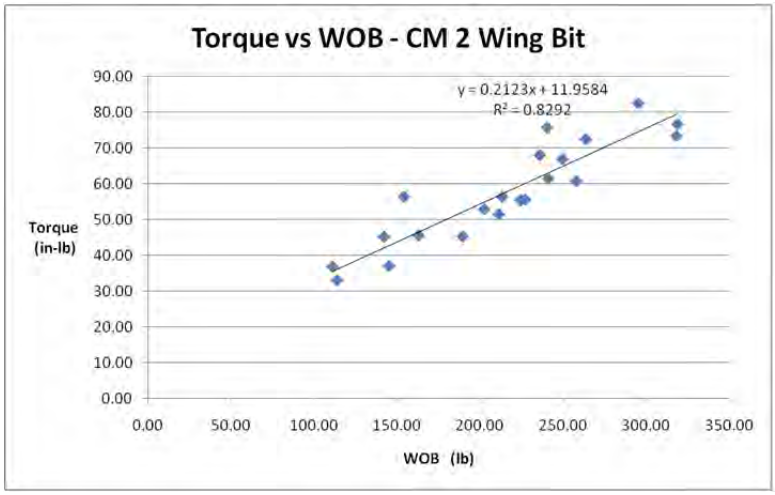

Figure 49 Torque as a Linear Function of Weight on Bit for Marble Drilled With a 2-Wing Bit

$$Torque = f(WOB) = A_0 + A_1 * WOB \quad (44)$$

$$Torque = f(WOB) = 11.958 + 0.212 * WOB \quad (45)$$

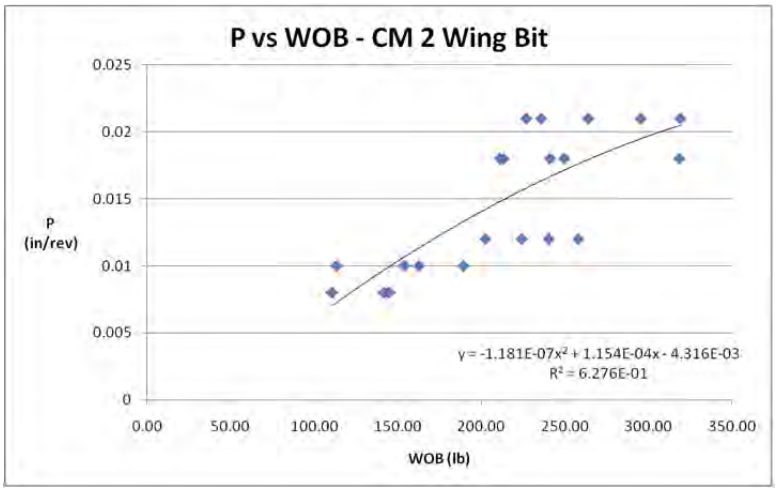

Figure 50 Rate of Penetration as a Function of Weight on Bit for Marble Drilled With a 2-Wing Bit

Similarly Weight on Bit was plotted against Penetration per Revolution, as can be seen in Figure 50. Under Assumption 3 a second order polynomial relationship was assumed, and the coefficients for the Penetration per Revolution equation were computed by regression.

$$ROP = g(WOB) = B_2 * WOB^2 + B_1 * WOB + B_0 \quad (46)$$

$$ROP = g(WOB) = -1.18\text{E}-07 * WOB^2 + 1.15\text{E}-04 * WOB - 4.32\text{E}-03 \quad (47)$$

The Torque and Penetration per Revolution equations were substituted into the MSE_H equation.

$$\text{MSE}_\text{H} = \frac{\text{WOB}}{\text{Area}} + \frac{2\,\pi * (\text{A}_0 + \text{A}_1 * \text{WOB})}{\text{Area} * (\text{B}_2 * \text{WOB}^2 + \text{B}_1 * \text{WOB} + \text{B}_0)} \quad (48)$$

$$\text{MSE}_\text{H} = \frac{\text{WOB}}{\text{Area}} + \frac{2\,\pi * (11.958 + 0.212 * WOB)}{\text{Area} * (-1.18\text{E}-07 * WOB^2 + 1.15\text{E}-04 * WOB - 4.32\text{E}-03)} \quad (49)$$

In Table 19 MSE was computed using both the conventional Equation 9 and the above equation. A comparison is plotted in Figure 51, where the proposed equation has a smoothing effect.

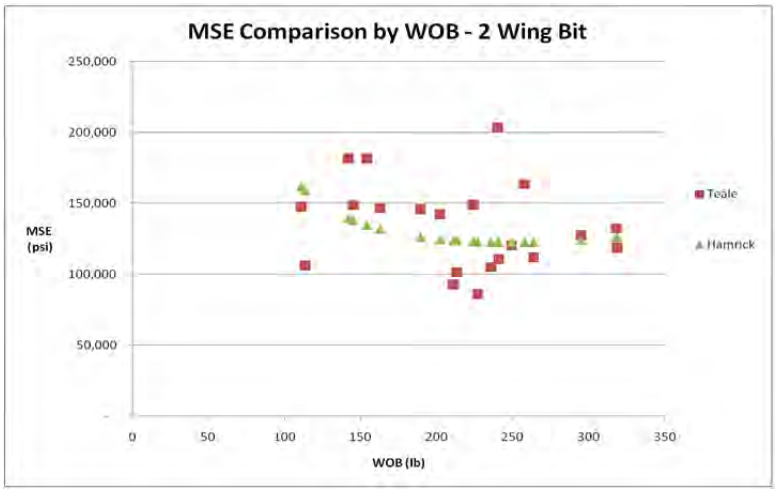

Figure 51 Comparison of Teale and Hamrick MSE Curves

Table 19 Carthage Marble Two Wing Bit Drilling Results

				Teale	Hamrick
RPM	in/Rev	WOB (lb)	Torque (in-lb)	MSE (ksi)	MSE (ksi)
21	0.008	111	36.8	148	162
21	0.018	211	51.5	92.6	124
21	0.021	227	55.6	85.9	123
43	0.008	142	45.2	181	140
43	0.010	163	45.5	147	132
43	0.012	224	55.4	149	123
43	0.018	241	61.5	111	123
43	0.021	264	72.6	112	123
65	0.010	114	33.0	106	159
65	0.012	202	52.9	142	125
65	0.018	213	56.4	101	124
65	0.021	236	68.1	105	123
86	0.010	154	56.5	182	135
86	0.012	240	75.8	203	123
86	0.018	250	66.9	120	123
86	0.021	295	82.6	127	124
100	0.008	145	37.0	149	138
100	0.010	189	45.3	146	126
100	0.012	258	60.8	164	123
100	0.018	318	73.5	132	126
100	0.021	319	76.8	119	126

The coefficients determined by regression were used in Equation 13 to compute the polynomial unique to this variant.

$$0 = B_2 * WOB^4 + 2B_1B_2 * WOB^3 + ({B_1}^2 + 2B_2B_0 - 2\pi A_1B_2) * WOB^2 + (2B_1B_0 - 4\pi A_0B_2) * WOB + ({B_0}^2 + 2A_1B_0 - 2\pi A_0B_1)0 \quad (50)$$

$$0 = 1.39E-14 * WOB^4 - 2.7E-11 * WOB^3 + 1.72E-07 * WOB^2 + 1.68E-05 * WOB - 0.0144 \quad (51)$$

This polynomial has four roots, which are indicated in Table 20. Only the positive real root has physical meaning, indicating that the optimum Weight on Bit is 249 pounds.

Table 20 Roots of MSEH Equation for Marble Drilled With a 2-Wing Bit

Real solutions:
Root 1: -330.7
Root 2: 248.5
Complex roots:
Root 3: 1018.248-3396.402 * i
Root 4: 1018.248+3396.402 * i

Using the modified Torque and Penetration per Revolution equations, optimum values were computed and illustrated in Table 21

Table 21 Optimum Values of Parameters for Marble Drilled With a 2-Wing bit

Parameter	Optimum Values
WOB (lb)	249
Torque (in-lb)	64.7
Penetration (in/rev)	0.017

Plots of MSE against Weight on Bit, Torque and Penetration per Revolution can be seen in Figure 52, Figure 53, and Figure 54.

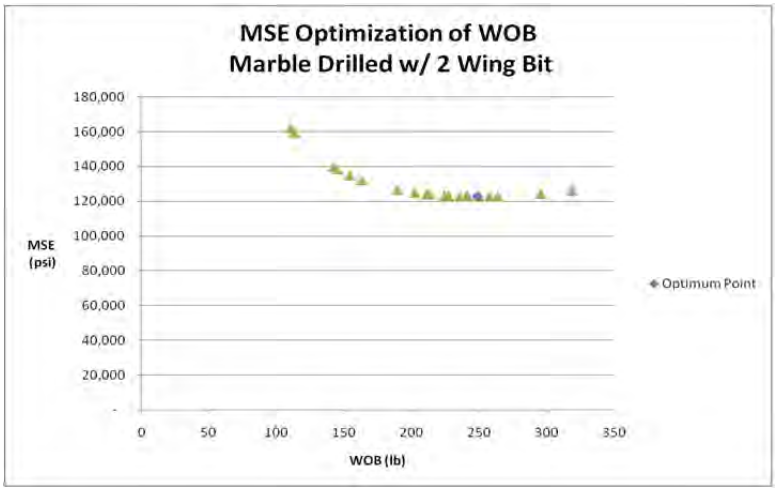

Figure 52 Optimum Weight on Bit Point Indicated for Marble Drilled With Two-Wing Bit

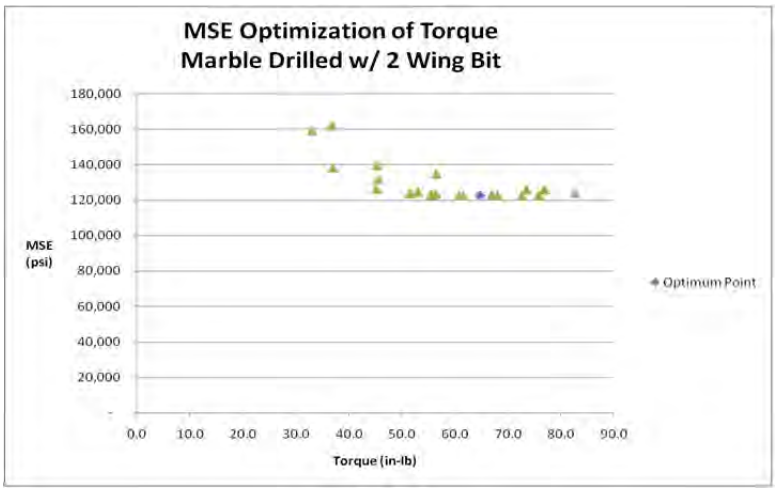

Figure 53 Optimum Torque Point Indicated for Marble Drilled With Two-Wing Bit

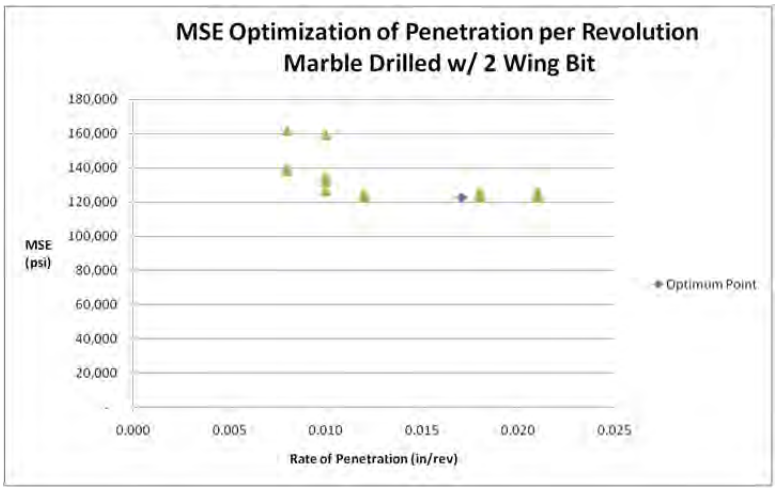

Figure 54 Optimum Rate of Penetration Point Indicated for Marble Drilled With Two-Wing Bit

Terretek Sandstone

Ambient Temperature and Pressure

Samples of Terretek Sandstone at ambient temperature and pressure were drilled using a standard ½ inch masonry bit at various RPM and Rate of Penetration settings. The data for this variant is displayed in Table 22 The Weight on Bit data plotted against Torque can be seen in Figure 55. Under Assumption 2 a linear relationship was assumed, and the coefficients for the Torque equation were computed by regression.

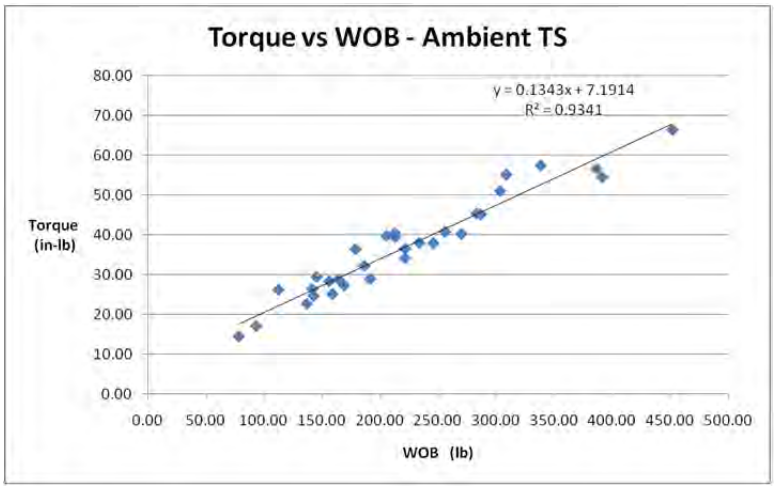

Figure 55 Torque as a Linear Function of Weight on Bit for Ambient Terretek Sandstone

$$Torque = f(WOB) = A_0 + A_1 * WOB \quad (52)$$

$$Torque = f(WOB) = 7.191 + 0.134 * WOB \quad (53)$$

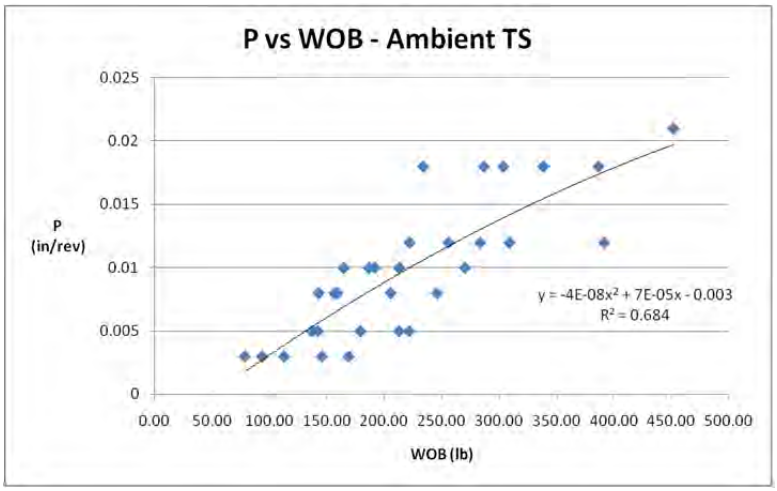

Figure 56 Rate of Penetration as a Function of Weight on Bit for Ambient Terretek Sandstone

Similarly Weight on Bit was plotted against Penetration per Revolution, as can be seen in Figure 56.Under Assumption 3 a second order polynomial relationship was assumed, and the coefficients for the Penetration per Revolution equation were computed by regression.

$$ROP = g(WOB) = B_2 * WOB^2 + B_1 * WOB + B_0 \quad (54)$$

$$ROP = g(WOB) = -4.00\text{E}-08 * WOB^2 + 7.00\text{E}-05 * WOB - 0.003 \quad (55)$$

The Torque and Penetration per Revolution equations were substituted into the MSE_H equation.

$$\mathrm{MSE_H} = \frac{\mathrm{WOB}}{\mathrm{Area}} + \frac{2\,\pi * (\mathrm{A_0} + \mathrm{A_1} * \mathrm{WOB})}{\mathrm{Area} * (\mathrm{B_2} * \mathrm{WOB}^2 + \mathrm{B_1} * \mathrm{WOB} + \mathrm{B_0})} \quad (56)$$

$$\mathrm{MSE_H} = \frac{\mathrm{WOB}}{\mathrm{Area}} + \frac{2\,\pi * (7.191 + 0.134 * WOB)}{\mathrm{Area} * (-4.00\text{E}-08 * WOB^2 + 7.00\text{E}-05 * WOB - 0.003)} \quad (57)$$

In Table 22 MSE was computed using both the conventional Equation 9 and the above equation. A comparison is plotted in Figure 57, where the proposed equation has a smoothing effect.

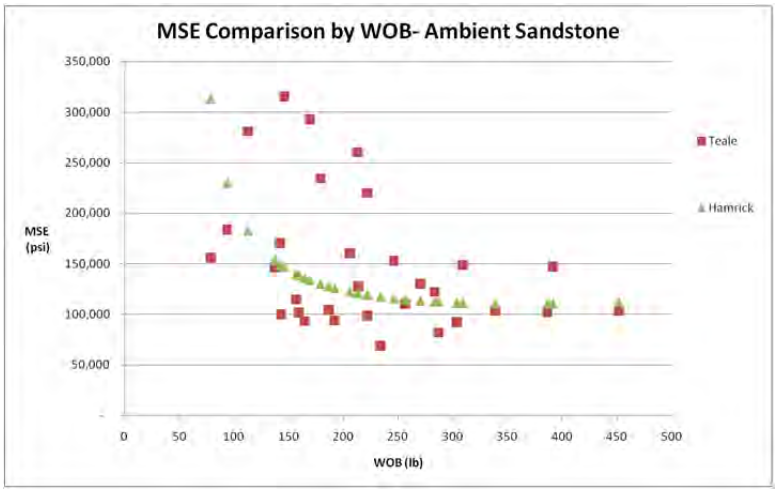

Figure 57 Comparison of Teale and Hamrick MSE Curves

Table 22 Comparison of Teale and Hamrick MSE computations for Ambient Sandstone

				Teale	Hamrick
RPM	in/Rev	WOB (lb)	Torque (ft-lb)	MSE (ksi)	MSE (ksi)
21	0.003	169	27.4	293	134
21	0.005	221	34.2	220	119
21	0.008	246	37.9	153	116
21	0.010	270	40.3	130	114
21	0.012	391	54.4	147	111
21	0.018	386	56.5	102	111
21	0.021	452	66.3	103	112
42	0.003	146	29.5	316	147
42	0.005	213	40.5	260	121
42	0.008	143	24.8	100	149
42	0.010	165	28.9	93.3	136
42	0.012	222	36.5	98.5	119
42	0.018	234	38.0	68.8	117
65	0.003	94	17.2	184	230
65	0.005	142	26.5	170	150
65	0.008	157	28.4	115	140
65	0.010	187	32.3	104	128
65	0.012	256	40.8	110	115
65	0.018	287	45.2	81.7	112
86	0.003	113	26.3	281	183
86	0.005	179	36.5	234	130
86	0.008	206	39.8	160	123
86	0.010	213	39.5	127	121
86	0.012	309	55.1	149	111
86	0.018	338	57.4	104	111
100	0.003	79	14.6	156	313
100	0.005	137	22.8	146	153
100	0.008	159	25.3	102	139
100	0.010	192	29.0	93.8	126
100	0.012	283	45.3	122	113
100	0.018	303	51.1	92.3	112

The coefficients determined by regression were used in Equation 13 to compute the polynomial unique to this variant.

$$0 = B_2 * WOB^4 + 2B_1B_2 * WOB^3 + (B_1{}^2 + 2B_2B_0 - 2\pi A_1B_2) * WOB^2 + (2B_1B_0 - 4\pi A_0B_2) * WOB + (B_0{}^2 + 2A_1B_0 - 2\pi A_0B_1)0 \quad (58)$$

$$0 = -1.6E-15 * WOB^4 - 5.5E-12 * WOB^3 + 3.88E-08 * WOB^2 + 3.15E-06 * WOB - 0.00597 \quad (59)$$

This polynomial has four roots, which are indicated in Table 23.[35] Only the positive real root has physical meaning, indicating that the optimum Weight on Bit is 361 pounds.

Table 23 Roots of MSE_H Equation for Ambient Terretek Sandstone

Real solutions:
Root 1: -419.4
Root 2: 361.1
Complex roots:
Root 3: 1759.88-4638.91 * i
Root 4: 1759.88+4638.91 * i

Using the modified Torque and Penetration per Revolution equations, optimum values were computed and illustrated in Table 24.

Table 24 Optimum Values of Parameters for Ambient Terretek Sandstone

Parameter	Optimum Values
WOB (lb)	361
Torque (in-lb)	55.7
Penetration (in/rev)	0.016

Plots of MSE against Weight on Bit, Torque and Penetration per Revolution can be seen in Figure 58, Figure 59, and Figure 60.

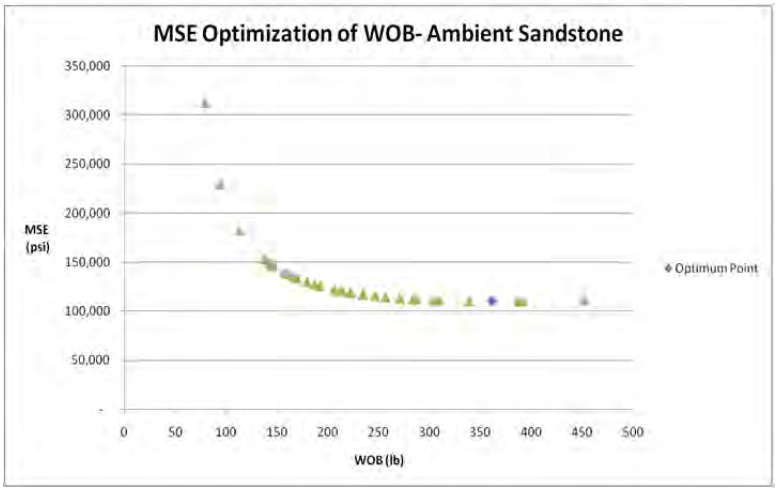

Figure 58 Optimum Weight on Bit Point Indicated for Ambient Terretek Sandstone

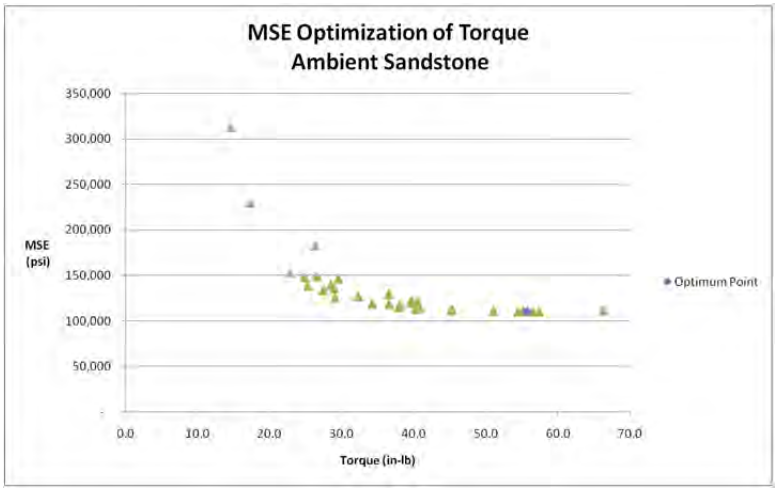

Figure 59 Optimum Torque Point Indicated for Ambient Terretek Sandstone

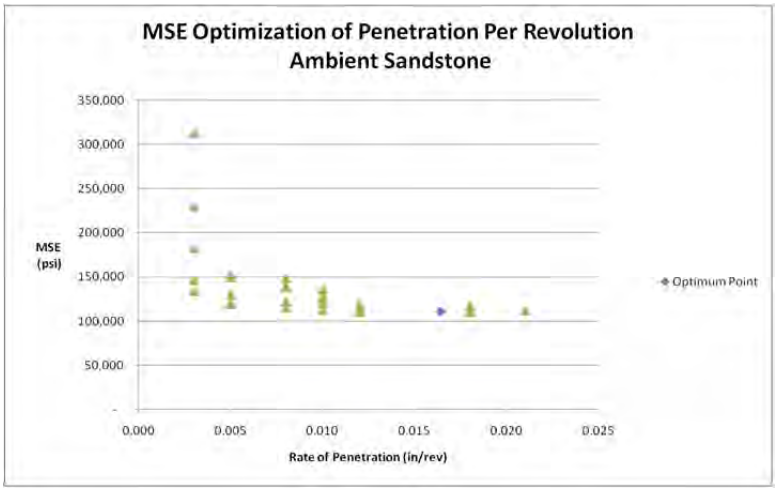

Figure 60 Optimum Rate of Penetration Point Indicated for Ambient Terretek Sandstone

Elevated Temperature and Ambient Pressure

Samples of Terretek Sandstone were heat soaked in an oven at 450 F for a minimum of two hours, then drilled using a standard ½ inch masonry bit at various RPM and Rate of Penetration settings. The results for each data point from testing Terretek Sandstone under these conditions can be found in Table 25.

The Weight on Bit data plotted against Torque can be seen in Figure 61. Under Assumption 2 a linear relationship was assumed, and the coefficients for the Torque equation were computed by regression.

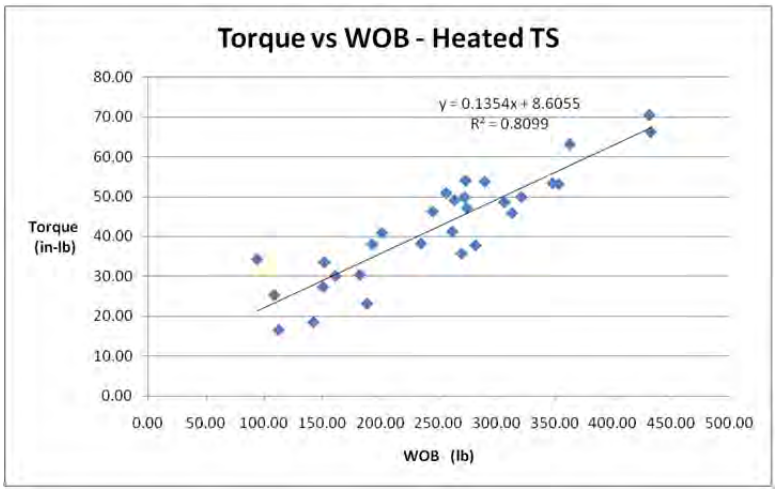

Figure 61 Torque as a Linear Function of Weight on Bit for Heated Sandstone

$$Torque = f(WOB) = A_0 + A_1 * WOB \quad (60)$$

$$Torque = f(WOB) = 8.6055 + 0.1354 * WOB \quad (61)$$

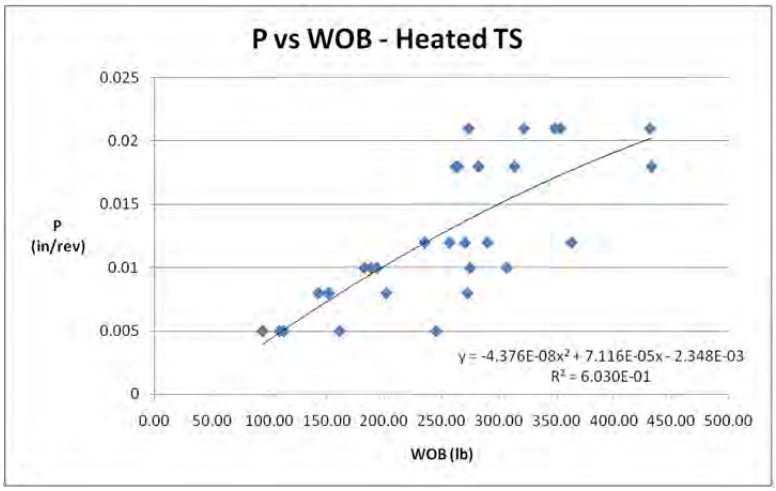

Figure 62 Rate of Penetration as a Function of Weight on Bit for Heated Marble

Similarly Weight on Bit was plotted against Penetration per Revolution, as can be seen in Figure 62. Under Assumption 3 a second order polynomial relationship was assumed, and the coefficients for the Penetration per Revolution equation were computed by regression.

$$ROP = g(WOB) = B_2 * WOB^2 + B_1 * WOB + B_0 \quad (62)$$

$$ROP = g(WOB) = -4.38\text{E}-08 * WOB^2 + 7.12\text{E}-05 * WOB - 2.35\text{E}-03 \quad (63)$$

The Torque and Penetration per Revolution equations were substituted into the MSE_H equation.

$$\text{MSE}_\text{H} = \frac{\text{WOB}}{\text{Area}} + \frac{2\,\pi * (\text{A}_0 + \text{A}_1 * \text{WOB})}{\text{Area} * (\text{B}_2 * \text{WOB}^2 + \text{B}_1 * \text{WOB} + \text{B}_0)} \quad (64)$$

$$\text{MSE}_\text{H} = \frac{\text{WOB}}{\text{Area}} + \frac{2\,\pi * (8.6055 + 0.1354 * WOB)}{\text{Area} * (-4.38\text{E}-08 * WOB^2 + 7.12\text{E}-05 * WOB - 2.35\text{E}-03)} \quad (65)$$

In Table 25 MSE was computed using both the conventional Equation 9 and the above equation. A comparison is plotted in Figure 33, where the proposed equation has a smoothing effect.

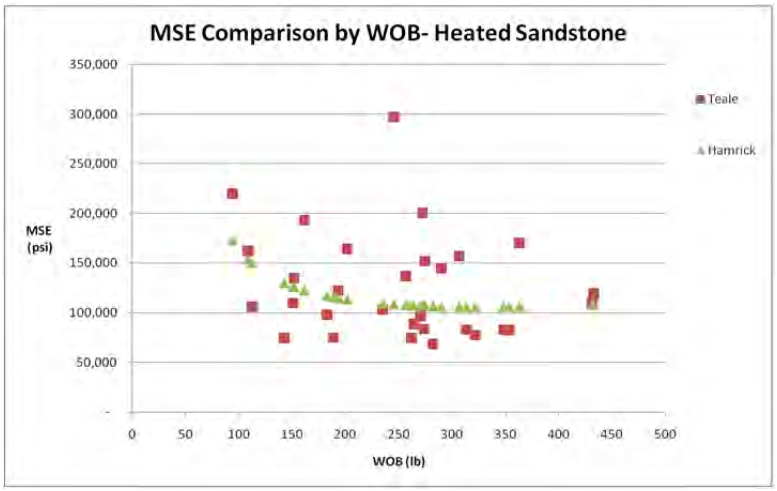

Figure 63 Comparison of Teale and Hamrick MSE Curves

Table 25 Comparison of Teale and Hamrick MSE Computations for Heated Sandstone

				Teale	Hamrick
RPM	in/Rev	WOB (lb)	Torque (in-lb)	MSE (ksi)	MSE (ksi)
21	0.005	94	34.3	220	173
21	0.008	152	33.5	135	126
21	0.010	193	38.0	123	115
21	0.012	257	50.9	137	108
21	0.018	264	49.1	88.6	107
21	0.021	273	54.0	83.6	107
43	0.005	161	30.1	193	123
43	0.008	201	40.8	164	113
43	0.010	274	47.1	152	107
43	0.012	290	53.7	145	106
43	0.018	313	45.8	83.0	106
43	0.021	348	53.3	83.0	106
65	0.005	245	46.2	297	109
65	0.008	272	49.7	200	107
65	0.010	306	48.5	157	106
65	0.012	363	63.1	170	106
65	0.018	433	66.1	120	108
65	0.021	431	70.4	109	108
86	0.005	112	16.5	106	150
86	0.008	142	18.5	74.6	130
86	0.010	189	23.1	75.0	116
86	0.012	270	35.6	96.4	107
86	0.018	282	37.7	68.5	107
86	0.021	353	53.1	82.7	106
100	0.005	109	25.3	162	154
100	0.008	151	27.3	110	127
100	0.010	182	30.3	98.0	117
100	0.012	235	38.2	103	109
100	0.018	262	41.2	74.5	107
100	0.021	321	49.8	77.6	106

The coefficients determined by regression were used in Equation 0 to compute the polynomial unique to this variant.

$$0 = B_2 * WOB^4 + 2B_1B_2 * WOB^3 + (B_1{}^2 + 2B_2B_0 - 2\pi A_1B_2) * WOB^2 + (2B_1B_0 - 4\pi A_0B_2) * WOB + (B_0{}^2 + 2A_1B_0 - 2\pi A_0B_1)0 \quad (66)$$

$$0 = 1.91E-15 * WOB^4 - 6.2E-12 * WOB^3 + 4.25E-08 * WOB^2 + 4.4E-06 * WOB - 0.00584 \quad (67)$$

This polynomial has four roots, which are indicated in Table 26.[35] Only the positive real root has physical meaning, indicating that the optimum Weight on Bit is 329 pounds.

Table 26 Roots of MSE_H Equation for Heated Sandstone

Real solutions:
Root 1: -410.5
Root 2: 328.7
Complex roots:
Root 3: 1666.998-4452.107 * i
Root 4: 1666.998+4452.107 * i

Using the modified Torque and Penetration per Revolution equations, optimum values were computed and illustrated in Table 27.

Table 27 Optimum Values of Parameters for Heated Sandstone

Parameter	Optimum Values
WOB (lb)	329
Torque (ft-lb)	53.1
Penetration (in/rev)	0.016

Plots of MSE against Weight on Bit, Torque and Penetration per Revolution can be seen in Figure 64, Figure 65, and Figure 66.

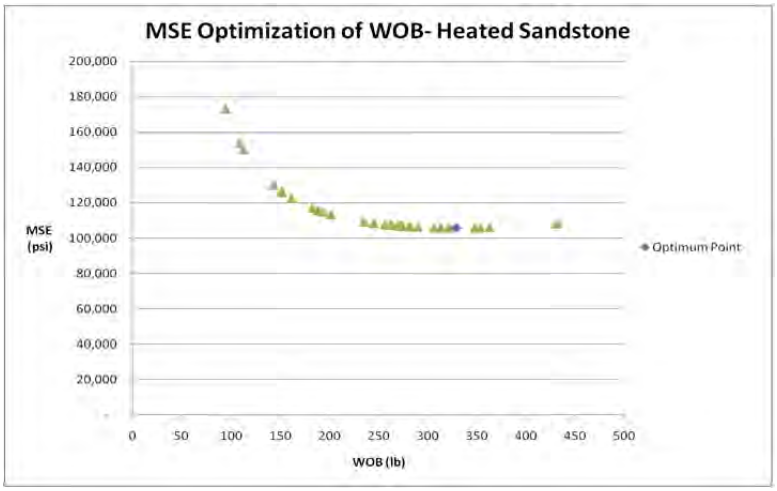

Figure 64 Optimum Weight on Bit Point Indicated for Heated Sandstone

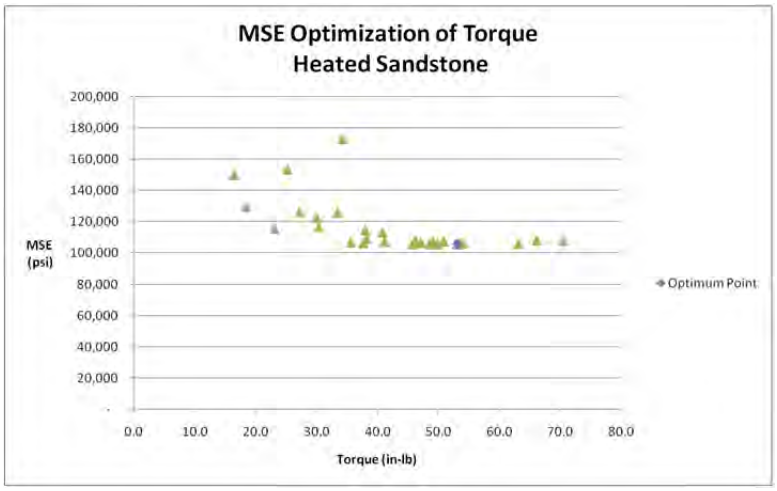

Figure 65 Optimum Torque Point Indicated for Heated Sandstone

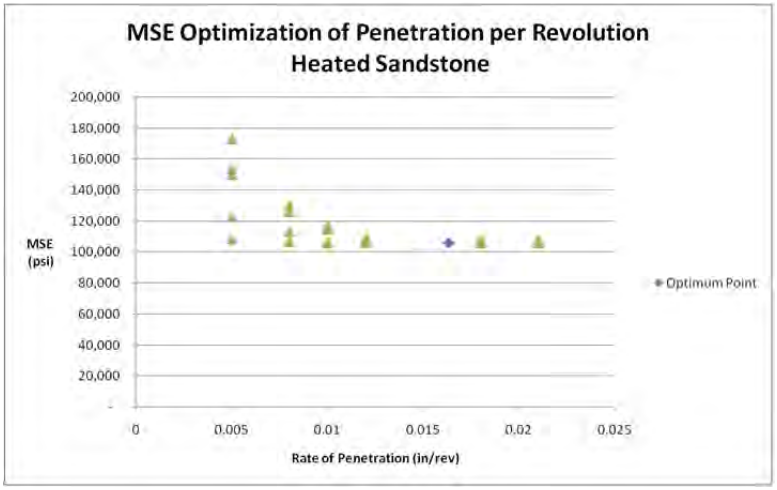

Figure 66 Optimum Rate of Penetration Point Indicated for Heated Sandstone

Elevated Confining Pressure

Samples of Terretek Sandstone were placed in a Hoek Cell and pressurized to 1500 psi confining pressure in the drilling apparatus, as described in the Drilling Experiments Section of this work. They were then drilled using a standard ½ inch masonry bit at various RPM and Rate of Penetration settings. The results for each data point from testing Terretek Sandstone under these conditions can be found in Table 28. The Weight on Bit data plotted against Torque can be seen in Figure 31. Under Assumption 2 a linear relationship was assumed, and the coefficients for the Torque equation were computed by regression.

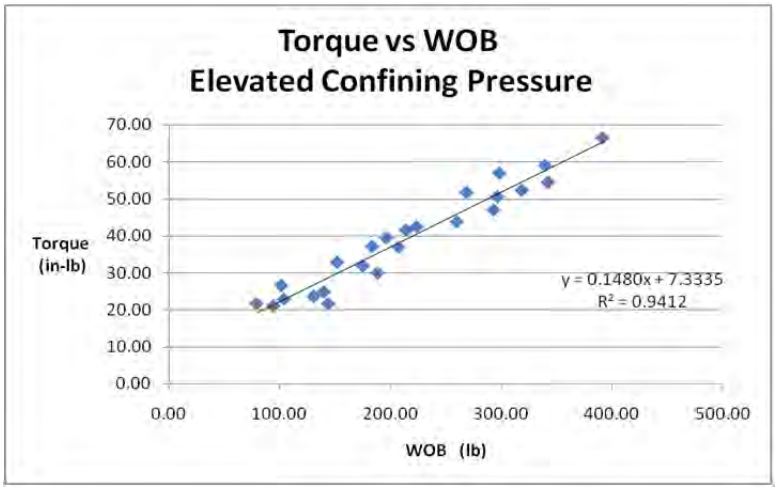

Figure 67 Torque as a Linear Function of Weight on Bit for Sandstone at Elevated Confining Pressure

$$Torque = f(WOB) = A_0 + A_1 * WOB \quad (68)$$

$$Torque = f(WOB) = 7.3335 + 0.148 * WOB \quad (69)$$

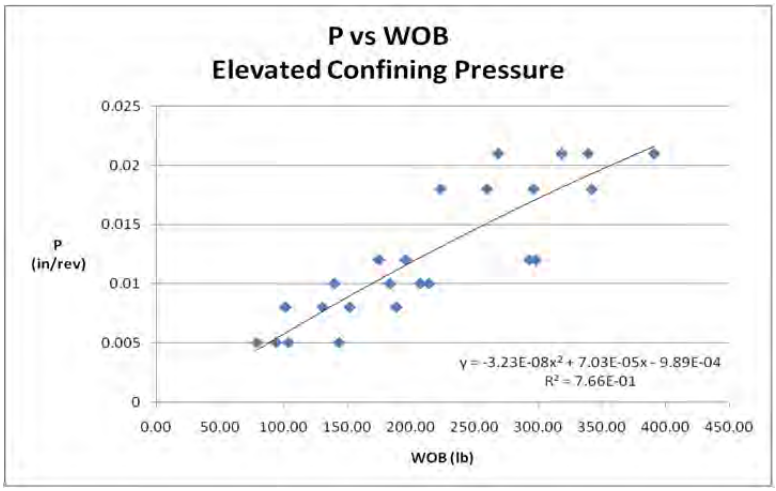

Figure 68 Rate of Penetration as a Function of Weight on Bit for Sandstone at Elevated Confining Pressure

Similarly Weight on Bit was plotted against Penetration per Revolution, as can be seen in Figure 68. Under Assumption 3 a second order polynomial relationship was assumed, and the coefficients for the Penetration per Revolution equation were computed by regression.

$$ROP = g(WOB) = B_2 * WOB^2 + B_1 * WOB + B_0 \quad (70)$$

$$ROP = g(WOB) = -3.23\text{E}-08 * WOB^2 + 7.03\text{E}-05 * WOB - 9.89\text{E}-04 \quad (71)$$

The Torque and Penetration per Revolution equations were substituted into the MSE_H equation.

$$\text{MSE}_\text{H} = \frac{\text{WOB}}{\text{Area}} + \frac{2\,\pi * (\text{A}_0 + \text{A}_1 * \text{WOB})}{\text{Area} * (\text{B}_2 * \text{WOB}^2 + \text{B}_1 * \text{WOB} + \text{B}_0)} \quad (72)$$

$$\text{MSE}_\text{H} = \frac{\text{WOB}}{\text{Area}} + \frac{2\,\pi * (7.3335 + 0.148 * WOB)}{\text{Area} * (-3.23\text{E}-08 * WOB^2 + 7.03\text{E}-05 * WOB - 9.89\text{E}-04)} \quad (73)$$

In Table 28 MSE was computed using both the conventional Equation 9 and the above equation. A comparison is plotted in Figure 69 where the proposed equation has a smoothing effect.

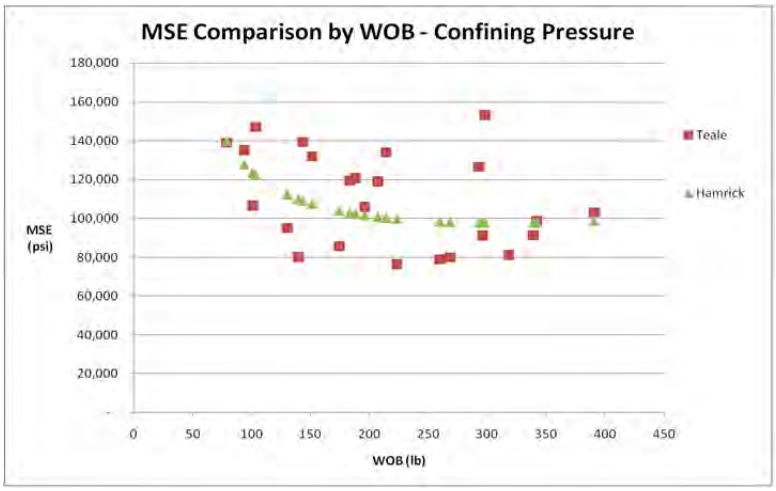

Figure 69 Comparison of Teale and Hamrick MSE Curves

Table 28 Terretek Sandstone at Elevated Confining Pressure Results

				Teale	Hamrick
RPM	in/Rev	WOB (lb)	Torque (in-lb)	MSE (ksi)	MSE (ksi)
21	0.005	143	21.7	139	109
21	0.008	188	29.9	121	102
21	0.010	207	36.9	119	101
21	0.012	293	46.9	127	97.9
21	0.018	296	50.6	91.4	97.8
21	0.021	339	58.9	91.5	97.9
43	0.005	79	21.7	139	140
43	0.008	101	26.6	107	124
43	0.010	183	37.1	120	103
43	0.012	196	39.4	106	102
43	0.018	223	42.4	76.5	100
43	0.021	269	51.7	80.1	98.2
65	0.005	94	21.1	135	128
65	0.008	130	23.6	95.1	112
65	0.010	140	24.8	80.2	110
65	0.012	175	31.8	85.8	104
65	0.018	260	43.8	79.1	98.4
65	0.021	318	52.3	81.2	97.8
100	0.005	104	22.9	147	122
100	0.008	152	32.8	132	107
100	0.010	214	41.5	134	100
100	0.012	298	56.9	153	97.8
100	0.018	342	54.5	98.6	97.9
100	0.021	391	66.4	103	98.8

The coefficients determined by regression were used in Equation 13 to compute the polynomial unique to this variant.

$$\begin{aligned} 0 = {} & B_2 * WOB^4 + 2B_1B_2 * WOB^3 + (B_1{}^2 + 2B_2B_0 \\ & - 2\pi A_1B_2) * WOB^2 \\ & + (2B_1B_0 - 4\pi A_0B_2) * WOB \\ & + (B_0{}^2 + 2A_1B_0 - 2\pi A_0B_1)0 \end{aligned} \tag{74}$$

$$\begin{aligned} 0 = {} & 1.04329E-15 * WOB^4 - 4.54138E-12 \\ & * WOB^3 + 3.50421E-08 * WOB^2 \\ & + 2.83757E-06 * WOB - 0.00416 \end{aligned} \tag{75}$$

This polynomial has four roots, which are indicated in Table 29.[35] Only the positive real root has physical meaning, indicating that the optimum Weight on Bit is 312 pounds.

Table 29 Roots of MSE_H Equation for Sandstone at Elevated Confining Pressure

Real solutions:
Root 1: -376.3
Root 2: 311.6
Complex roots:
Root 3: 2208.859-5395.593 * i
Root 4: 2208.859+5395.593 * i

Using the modified Torque and Penetration per Revolution equations, optimum values were computed and illustrated in Table 30.

Table 30 Optimum Values of Parameters for Heated Sandstone

Parameter	Optimum Values
WOB (lb)	312
Torque (in-lb)	53.4
Penetration (in/rev)	0.018

Plots of MSE against Weight on Bit, Torque and Penetration per Revolution can be seen in Figure 70, Figure 71, and Figure 72.

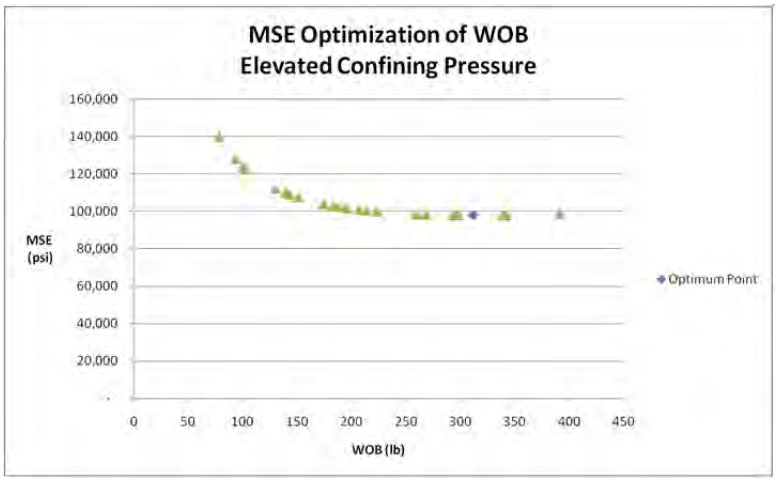

Figure 70 Optimum Weight on Bit Point Indicated for Sandstone at Elevated Confining Pressure

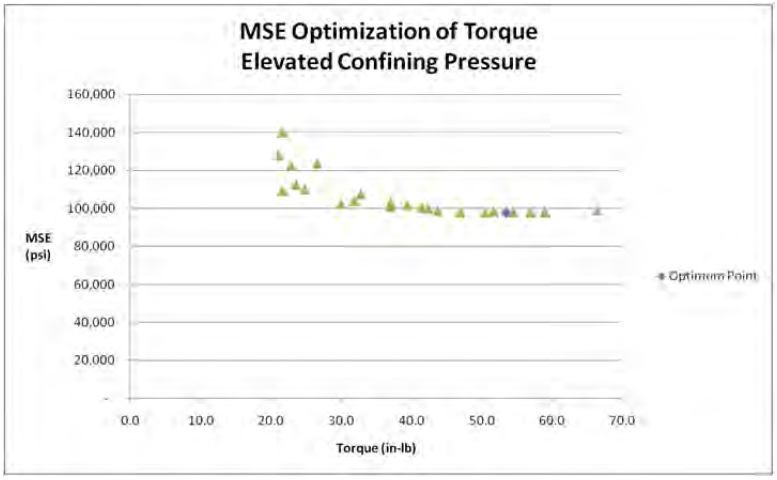

Figure 71 Optimum Torque Point Indicated for Sandstone at Elevated Confining Pressure

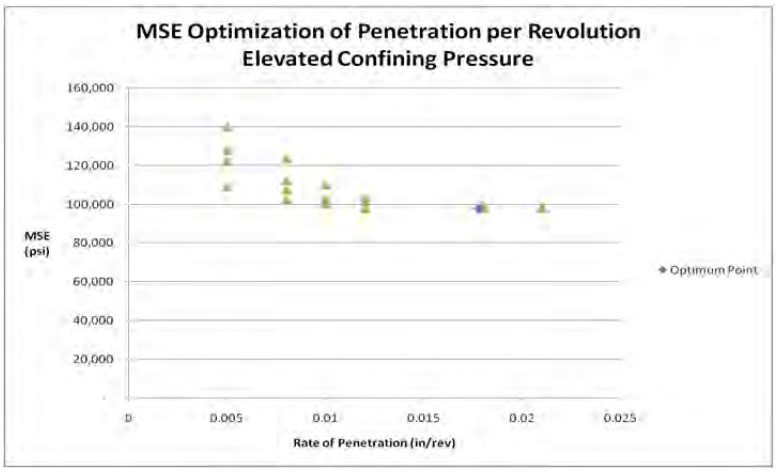

Figure 72 Optimum Rate of Penetration Point Indicated for Sandstone at Elevated Confining Pressure

2-Wing Bit

Samples of Terretek Sandstone were drilled in the drilling apparatus at ambient temperature and pressure using a 2-wing ½ inch drill bit as described in the Drilling Experiments Section of this work. They were then drilled at various RPM and Rate of Penetration settings. The results for each data point from testing Terretek Sandstone under these conditions can be found in Table 31. The Weight on Bit data plotted against Torque can be seen in Figure 73. Under Assumption 2 a linear relationship was assumed, and the coefficients for the Torque equation were computed by regression.

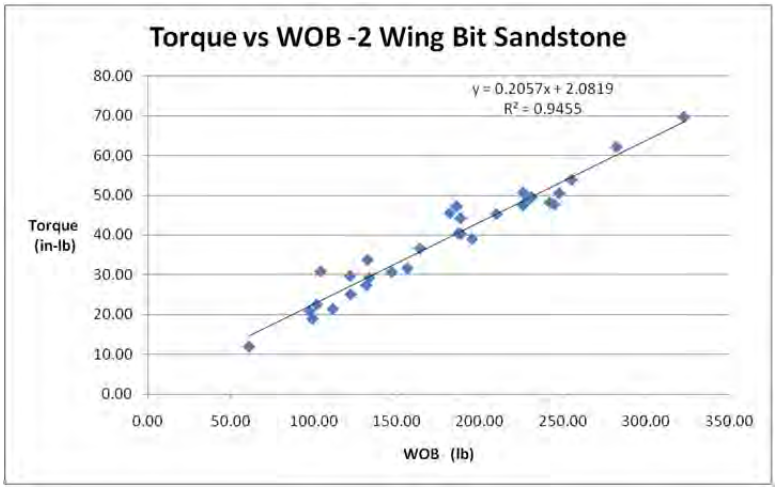

Figure 73 Torque as a Linear Function of Weight on Bit for Sandstone Drilled With a 2-Wing Bit

$$Torque = f(WOB) = A_0 + A_1 * WOB \quad (76)$$

$$Torque = f(WOB) = 2.0819 + 0.2057 * WOB \quad (77)$$

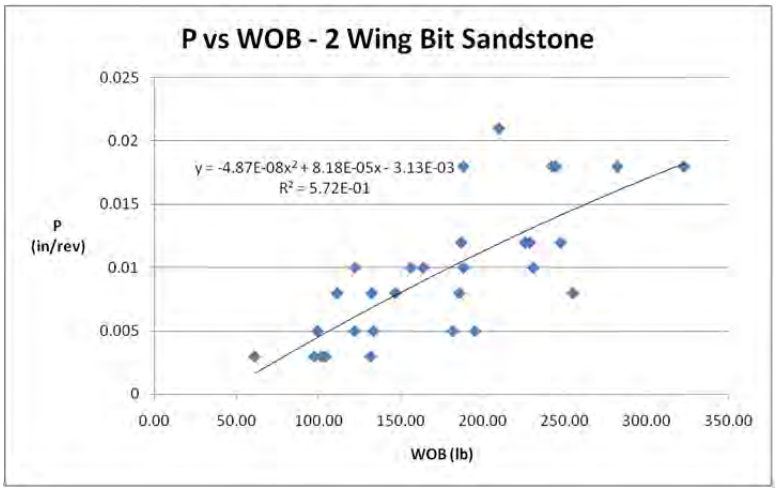

Figure 74 Rate of Penetration as a Function of Weight on Bit for Sandstone Drilled With a 2-Wing Bit

Similarly Weight on Bit was plotted against Penetration per Revolution, as can be seen in Figure 74. Under Assumption 3 a second order polynomial relationship was assumed, and the coefficients for the Penetration per Revolution equation were computed by regression.

$$ROP = g(WOB) = B_2 * WOB^2 + B_1 * WOB + B_0 \quad (78)$$

$$ROP = g(WOB) = -5.00\text{E}-08 * WOB^2 + 8.18\text{E}-05 * WOB - 3.13\text{E}-03 \quad (79)$$

The Torque and Penetration per Revolution equations were substituted into the MSE_H equation.

$$\text{MSE}_\text{H} = \frac{\text{WOB}}{\text{Area}} + \frac{2\,\pi * (\text{A}_0 + \text{A}_1 * \text{WOB})}{\text{Area} * (\text{B}_2 * \text{WOB}^2 + \text{B}_1 * \text{WOB} + \text{B}_0)} \quad (80)$$

$$\text{MSE}_\text{H} = \frac{\text{WOB}}{\text{Area}} + \frac{2\,\pi * (2.0819 + 0.2057 * WOB)}{\text{Area} * (-5.00\text{E}-08 * WOB^2 + 8.18\text{E}-05 * WOB - 3.13\text{E}-03)} \quad (81)$$

In Table 31 MSE was computed using both the conventional Equation 9 and the above equation. A comparison is plotted in Figure 75, where the proposed equation has a smoothing effect.

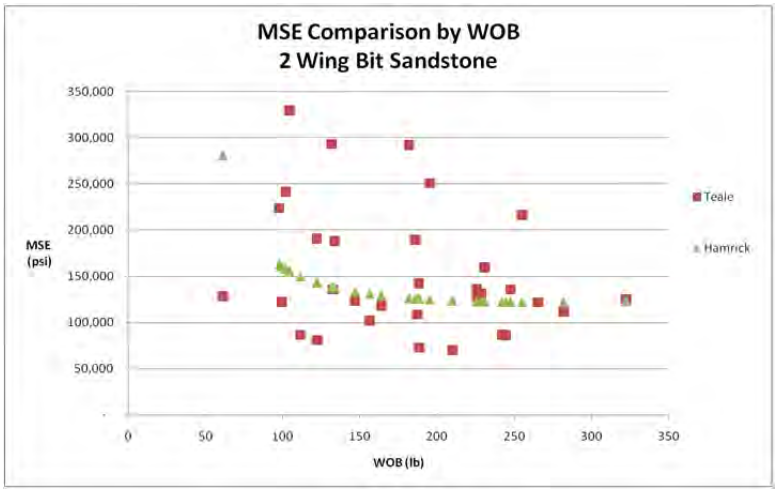

Figure 75 Comparison of Teale and Hamrick MSE Curves

Table 31 Terretek Sandstone Two Wing Bit Drilling Results

				Teale	Hamrick
RPM	in/Rev	WOB (lb)	Torque (in-lb)	MSE (ksi)	MSE (ksi)
21	0.003	61	12.0	128	281
21	0.005	99	19.0	122	161
21	0.008	111	21.5	86.5	150
21	0.010	122	25.1	81.0	143
21	0.012	187	40.4	109	126
21	0.018	188	40.3	72.6	125
21	0.021	210	45.2	70.0	123
43	0.003	97	20.9	224	163
43	0.005	133	29.3	188	138
43	0.008	147	30.7	124	133
43	0.010	156	31.6	102	131
43	0.012	226	47.4	128	123
43	0.018	242	48.1	86.7	122
65	0.003	104	30.9	330	156
65	0.005	182	45.5	292	126
65	0.008	186	47.2	190	126
65	0.010	188	44.2	142	125
65	0.012	226	50.6	136	123
65	0.018	323	69.5	125	123
86	0.003	102	22.6	241	158
86	0.005	122	29.7	191	143
86	0.008	132	33.7	136	138
86	0.010	164	36.6	118	129
86	0.012	229	48.8	131	122
86	0.018	282	62.0	112	122
100	0.003	132	27.4	293	139
100	0.005	195	39.0	251	125
100	0.008	255	53.8	217	122
100	0.010	231	49.5	160	122
100	0.012	247	50.4	136	122
100	0.018	244	47.7	86.0	122

The coefficients determined by regression were used in Equation 13 to compute the polynomial unique to this variant.

$$0 = B_2 * WOB^4 + 2B_1B_2 * WOB^3 + (B_1{}^2 + 2B_2B_0 - 2\pi A_1B_2) * WOB^2 + (2B_1B_0 - 4\pi A_0B_2) * WOB + (B_0{}^2 + 2A_1B_0 - 2\pi A_0B_1)0 \quad (82)$$

$$0 = 2.5E-15 * WOB^4 - 8.2E-12 * WOB^3 + 7.16E-08 * WOB^2 + 7.96E-07 * WOB - 0.00511 \quad (83)$$

This polynomial has four roots, which are indicated in Table 32.[35] Only the positive real root has physical meaning, indicating that the optimum Weight on Bit is 265 pounds.

Table 32 Roots of MSE_H Equation for Sandstone Drilled With a 2-Wing Bit

Real solutions:
Root 1: -268.1
Root 2: 265.2
Complex roots:
Root 3: 1637.289-5104.188 * i
Root 4: 1637.289+5104.188 * i

Using the modified Torque and Penetration per Revolution equations, optimum values were computed and illustrated in Table 33.

Table 33 Optimum Values of Parameters for Sandstone Drilled With a 2-Wing bit

Parameter	Optimum Values
WOB (lb)	265
Torque (in-lb)	56.6
Penetration (in/rev)	0.015

Plots of MSE against Weight on Bit, Torque and Penetration per Revolution can be seen in Figure 76, Figure 77, and Figure 78

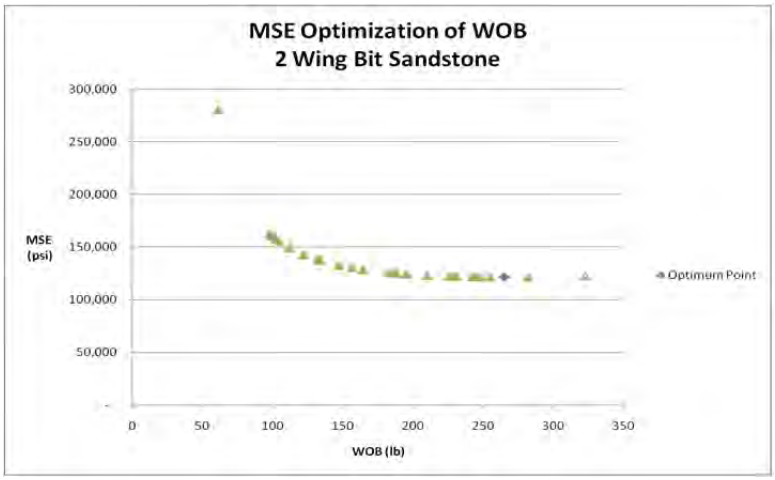

Figure 76 Optimum Weight on Bit Point Indicated for Sandstone at Elevated Confining Pressure

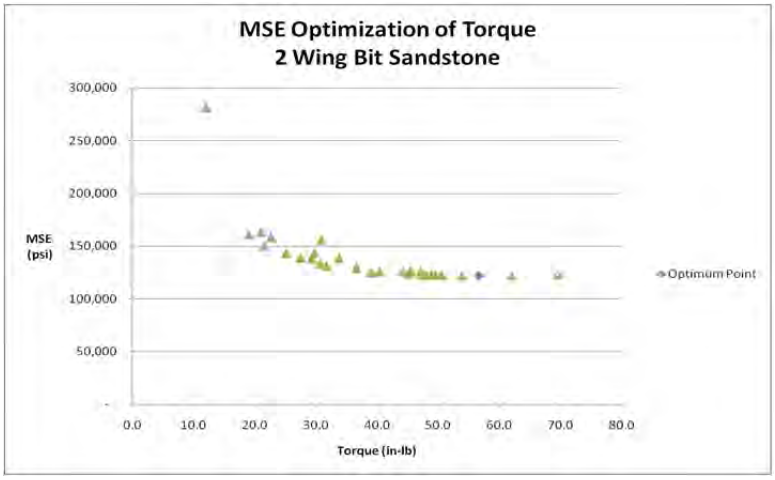

Figure 77 Optimum Torque Point Indicated for Sandstone at Elevated Confining Pressure

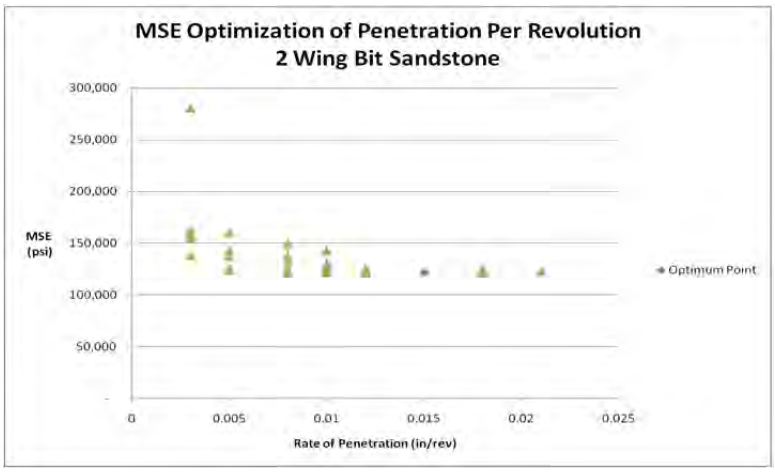

Figure 78 Optimum Rate of Penetration Point Indicated for Sandstone at Elevated Confining Pressure

Corroborative Results From Published Data

Deeptrek Test 17 – Impregnated Bit in Mancos Shale

The method was applied to data generated in the Deeptrek study. This data set was generated by drilling with a 6 inch diameter diamond impregnated bit in Mancos Shale.[28] The data is found in Table 34. The Weight on Bit data plotted against Torque can be seen in Figure 79. Under Assumption 2 a linear relationship was assumed, and the coefficients for the Torque equation were computed by regression.

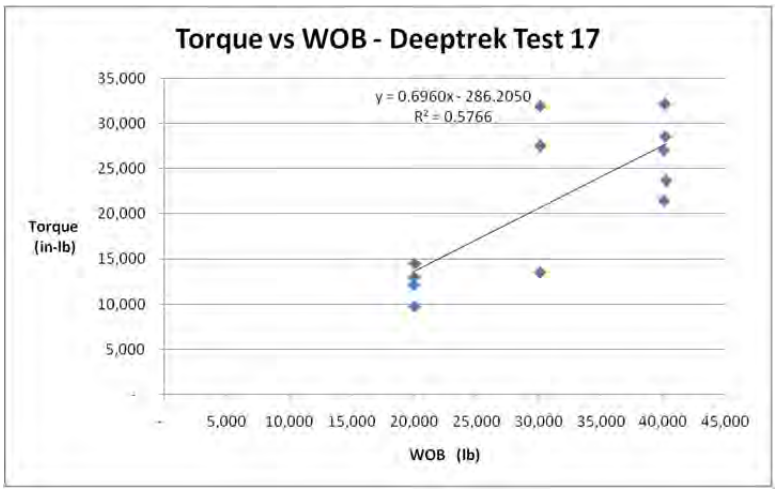

Figure 79 Torque as a Linear Function of Weight on Bit for Impregnated Bit in Mancos Shale

$$Torque = f(WOB) = A_0 + A_1 * WOB \quad (84)$$

$$Torque = f(WOB) = -286.21 + 0.696 * WOB \quad (85)$$

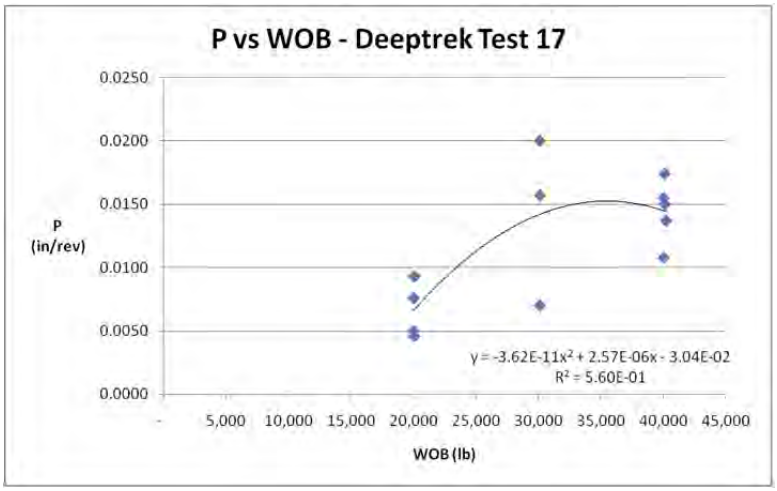

Figure 80 Rate of Penetration as a Function of Weight on Bit for Impregnated Bit in Mancos Shale

Similarly Weight on Bit was plotted against Penetration per Revolution, as can be seen in Figure 80. Under Assumption 3 a second order polynomial relationship was assumed, and the coefficients for the Penetration per Revolution equation were computed by regression.

$$ROP = g(WOB) = B_2 * WOB^2 + B_1 * WOB + B_0 \quad (86)$$

$$ROP = g(WOB) = -3.62\text{E}-11 * WOB^2 + 2.57\text{E}-06 * WOB - 3.04\text{E}-02 \quad (87)$$

The Torque and Penetration per Revolution equations were substituted into the MSE_H equation.

$$\text{MSE}_\text{H} = \frac{\text{WOB}}{\text{Area}} + \frac{2\,\pi * (\text{A}_0 + \text{A}_1 * \text{WOB})}{\text{Area} * (\text{B}_2 * \text{WOB}^2 + \text{B}_1 * \text{WOB} + \text{B}_0)} \quad (88)$$

$$\text{MSE}_\text{H} = \frac{\text{WOB}}{\text{Area}} + \frac{2\,\pi * (-286.21 + 0.696 * WOB)}{\text{Area} * (-3.62\text{E}-11 * WOB^2 + 2.57\text{E}-06 * WOB - 3.04\text{E}-02)} \quad (89)$$

In Table 34 MSE was computed using both the conventional Equation 9 and the above equation. A comparison is plotted in Figure 81.

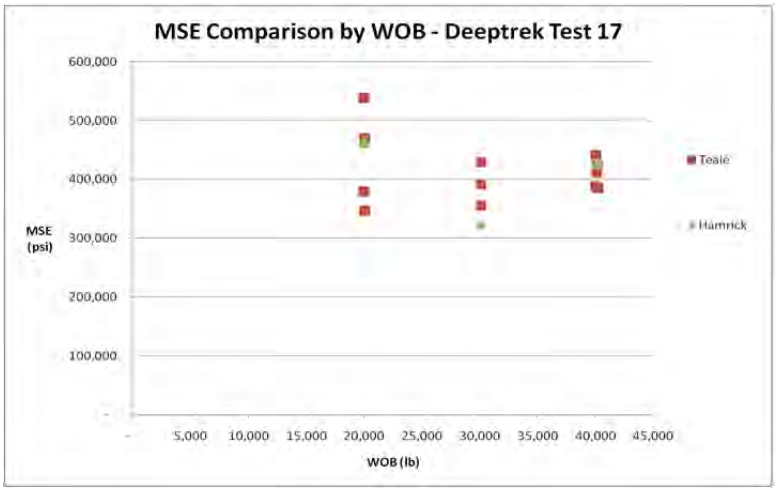

Figure 81 Comparison of Teale and Hamrick MSE Curves

Table 34 Deeptrek Test 17 – Impregnated Bit in Mancos Shale Results

				Teale	Hamrick
RPM	in/Rev	WOB (lb)	Torque (in-lb)	MSE (ksi)	MSE (ksi)
60	0.0200	30,100	31,900	356	325
60	0.0093	20,100	14,500	347	462
60	0.0174	40,100	32,200	412	427
120	0.0157	30,100	27,500	391	325
120	0.0137	40,300	23,600	385	430
120	0.0076	20,021	12,900	379	464
180	0.0050	20,000	12,100	539	465
180	0.0155	40,0 00	27,000	389	425
180	0.0150	40,200	28,500	424	428
221	0.0070	30,100	13,500	429	325
221	0.0108	40,100	21,400	442	426
221	0.0046	20,100	9,710	470	462

The coefficients determined by regression were used in Equation 13 to compute the polynomial unique to this variant.

$$0 = B_2 * WOB^4 + 2B_1B_2 * WOB^3 + (B_1{}^2 + 2B_2B_0 - 2\pi A_1B_2) * WOB^2 + (2B_1B_0 - 4\pi A_0B_2) * WOB + (B_0{}^2 + 2A_1B_0 - 2\pi A_0B_1)0 \quad (90)$$

$$0 = 1.31E-21 * WOB^4 - 1.9E-16 * WOB^3 + 1.67E-10 * WOB^2 - 2.9E-07 * WOB - 0.1274 \quad (91)$$

This polynomial has four roots, which are indicated in Table 35.[35] Only the positive real root has physical meaning, indicating that the optimum Weight on Bit is 28,900 pounds.

Table 35 Roots of MSE_H Equation for Impregnated Bit in Mancos Shale

Real solutions:
Root 1: -26,327.3
Root 2: 28,864.4
Complex roots:
Root 3: 69725.95-350810.485 * i
Root 4: 69725.95+350810.485 * i

Using the modified Torque and Penetration per Revolution equations, optimum values were computed and illustrated in Table 36.

Table 36 Optimum Values of Parameters for Impregnated Bit in Mancos Shale

Parameter	Optimum Values
WOB (lb)	28,900
Torque (in-lb)	19,800
Penetration (in/rev)	0.014

Plots of MSE against Weight on Bit, Torque and Penetration per Revolution can be seen in Figure 82, Figure 83, and Figure 84

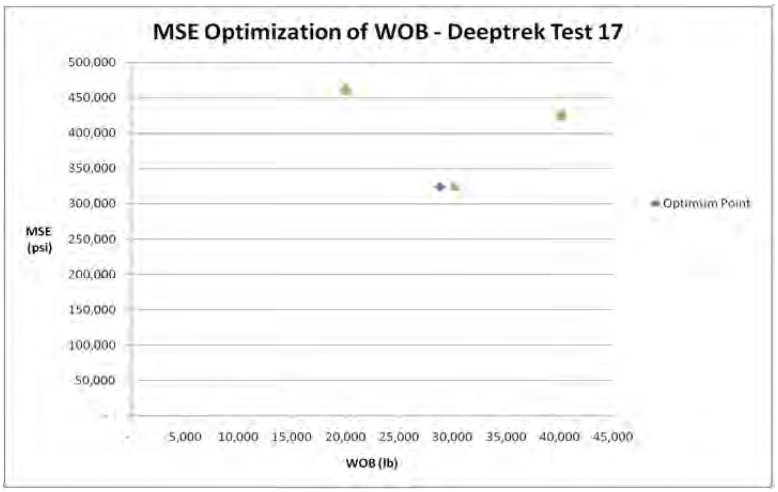

Figure 82 Optimum Weight on Bit Point Indicated for Impregnated Bit in Mancos Shale

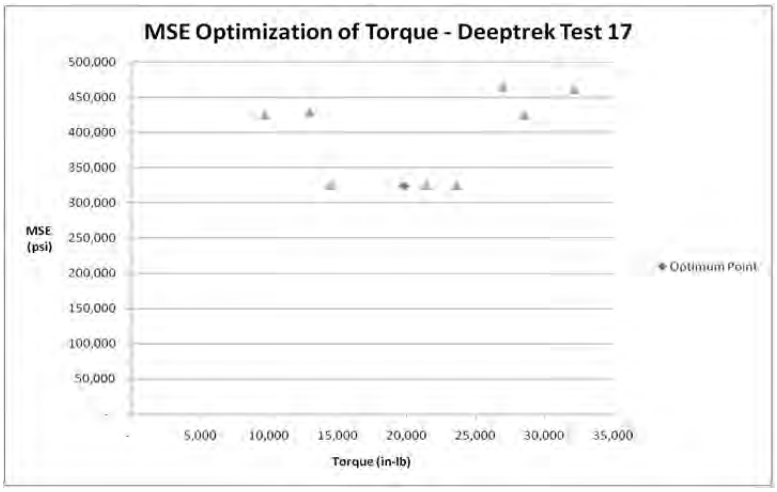

Figure 83 Optimum Torque Point Indicated for Impregnated Bit in Mancos Shale

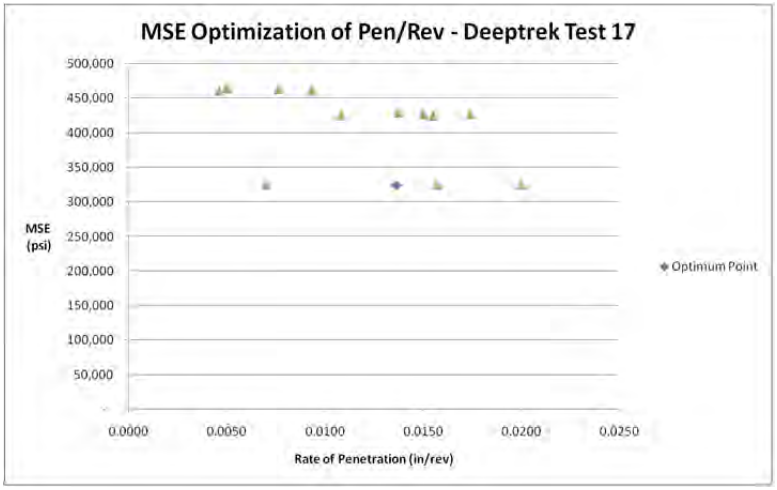

Figure 84 Optimum Rate of Penetration Point Indicated for Impregnated Bit in Mancos Shale

Deeptrek Test 3 – Roller Cone Bit in Terretek Sandstone

The method was applied to data generated in the Deeptrek study. This data set was generated by drilling with a 6 inch diameter roller cone bit in Terretek Sandstone.[28] The data is found in Table 37. The Weight on Bit data plotted against Torque can be seen in Figure 85. Under Assumption 2 a linear relationship was assumed, and the coefficients for the Torque equation were computed by regression.

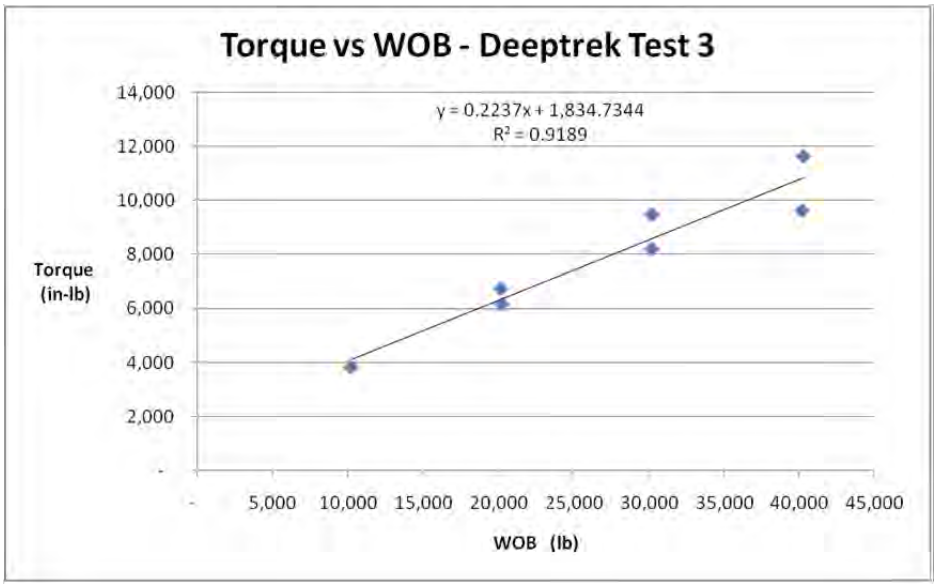

Figure 85 Torque as a Linear Function of Weight on Bit for Roller Cone Bit in Terretek Sandstone

$$Torque = f(WOB) = A_0 + A_1 * WOB \quad (92)$$

$$Torque = f(WOB) = 1{,}834.73 + 0.2237 * WOB \quad (93)$$

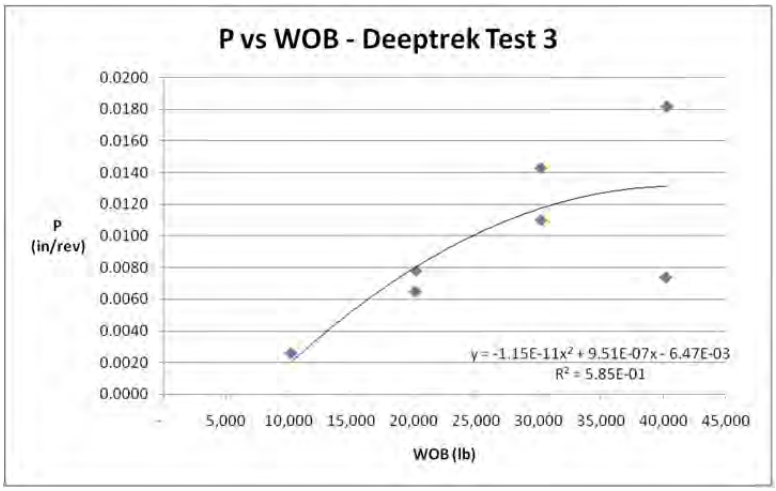

Figure 86 Rate of Penetration as a Function of Weight on Bit for Roller Cone Bit in Terretek Sandstone Shale

Similarly Weight on Bit was plotted against Penetration per Revolution, as can be seen in Figure 86. Under Assumption 3 a second order polynomial relationship was assumed, and the coefficients for the Penetration per Revolution equation were computed by regression.

$$ROP = g(WOB) = B_2 * WOB^2 + B_1 * WOB + B_0 \quad (94)$$

$$ROP = g(WOB) = -1.15\text{E}-11 * WOB^2 + 9.51\text{E}-07 * WOB - 6.47\text{E}-03 \quad (95)$$

The Torque and Penetration per Revolution equations were substituted into the MSE_H equation.

$$\text{MSE}_\text{H} = \frac{\text{WOB}}{\text{Area}} + \frac{2\,\pi * (\text{A}_0 + \text{A}_1 * \text{WOB})}{\text{Area} * (\text{B}_2 * \text{WOB}^2 + \text{B}_1 * \text{WOB} + \text{B}_0)} \quad (96)$$

$$\text{MSE}_\text{H} = \frac{\text{WOB}}{\text{Area}} + \frac{2\,\pi * (1{,}834.73 + 0.2237 * WOB)}{\text{Area} * (-1.15\text{E}-11 * WOB^2 + 9.51\text{E}-07 * WOB - 6.47\text{E}-03)} \quad (97)$$

In Table 37 MSE was computed using both the conventional Equation 9 and the above equation. A comparison is plotted in Figure 87, where the proposed equation has a smoothing effect.

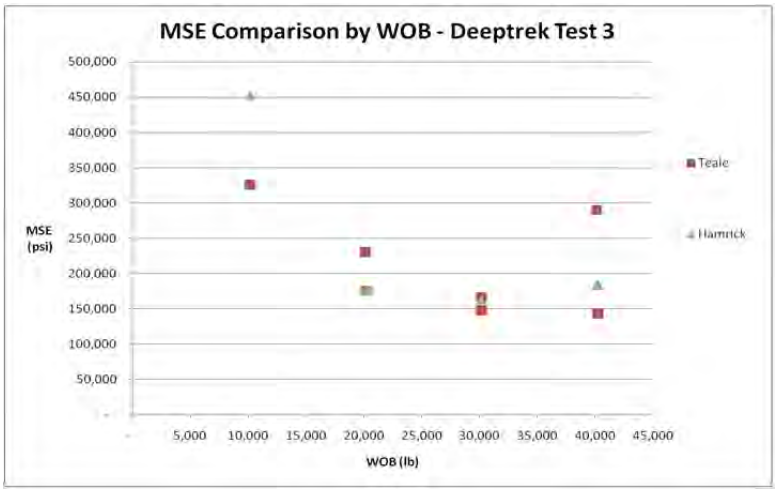

Figure 87 Comparison of Teale and Hamrick MSE Curves

Table 37 Deeptrek Test 3 – Roller Cone Bit in Terretek Sandstone Results

				Teale	Hamrick
RPM	in/Rev	WOB (lb)	Torque (in-lb)	MSE (ksi)	MSE (ksi)
71	0.0026	10,200	3,810	327	453
71	0.0065	20,100	6,730	231	176
71	0.0078	20,200	6,150	176	176
71	0.0143	30,200	9,480	148	163
71	0.0110	30,200	8,210	167	163
71	0.0074	40,200	9,620	290	184
71	0.0182	40,300	11,600	144	184

The coefficients determined by regression were used in Equation 13 to compute the polynomial unique to this variant.

$$0 = B_2 * WOB^4 + 2B_1B_2 * WOB^3 + (B_1{}^2 + 2B_2B_0 - 2\pi A_1B_2) * WOB^2 + (2B_1B_0 - 4\pi A_0B_2) * WOB + (B_0{}^2 + 2A_1B_0 - 2\pi A_0B_1)0 \quad (98)$$

$$0 = 1.31E-21 * WOB^4 - 1.9E-16 * WOB^3 + 1.67E-10 * WOB^2 - 2.9E-07 * WOB - 0.1274 \quad (99)$$

This polynomial has four roots, which are indicated in Table 38.[35] Only the positive real root has physical meaning, indicating that the optimum Weight on Bit is 27,860 pounds.

Table 38 Roots of MSE_H Equation for Roller Cone Bit in Terretek Sandstone

Real solutions:
Root 1: -40,660
Root 2: 27,860.8
Complex roots:
Root 3: 89095.265-354486.684 * i
Root 4: 89095.265+354486.684 * i

Using the modified Torque and Penetration per Revolution equations, optimum values were computed and illustrated in Table 39.

Table 39 Optimum Values of Parameters for Roller Cone Bit in Terretek Sandstone

Parameter	Optimum Values
WOB (lb)	27,900
Torque (in-lb)	8070
Penetration (in/rev)	0.011

Plots of MSE against Weight on Bit, Torque and Penetration per Revolution can be seen in Figure 88, Figure 89, and Figure 90.

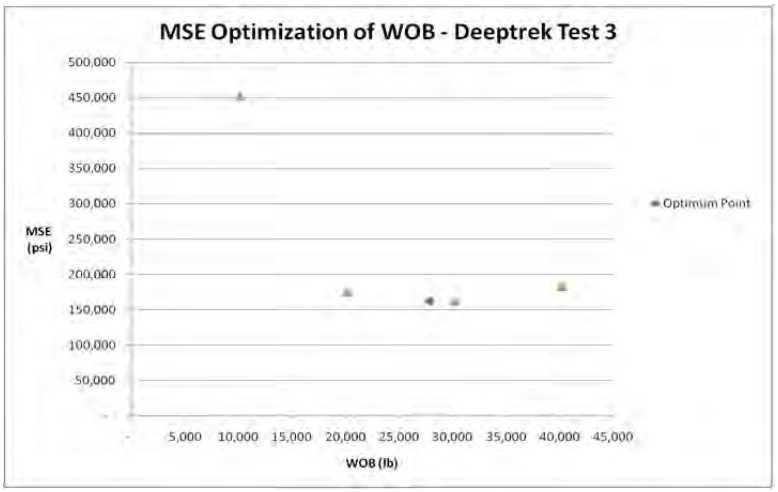

Figure 88 Optimum Weight on Bit Point Indicated for Roller Cone Bit in Terretek Sandstone

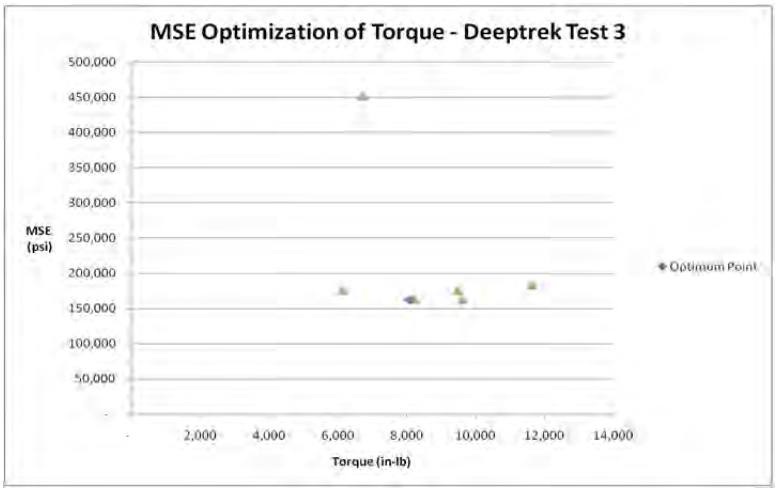

Figure 89 Optimum Torque Point Indicated for Roller Cone Bit in Terretek Sandstone

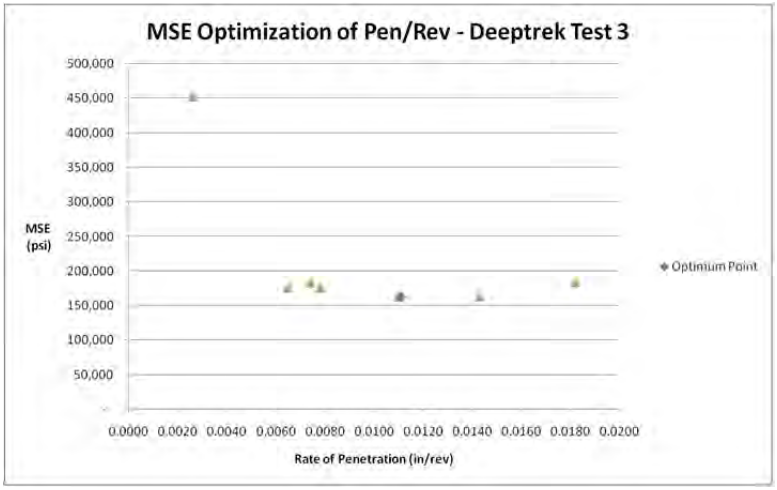

Figure 90 Optimum Rate of Penetration Point Indicated for Roller Cone Bit in Sandstone

Deeptrek Test 5 – PDC Bit in Carthage Marble

The method was applied to data generated in the Deeptrek study. This data set was generated by drilling with a 6 inch diameter PDC bit in Carthage Marble.[28] The data for this variant is displayed in Table 40. The Weight on Bit data plotted against Torque can be seen in Figure 91. Under Assumption 2 a linear relationship was assumed, and the coefficients for the Torque equation were computed by regression.

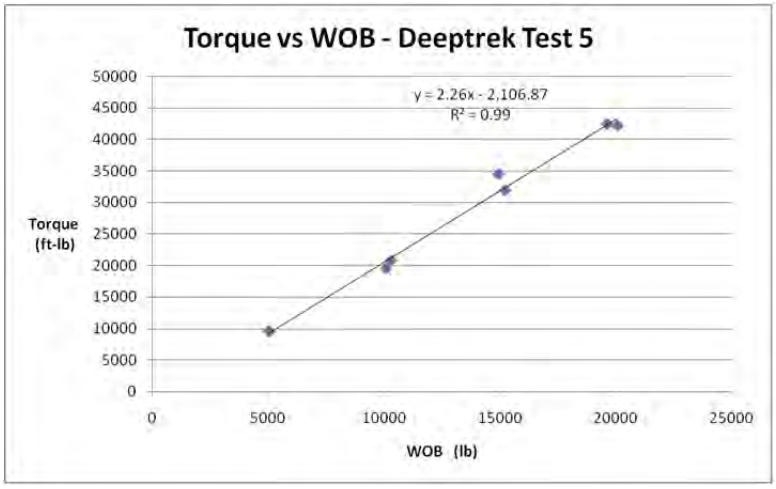

Figure 91 Torque as a Linear Function of Weight on Bit for PDC Bit in Marble

$$Torque = f(WOB) = A_0 + A_1 * WOB \quad (100)$$

$$Torque = f(WOB) = -2{,}106.87 + 2.26 * WOB \quad (101)$$

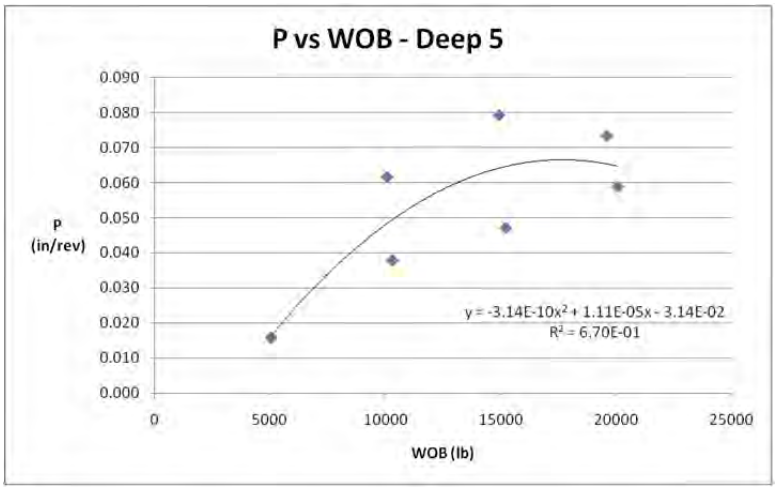

Figure 92 Rate of Penetration as a Function of Weight on Bit for PDC Bit in Marble

Similarly Weight on Bit was plotted against Penetration per Revolution, as can be seen in Figure 92. Under Assumption 3 a second order polynomial relationship was assumed, and the coefficients for the Penetration per Revolution equation were computed by regression.

$$ROP = g(WOB) = B_2 * WOB^2 + B_1 * WOB + B_0 \quad (102)$$

$$ROP = g(WOB) = -3.14\text{E}-10 * WOB^2 + 1.11\text{E}-05 * WOB - 3.14\text{E}-02 \quad (103)$$

The Torque and Penetration per Revolution equations were substituted into the MSE_H equation.

$$\mathrm{MSE_H} = \frac{\mathrm{WOB}}{\mathrm{Area}} + \frac{2\,\pi * (\mathrm{A_0} + \mathrm{A_1} * \mathrm{WOB})}{\mathrm{Area} * (\mathrm{B_2} * \mathrm{WOB}^2 + \mathrm{B_1} * \mathrm{WOB} + \mathrm{B_0})} \quad (104)$$

$$\mathrm{MSE_H} = \frac{\mathrm{WOB}}{\mathrm{Area}} + \frac{2\,\pi * (-2{,}106.87 + 2.26 * WOB)}{\mathrm{Area} * (-3.14\text{E}-10 * WOB^2 + 1.11\text{E}-05 * WOB - 3.14\text{E}-02)} \quad (105)$$

In Table 40 MSE was computed using both the conventional Equation 9 and the above equation. A comparison is plotted in Figure 93, where the proposed equation has a smoothing effect.

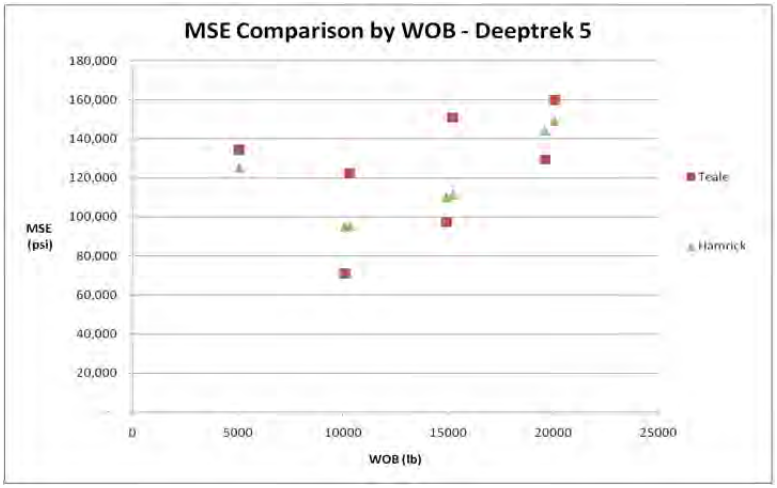

Figure 93 Comparison of Teale and Hamrick MSE Curves

Table 40 Deeptrek Test 5 – PDC Bit in Marble Results

	Penetr	WOB	Torque	Teale	Hamrick
RPM	in/Rev	(lb)	(in-lb)	MSE (ksi)	MSE (ksi)
90	0.016	5,040	9,550	135	125
90	0.038	10,300	20,800	122	95.4
90	0.047	15,200	31,900	151	111
90	0.059	20,100	42,200	160	149
121	0.062	10,100	19,500	70.9	95.1
121	0.073	19,600	42,500	129	144
121	0.079	14,900	34,500	97.3	110

The coefficients determined by regression were used in Equation 13 to compute the polynomial unique to this variant.

$$\begin{aligned} 0 = {} & B_2 * WOB^4 + 2B_1B_2 * WOB^3 + (B_1{}^2 + 2B_2B_0 \\ & - 2\pi A_1B_2) * WOB^2 \\ & + (2B_1B_0 - 4\pi A_0B_2) * WOB \\ & + (B_0{}^2 + 2A_1B_0 - 2\pi A_0B_1)0 \end{aligned} \tag{106}$$

$$0 = 9.86\text{EE} - 20 * \text{WOB}^4 - 7\text{EE} - 15 * \text{WOB}^3 + 4.61\text{E} - 09 * \text{WOB}^2 - 9\text{E} - 06 * \text{WOB} - 0.299 \quad (107)$$

This polynomial has four roots, which are indicated in Table 41.[35] Only the positive real root has physical meaning, indicating that the optimum Weight on Bit is 9149 pounds.

Table 41 Four Roots of MSE Minimization Function For Deeptrek Test 5 Example

Real solutions:
Root 1: -7096.1
Root 2: 9149.0
Complex roots:
Root 3: 34323.9-213330.1 * i
Root 4: 34323.9+213330.1 * i

Using the modified Torque and Penetration per Revolution equations, optimum values were computed and illustrated in Table 42

Table 42 Optimum Values of Parameters in Deeptrek Test 5

Parameter	Optimum Values
WOB (lb)	9150
Torque (in-lb)	18,600
Penetration (in/rev)	0.044

Plots of MSE against Weight on Bit, Torque and Penetration per Revolution can be seen in Figure 94, Figure 95, and Figure 96

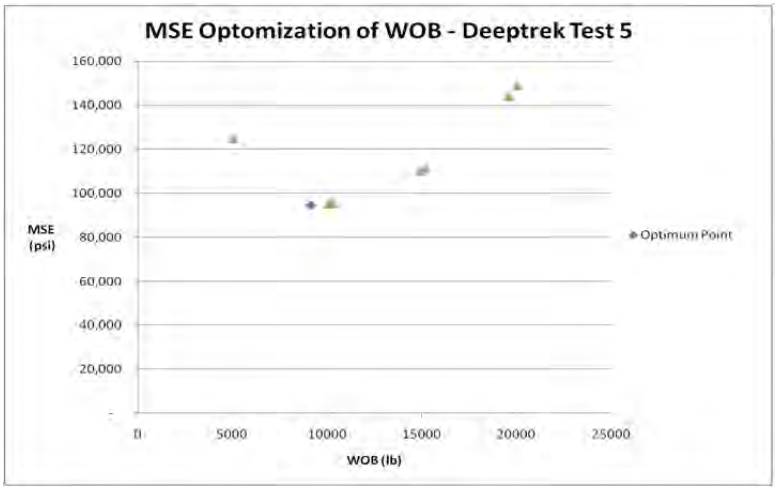

Figure 94 Optimum Weight on Bit Point Indicated for PDC Bit in Marble

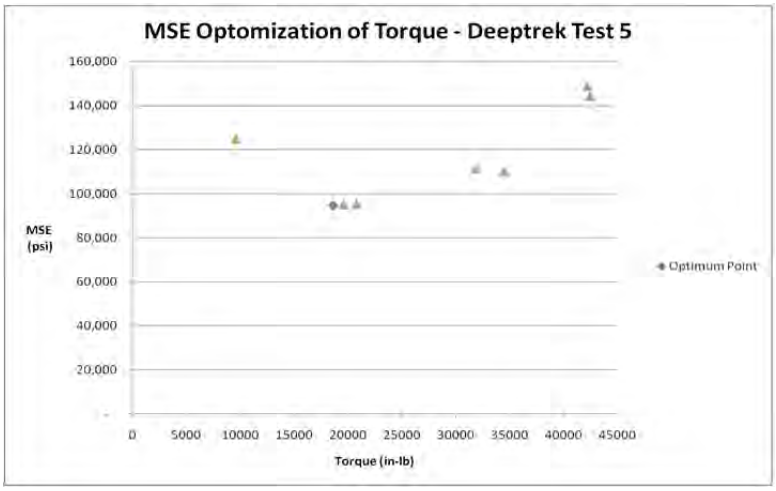

Figure 95 Optimum Torque Point Indicated for PDC Bit in Marble

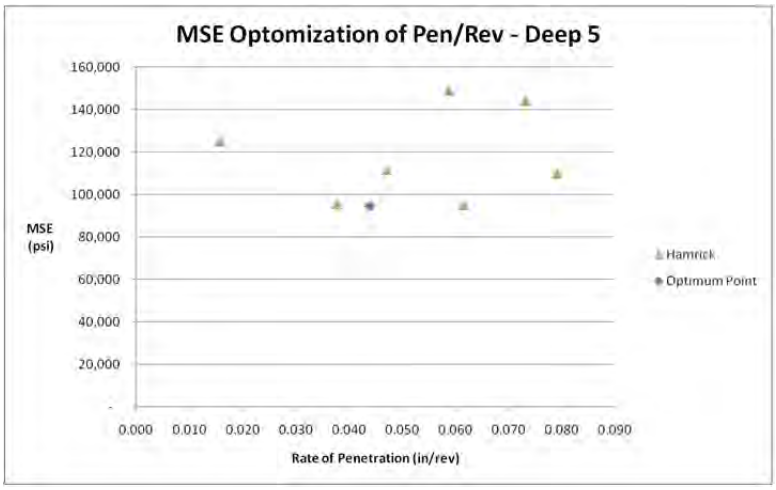

Figure 96 Optimum Penetration per Revolution Point Indicated for PDC Bit in Marble

PDC Coring Bit in Basalt

The method was applied to data generated by Hamade in 2009 for basalt drilling.[27] That work used a PDC coring bit 1.49 inch OD and 0.984 inch ID and various rake angles. The data was normalized for this work so that the effect of rake angle was removed, and can be found in Table 43. The Weight on Bit data plotted against Torque can be seen in Figure 97. Under Assumption 2 a linear relationship was assumed, and the coefficients for the Torque equation were computed by regression.

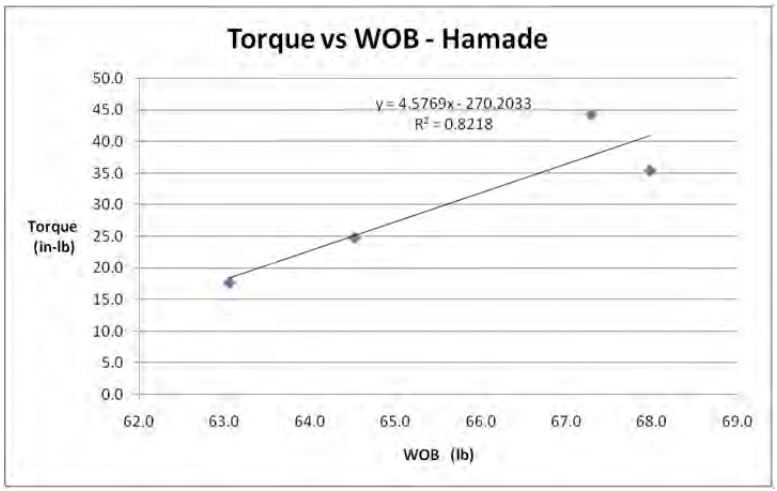

Figure 97 Torque as a Linear Function of Weight on Bit for Basalt

$$Torque = f(WOB) = A_0 + A_1 * WOB \quad (108)$$

$$Torque = f(WOB) = -270.2 + 4.58 * WOB \quad (109)$$

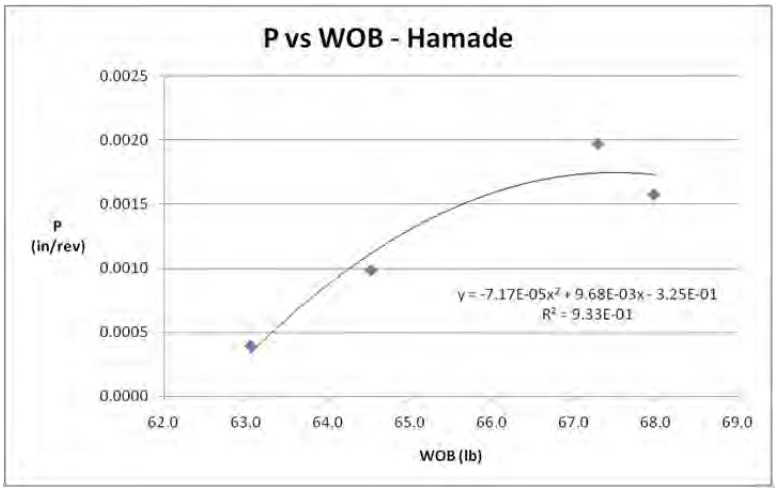

Figure 98 Rate of Penetration as a Function of Weight on Bit for Basalt

Similarly Weight on Bit was plotted against Penetration per Revolution, as can be seen in Figure 98. Under Assumption 3 a second order polynomial relationship was assumed, and the coefficients for the Penetration per Revolution equation were computed by regression.

$$ROP = g(WOB) = B_2 * WOB^2 + B_1 * WOB + B_0 \quad (110)$$

$$ROP = g(WOB) = -7.17\text{E}-05 * WOB^2 + 9.68\text{E}-03 * WOB - 3.25\text{E}-01 \quad (111)$$

The Torque and Penetration per Revolution equations were substituted into the MSE_H equation.

$$\text{MSE}_\text{H} = \frac{\text{WOB}}{\text{Area}} + \frac{2\,\pi * (\text{A}_0 + \text{A}_1 * \text{WOB})}{\text{Area} * (\text{B}_2 * \text{WOB}^2 + \text{B}_1 * \text{WOB} + \text{B}_0)} \quad (112)$$

$$\text{MSE}_\text{H} = \frac{\text{WOB}}{\text{Area}} + \frac{2\,\pi * (-270.2 + 4.58 * WOB)}{\text{Area} * (-7.17\text{E}-05 * WOB^2 + 9.68\text{E}-03 * WOB - 3.25\text{E}-01)} \quad (113)$$

In Table 43 MSE was computed using both the conventional Equation 9 and the above equation. A comparison is plotted in Figure 99.

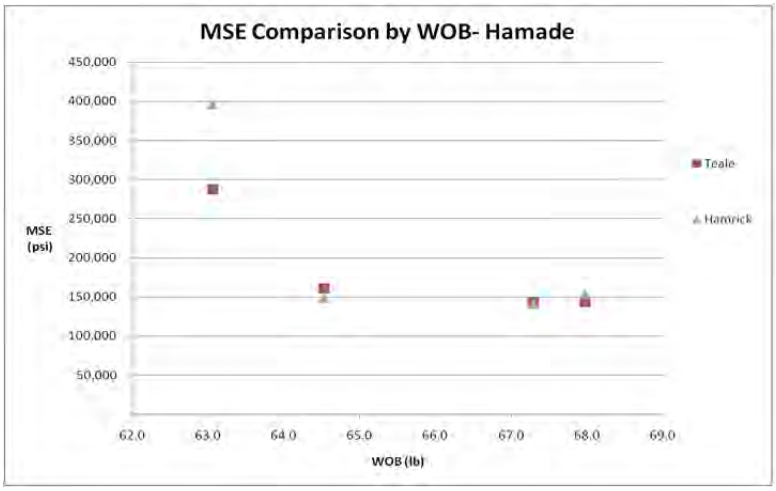

Figure 99 Comparison of Teale and Hamrick MSE Curves

Table 43 Basalt With PDC Coring Bit Results

				Teale	Hamrick
RPM	in/Rev	WOB (lb)	Torque (in-lb)	MSE (ksi)	MSE (ksi)
100	0.0010	64.5	24.8	161	149
100	0.0004	63.1	17.7	287	396
100	0.0020	67.3	44.3	144	141
100	0.0016	68.0	35.4	144	154

The coefficients determined by regression were used in Equation 13 to compute the polynomial unique to this variant.

$$0 = B_2 * WOB^4 + 2B_1B_2 * WOB^3 + (B_1{}^2 + 2B_2B_0 - 2\pi A_1B_2) * WOB^2 + (2B_1B_0 - 4\pi A_0B_2) * WOB + (B_0{}^2 + 2A_1B_0 - 2\pi A_0B_1)0 \quad (114)$$

$$0 = 5.14E-09 * WOB^4 - 1.4E-06 * WOB^3 + 0.0022 * WOB^2 + -0.2498 * WOB + 7.193 \quad (115)$$

This polynomial has four roots, which are indicated in Table 44.[35] Only the positive real root has physical meaning, indicating that the optimum Weight on Bit is 66 pounds.

Table 44 Roots of MSE_H Equation for Basalt

Real solutions:
Root 1: 52.1
Root 2: 65.9
Complex roots:
Root 3: 75.967-633.425 * i
Root 4: 75.967+633.425 * i

Using the modified Torque and Penetration per Revolution equations, optimum values were computed and illustrated in Table 45.

Table 45 Optimum Values of Parameters for Basalt

Parameter	Optimum Values
WOB (lb)	65.9
Torque (in-lb)	31.4
Penetration (in/rev)	0.0015

Plots of MSE against Weight on Bit, Torque and Penetration per Revolution can be seen in Figure 100, Figure 101, and Figure 102.

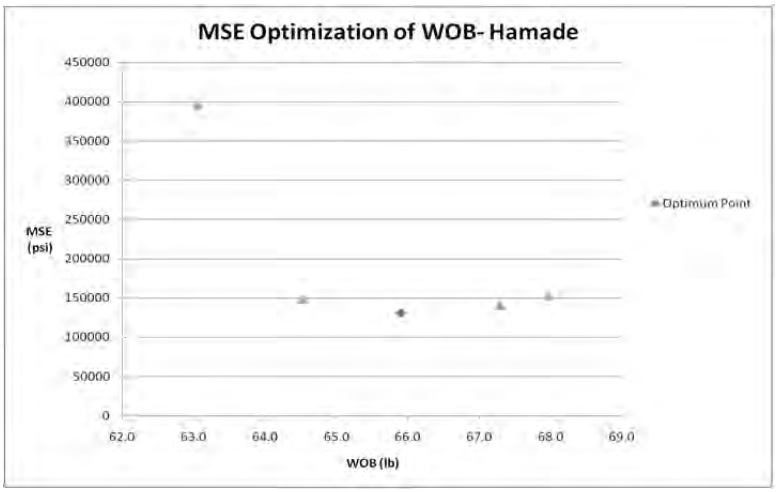

Figure 100 Optimum Weight on Bit Point Indicated for Basalt

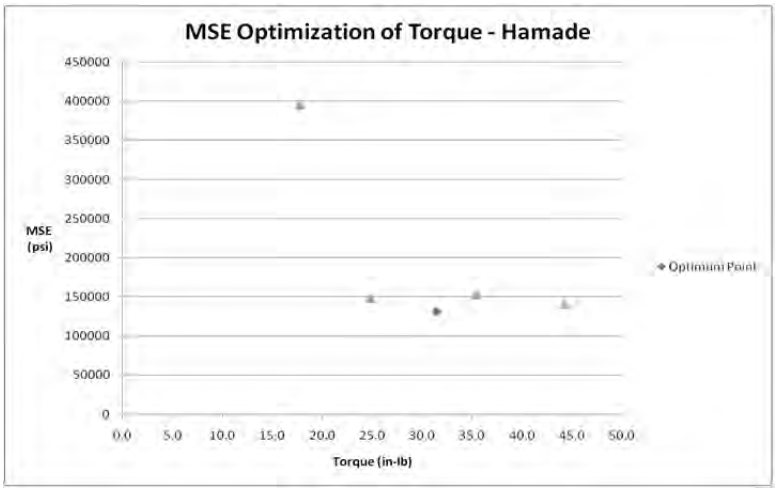

Figure 101 Optimum Torque Point Indicated for Basalt

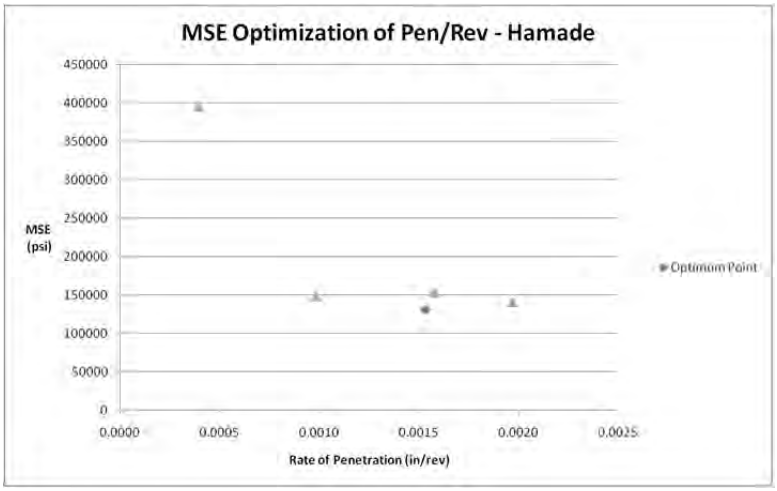

Figure 102 Optimum Rate of Penetration Point Indicated for Basalt

Appendix C

Raw data for each data point can be found in the enclosed electronic media. Each of the eight variants of the testing conducted for this work is listed in the tables below. The file name for each can be found in its caption, and the table indicates the sheet within the spreadsheet file where the raw data for that data point resides.

All data to support this document is contained in the attached zip file:
Data_Sets_Hamrick_Dissertation

Table 46 Carthage Marble, Ambient Temp, Ambient Pressure, Standard Bit. All data for this variant can be found in the attached spreadsheet File Name "Data Sets Hamrick Dissertation Ambient Marble"

RPM	in/Rev	WOB (lb)	Torque (in-lb)	Sheet Name
21	0.018	214	30.5	CMAmb21018
21	0.021	275	33.8	CMAmb21021
21	0.047	762	61.5	CMAmb21047
43	0.008	105	20.0	CMAmb43008
43	0.018	216	33.2	CMAmb43018
43	0.021	245	32.2	CMAmb43021
43	0.033	480	61.2	CMAmb43033
65	0.018	199	32.6	CMAmb65018
65	0.021	235	34.2	CMAmb65021
65	0.027	325	43.8	CMAmb65027
86	0.008	97	19.6	CMAmb86008
86	0.018	212	32.4	CMAmb86018
86	0.027	302	40.5	CMAmb86027
86	0.033	213	31.5	CMAmb86033
86	0.047	382	38.1	CMAmb86047
115	0.008	82	18.6	CMAmb115008
115	0.018	179	33.9	CMAmb115018
115	0.027	279	39.5	CMAmb115027
115	0.033	332	33.0	CMAmb115033
133	0.008	103	19.9	CMAmb133008
133	0.018	192	30.0	CMAmb133018
133	0.027	372	50.3	CMAmb133027
133	0.033	382	38.4	CMAmb133033
133	0.047	370	39.3	CMAmb133047
151	0.008	102	17.9	CMAmb151008
151	0.018	236	30.8	CMAmb151018
151	0.027	420	47.8	CMAmb151027
151	0.047	402	33.4	CMAmb151047
151	0.056	459	41.4	CMAmb151056

Table 47 Carthage Marble Heated to 450 F. All data for this variant can be found in the attached spreadsheet File Name "Data Sets Hamrick Dissertation Heated Marble"

RPM	in/Rev	WOB (lb)	Torque (in-lb)	Sheet Name
21	0.003	34	12.3	CMHot21003
21	0.005	49	14.0	CMHot21005
21	0.008	76	13.6	CMHot21008
21	0.01	68	17.7	CMHot21010
21	0.018	104	22.2	CMHot21018
21	0.027	188	30.9	CMHot21027
21	0.047	486	50.0	CMHot21047
21	0.056	562	65.1	CMHot21056
21	0.071	612	57.2	CMHot21071
43	0.003	36	7.1	CMHot43003
43	0.005	53	9.1	CMHot43005
43	0.008	68	14.4	CMHot43008
43	0.010	72	12.0	CMHot43010
43	0.018	128	24.5	CMHot43018
43	0.027	148	26.9	CMHot43027
43	0.033	378	38.5	CMHot43033
43	0.047	445	47.2	CMHot43047
43	0.056	477	45.0	CMHot43056
43	0.071	668	48.5	CMHot43071
65	0.003	34	8.1	CMHot65003
65	0.005	46	8.6	CMHot65005
65	0.010	46	12.0	CMHot65010
65	0.047	424	41.5	CMHot65047
65	0.056	531	50.0	CMHot65056
100	0.003	41	7.9	CMHot100003
100	0.005	48	8.0	CMHot100005
100	0.010	76	11.3	CMHot100010
100	0.021	137	12.7	CMHot100021
100	0.047	335	30.0	CMHot100047
100	0.056	456	40.0	CMHot100056
100	0.071	596	48.0	CMHot100071
133	0.003	37	5.3	CMHot133003
133	0.005	64	8.7	CMHot133005
133	0.010	89	14.3	CMHot133010
133	0.012	92	18.4	CMHot133012
133	0.018	118	12.6	CMHot133018
133	0.033	364	26.0	CMHot133033
133	0.056	484	45.3	CMHot133056
133	0.071	611	50.2	CMHot133071

Table 48 Carthage Marble Under 1500 psi Confining Pressure. All data for this variant can be found in the attached spreadsheet File Name "Data Sets Hamrick Dissertation Pressurized Marble"

RPM	in/Rev	WOB (lb)	Torque (in-lb)	Sheet Name
21	0.008	61	12.0	CM Hoek 21 008
21	0.012	98	16.9	CM Hoek 21
21	0.018	114	17.8	CM Hoek 21 018
21	0.027	149	22.1	CM Hoek 21 027
21	0.033	355	29.6	CM Hoek 21 033
43	0.008	51	12.6	CM Hoek 43 008
43	0.012	95	18.0	CM Hoek 43 012
43	0.018	128	22.1	CM Hoek 43 018
43	0.027	145	22.2	CM Hoek 43 027
43	0.033	397	35.0	CM Hoek 43 033
65	0.008	65	11.7	CM Hoek 65 008
65	0.012	129	21.7	CM Hoek 65 012
65	0.018	119	22.1	CM Hoek 65 018
65	0.027	212	31.0	CM Hoek 65 027
86	0.008	65	11.9	CM Hoek 86 008
86	0.012	120	18.2	CM Hoek 86 012
86	0.018	117	21.5	CM Hoek 86 018
86	0.027	197	26.7	CM Hoek 86 027
86	0.033	464	43.1	CM Hoek 86 033
100	0.008	77	14.8	CM Hoek 100 008
100	0.012	138	21.1	CM Hoek 100 012
100	0.018	105	19.4	CM Hoek 100 018
100	0.027	215	36.6	CM Hoek 100 027
100	0.033	383	51.3	CM Hoek 100 033

Table 49 Carthage Marble Drilled with 2-Wing Bit. All data for this variant can be found in the attached spreadsheet File Name "Data Sets Hamrick Dissertation 2 Wing Bit Marble"

RPM	in/Rev	WOB (lb)	Torque (in-lb)	Sheet Name
21	0.008	111	36.8	CM 2Wing 21 008
21	0.018	211	51.5	CM 2Wing 21 018
21	0.021	227	55.6	CM 2Wing 21 021
43	0.008	142	45.2	CM 2Wing 43 008
43	0.010	163	45.5	CM 2Wing 43 010
43	0.012	224	55.4	CM 2Wing 43 012
43	0.018	241	61.5	CM 2Wing 43 018
43	0.021	264	72.6	CM 2Wing 43 021
65	0.010	114	33.0	CM 2Wing 65 010
65	0.012	202	52.9	CM 2Wing 65 012
65	0.018	213	56.4	CM 2Wing 65 018
65	0.021	236	68.1	CM 2Wing 65 021
86	0.010	154	56.5	CM 2Wing 86 010
86	0.012	240	75.8	CM 2Wing 86 012
86	0.018	250	66.9	CM 2Wing 86 018
86	0.021	295	82.6	CM 2Wing 86 021
100	0.008	145	37.0	CM 2Wing 100 008
100	0.010	189	45.3	CM 2Wing 100 010
100	0.012	258	60.8	CM 2Wing 100 012
100	0.018	318	73.5	CM 2Wing 100 018
100	0.021	319	76.8	CM 2Wing 100 021

Table 50 Terretek Sandstone, Ambient Temp, Ambient Pressure, Standard Bit. All data for this variant can be found in the attached spreadsheet File Name "Data Sets Hamrick Dissertation Ambient Sandstone"

RPM	in/Rev	WOB (lb)	Torque (ft-lb)	Sheet Name
21	0.003	169	27.4	TS Amb 21 003
21	0.005	221	34.2	TS Amb 21 005
21	0.008	246	37.9	TS Amb 21 008
21	0.010	270	40.3	TS Amb 21 010
21	0.012	391	54.4	TS Amb 21 012
21	0.018	386	56.5	TS Amb 21 018
21	0.021	452	66.3	TS Amb 21 021
42	0.003	146	29.5	TS Amb 43 003
42	0.005	213	40.5	TS Amb 43 005
42	0.008	143	24.8	TS Amb 43 008
42	0.010	165	28.9	TS Amb 43 010
42	0.012	222	36.5	TS Amb 43 012
42	0.018	234	38.0	TS Amb 43 018
65	0.003	94	17.2	TS Amb 65 003
65	0.005	142	26.5	TS Amb 65 005
65	0.008	157	28.4	TS Amb 65 008
65	0.010	187	32.3	TS Amb 65 010
65	0.012	256	40.8	TS Amb 65 012
65	0.018	287	45.2	TS Amb 65 018
86	0.003	113	26.3	TS Amb 86 003
86	0.005	179	36.5	TS Amb 86 005
86	0.008	206	39.8	TS Amb 86 008
86	0.010	213	39.5	TS Amb 86 010
86	0.012	309	55.1	TS Amb 86 012
86	0.018	338	57.4	TS Amb 86 018
100	0.003	79	14.6	TS Amb 100 003
100	0.005	137	22.8	TS Amb 100 005
100	0.008	159	25.3	TS Amb 100 008
100	0.010	192	29.0	TS Amb 100 010
100	0.012	283	45.3	TS Amb 100 012
100	0.018	303	51.1	TS Amb 100 018

Table 51 Terretek Sandstone Heated to 450 F. All data for this variant can be found in the attached spreadsheet File Name "Data Sets Hamrick Dissertation Heated Sandstone"

RPM	in/Rev	WOB (lb)	Torque (in-lb)	Sheet Name
21	0.005	94	34.3	TS Hot 21 005
21	0.008	152	33.5	TS Hot 21 008
21	0.010	193	38.0	TS Hot 21 010
21	0.012	257	50.9	TS Hot 21 012
21	0.018	264	49.1	TS Hot 21 018
21	0.021	273	54.0	TS Hot 21 021
43	0.005	161	30.1	TS Hot 43 005
43	0.008	201	40.8	TS Hot 43 008
43	0.010	274	47.1	TS Hot 43 010
43	0.012	290	53.7	TS Hot 43 012
43	0.018	313	45.8	TS Hot 43 018
43	0.021	348	53.3	TS Hot 43 021
65	0.005	245	46.2	TS Hot 65 005
65	0.008	272	49.7	TS Hot 65 008
65	0.010	306	48.5	TS Hot 65 010
65	0.012	363	63.1	TS Hot 65 012
65	0.018	433	66.1	TS Hot 65 018
65	0.021	431	70.4	TS Hot 65 021
86	0.005	112	16.5	TS Hot 86 005
86	0.008	142	18.5	TS Hot 86 008
86	0.010	189	23.1	TS Hot 86 010
86	0.012	270	35.6	TS Hot 86 012
86	0.018	282	37.7	TS Hot 86 018
86	0.021	353	53.1	TS Hot 86 021
100	0.005	109	25.3	TS Hot 100 005
100	0.008	151	27.3	TS Hot 100 008
100	0.010	182	30.3	TS Hot 100 010
100	0.012	235	38.2	TS Hot 100 012
100	0.018	262	41.2	TS Hot 100 018
100	0.021	321	49.8	TS Hot 100 021

Table 52 Terretek Sandstone Under 1500 psi Confining Pressure. All data for this variant can be found in the attached spreadsheet File Name "Data Sets Hamrick Dissertation Pressurized Sandstone"

RPM	in/Rev	WOB (lb)	Torque (in-lb)	Sheet Name
21	0.005	143	21.7	TS Hoek 21 005
21	0.008	188	29.9	TS Hoek 21 008
21	0.010	207	36.9	TS Hoek 21 010
21	0.012	293	46.9	TS Hoek 21 012
21	0.018	296	50.6	TS Hoek 21 018
21	0.021	339	58.9	TS Hoek 21 021
43	0.005	79	21.7	TS Hoek 43 005
43	0.008	101	26.6	TS Hoek 43 008
43	0.010	183	37.1	TS Hoek 43 010
43	0.012	196	39.4	TS Hoek 43 012
43	0.018	223	42.4	TS Hoek 43 018
43	0.021	269	51.7	TS Hoek 43 021
65	0.005	94	21.1	TS Hoek 65 005
65	0.008	130	23.6	TS Hoek 65 008
65	0.010	140	24.8	TS Hoek 65 010
65	0.012	175	31.8	TS Hoek 65 012
65	0.018	260	43.8	TS Hoek 65 018
65	0.021	318	52.3	TS Hoek 65 021
100	0.005	104	22.9	TS Hoek 100 005
100	0.008	152	32.8	TS Hoek 100 008
100	0.010	214	41.5	TS Hoek 100 010
100	0.012	298	56.9	TS Hoek 100 012
100	0.018	342	54.5	TS Hoek 100 018
100	0.021	391	66.4	TS Hoek 100 021

Table 53 Terretek Sandstone Drilled with 2-Wing Bit. All data for this variant can be found in the attached spreadsheet File Name "Data Sets Hamrick Dissertation 2 Wing Bit Sandstone"

RPM	in/Rev	WOB (lb)	Torque (in-lb)	Sheet Name
21	0.003	61	12.0	TS 2Wing 21 003
21	0.005	99	19.0	TS 2Wing 21 005
21	0.008	111	21.5	TS 2Wing 21 008
21	0.010	122	25.1	TS 2Wing 21 010
21	0.012	187	40.4	TS 2Wing 21 012
21	0.018	188	40.3	TS 2Wing 21 018
21	0.021	210	45.2	TS 2Wing 21 021
43	0.003	97	20.9	TS 2Wing 43 003
43	0.005	133	29.3	TS 2Wing 43 005
43	0.008	147	30.7	TS 2Wing 43 008
43	0.010	156	31.6	TS 2Wing 43 010
43	0.012	226	47.4	TS 2Wing 43 012
43	0.018	242	48.1	TS 2Wing 43 018
65	0.003	104	30.9	TS 2Wing 65 003
65	0.005	182	45.5	TS 2Wing 65 005
65	0.008	186	47.2	TS 2Wing 65 008
65	0.010	188	44.2	TS 2Wing 65 010
65	0.012	226	50.6	TS 2Wing 65 012
65	0.018	323	69.5	TS 2Wing 65 018
86	0.003	102	22.6	TS 2Wing 86 003
86	0.005	122	29.7	TS 2Wing 86 005
86	0.008	132	33.7	TS 2Wing 86 008
86	0.010	164	36.6	TS 2Wing 86 010
86	0.012	229	48.8	TS 2Wing 86 012
86	0.018	282	62.0	TS 2Wing 86 018
100	0.003	132	27.4	TS 2Wing 100 003
100	0.005	195	39.0	TS 2Wing 100 005
100	0.008	255	53.8	TS 2Wing 100 008
100	0.010	231	49.5	TS 2Wing 100 010
100	0.012	247	50.4	TS 2Wing 100 012
100	0.018	244	47.7	TS 2Wing 100 018

References

[1] Well Drilling School. "http://welldrilliHistoryofWellConstruction." *http://welldrilliHistoryofWellConstruction* n. pag. Web. 20 Apr 2010. <http://welldrillingschool.com/courses/pdf/HistoryofWellConstruction.pdf>.

[2] American Society of Mechanical Engineers. "Hughes Two-Cone Drill Bit." *Historic Mechanical Engineering Landmark* 2009: n. pag. Web. 27 Apr 2010. <http://files.asme.org/MEMagazine/Web/20779.pdf>.

[3] US Energy Information Administration. United States. *International Energy Outlook 2010, Report #:DOE/EIA-0484*, 2010. Web. Aug 2010. <www.eia.doe.gov/>.

[4] Lambert S W, Rogers J D, Williamson J R, Boyer C M, and Frantz J H. "Benchmarking Deep Drilling Technologies." *2005 SPE Annual Technical Conference and Exhibition*. SPE Editorial Committee: Dallas, TX, Society of Petroleum Engineers. 2005. Print.

[5] Teale R. "The Concept of Specific Energy in Rock Drilling." *International Journal of Rock Mechanics* . 2. (1965): 57-73. Print.

[6] Gerbaud, Menand, and Sellami. "PDC Bits: All Comes From the Cutter/Rock Interaction." *IADC/SPE 98988 Drilling Conference*. Miami, FL, International Association of Drilling Contractors and Society of Petrolleum Engineers. 2006. Web. 11 Jun 2010.

[7] Rashidi B, Hareland G, and Nygaard R. "Real-Time Drill Bit Wear Prediction by Combining Rock Energy and Drilling Strength Concepts." *SPE 117109-PP 2008 Abu Dhabi International Petroleum Exhibition and Conference*. Abu Dhabi, Society of Petroleum Engineers. 2008. Print.

[8] Zeuch D H, and Finger J T. "Rock Breakage Mechanisms With a PDC Cutter." 60*th Annual Technical Conference and Exhibitionof the Society of Petroleum Engineers*. Society of Petroleum Engineers: Las Vegas, SPE . 1985. Print.

[9] Wojtanowicz A K, and Kuro E. "Dynamic Drilling Strategy For PDC Bits." *SPE/IADC 16118 1987 SPE/IADC Drilling Conference.* New Orleans, LA, Society of Petroleum Engineers and International Association of Drilling Contractors. 1987. Print.

[10] Huang S L, and Wang Z W . "The Mechanics of Diamond Core Drilling of Rocks." Int. J. Rock Mech. & Min. Sci. 34:3-4, paper No. 134.

[11] Ersoy A, and Waller M. "Drilling Detritus and the Operating Parameters of Thermally Stable PDC Core Bits." *International Journal of Rock Mechanics*. 34.7 (1997): 1109-1123. Print.

[12] Ersoy A, and Atici U. "Performance characteristics of circular diamond saws in cutting different types of rocks." *Diamond and Related Materials* 13 (2004) 22–37. Print.

[13] Caicedo H, and Calhoun W. "Unique ROP Predictor Using Bit-specific Coefficient of Sliding Friction and Mechanical Efficiency as a Function of Confined Compressive Strength Impacts Drilling Performance." *AADE 2005 National Technical Conference and Exhibition*. Houston. TX, American Association of Drilling Engineers. 2005. Print.

[14] Armenta M. "Identifying Inefficient Drilling Conditions Using Drilling Specific Energy." *SPE 116667. SPE Annual Technical Conference and Exhibition*. Denver, CO. Society of Petroleum Engineers. 2008. Print.

[15] DuPriest F, and Koederlitz W. "Maximizing Drill Rates With Real Time Surveillance of Mechanical Specific Energy." *SPE/IADC 92194 Drilling Conference*. Amsterdam, The Netherlands, Society of Petroleum Engineers, International Association of Drilling Contractors. 2005. Print.

[16] Koederlitz W and Weis J. "A Real-Time Implementation of MSE." *AADE-05-NTCE-66 AADE National Technical Conference and Exhibition*. Houston, TX, American Association of Drilling Engineers. 2005. Print

[17] DuPriest F. "Comprehensive Drill Rate Management Process to Maximize Rate of Penetration." *SPE Annual Technical Conference and Exhibition*. San Antonio, TX, Society of Petroleum Engineers. 2006. Print.

[18] Remmert S, Witt J, and DuPriest F. "Implementation of ROP Management Process in Qatar North Field." *SPE/IADC 105521 Drilling Conference*. Amsterdam, The Netherlands, Society of Petroleum Engineers, International Association of Drilling Contractors. 2007. Print.

[19] Burmaster K, Chando J, and Vaczi K. "Execution Success in Platform Drilling Campaign." *SPE/IADC 119262 Drilling Conference*. Amsterdam, The Netherlands, Society of Petroleum Engineers, International Association of Drilling Contractors. 2009. Print.

[20] Kilroy D, and DuPriest F. "Practices Implemented to Achieve Record Performance in Narrow Margin Drilling in Bass Straight Extended Reach." SPE 125246. *SPE Annual Technical Conference and Exhibition*. New Orleans, LA, Society of Petroleum Engineers. 2009. Print.

[21] Roehrlich M, and Belohlavek KU. "ROP Enhancement in Ultra-hard Rock." *IADC/SPE 99045 IADC/SPE Drilling Conference*. Miami, FL, Society of Petroleum Engineers, International Association of Drilling Contractors. 2006. Print.

[22] DuPriest F. "Maintaining Steerability While Extending Gauge Length to Manage Whirl." *SPE/IADC 119625 Drilling Conference*. Amsterdam, The Netherlands, Society of Petroleum Engineers, International Association of Drilling Contractors. 2009. Print.

[23] Reddish D J, and Yasar E. “A New Portable Rock Strength Index Test Based on Specific Energy of Drilling.” Int. J. Rock Mech. & Min. Sci. 33:5 pp 543-548. 1997. Print.

[24] Stavropoulou M. “Modeling of Small Diameter Rotary Drilling Tests on Marbles.” Int. J. Rock Mech. & Min. Sci. 43. Pp 1034-1051. 2006. Print.

[25] Abd Al-Jalil Y Q. "The Mechanics of Indentation of Rock –A Critical Review." The 41st U.S. Symposium on Rock Mechanics (USRMS)ARMA/USRMS 06-1082. American Rock Mechanics Association: Golden, CO, American Rock Mechanics Association. 2006. Print.

[26] Mosley S G, Bohn K P, and Goedickemeier M. “Core Drilling In Reinforced Concrete Using Polycrystalline Diamond (PCD) Cutters: Wear And Fracture Mechanisms.” *Int. Journal of Refractory Metals & Hard Materials* 27 (2009) 394–402

[27] Hamade R F, Manthrib S P, Pusavec F, Zacny K A, and Taylor L A. "Compact Core Drilling In Basalt Rock Using PCD Tool Inserts: Wear Characteristics And Cutting Forces." *Journal of Materials Processing Technology*. 210. (2010): 1326–1339. Print.

[28] Black A D, and Judizs A. “Optimization of Deep Drilling Performance – Development and Benchmark Testing of Advanced Diamond Product Drill Bits & HP/HT Fluids to Significantly Improve Rates of Penetration.” Topical Report, March, 2006, Contract DE-FC26-02NT41657, prepared by TerraTek, Inc. for NETL. Morgantown, West Virginia: National Energy Technology Laboratory (NETL). 2006. Print.

[29] Langeveld C J. "PDC Bit Dynamics." 1992 IADC/SPE Drilling Conference. IADC /SPE 23867: New Orleans, LA, American Society of Petroleum Engineers. 1992. Print.

[30] Langeveld C J. "PDC Bit Dynamics. (Supplement to IADC /SPE 23867" 1992 IADC/SPE Drilling Conference. IADC/SPE 23873: New Orleans, LA, American Society of Petroleum Engineers. 1992. Print.

[31] Mensa-Wilmot, Graham, Fear, and Martyn. "The Effects of Formation Hardness, Abrasiveness, Heterogeneity and Hole Size on PDC Bit Performance." 2001 IADC/SPE Drilling Conference IADC/SPE 67698: Amsterdam, The Netherlands, American Society of Petroleum Engineers. 2001. Print.

[32] Warren T M, and Sinor, L A. "PDC Bits: What’s Needed to Meet Tomorrow Challenge." University of Tulsa Centennial Petroleum Engineering Symposium, IADC/SPE 27978: Tulsa, OK, American Society of Petroleum Engineers. 1994. Print.

[33] Clayton R S, and Ivey B S. "Development of Whirl Resistant Bits." Latin American Caribbean Petroleum Conference IADC/SPE 26954: Buenos Aires, Argentina, American Society of Petroleum Engineers. 1994. Print.

[34] Huang H. "Intrinsic Length Scales in Tool-Rock Interaction." *International Journal of Geomechanics*. 8.1 (2008): 44. Print.

[35] "Polynomial Root Finder." Free Online Polynomial Roots Finder (factoring). Real and imaginary (complex) roots. Web. 17 Mar 2011. http://xrjunque.nom.es/precis/rootfinder.aspx>.